A

THESIS

ON

An Experimental Investigation into Stability and Thermal Conductivity of Nanofluids

Submitted In Partial Fulfillment of the Requirement for the award of degree of

MASTER OF ENGINEERING

IN

THERMAL ENGINEERING

Submitted by

APOORVA SINGH

ROLL NO: 801183004

Under the guidance of

Dr. S.S.MALLICK

(ASSISTANT PROFESSOR)

Dr. B. PAL

(ASSOCIATE PROFESSOR)

THAPAR UNIVERSITY

PATIALA- 147004, INDIA

Declaration

I hereby certify that the work which is being presented in on the topic "An experimental investigation into stability and thermal conductivity of nanofluids", in partial fulfillment of the requirements for the award of degree of Master of Engineering in Thermal engineering submitted in Mechanical Engineering Department of Thapar University, Patiala, is an authentic record of my own work carried out under the supervision of Dr. S.S. Mallick and Dr. B.Pal.

Apoorva Singh
(801183004)

This is to certify that the above statement made by the candidate is correct and true to the best of my knowledge.

15/7

Dr. S.S. Mallick
Thapar University
Patiala-147004

15/07/13

Dr. B.Pal
Thapar University
Patiala-147004

DR. AJAY BATISH
(Professor & Head)
Mech. Engg. Deptt.
Thapar University, Patiala

DR. S.K. MOHAPATRA
SENIOR PROFESSOR & DEAN
OF ACADEMIC AFFAIRS
THAPAR UNIV., PATIALA

Acknowledgement

No volume of words is enough to express my gratitude toward my guides, Dr. S.S. Mallick and Dr. B.Pal, TU, who has been very concerned and has aided for all the material essential for the preparation of this report. He has helped me explore this vast topic in an organized manner and provided me with all the ideas on how to work towards a research-oriented venture.

I would also like to thank the staff members and my colleagues who were always there at the need of the hour and provided with all the help and facilities, which I required, for the completion of my report work.

Most importantly, I would like to thank my parents and the almighty for showing me the right direction out of the blue, to help me stay calm in the oddest of the times and keep moving even at times when there was no hope.

Apoorva Singh
801183004

TABLE OF CONTENTS

ABSTRACT

This thesis presents an experimental investigation into the stability and thermal conductivity of nanofluids. In the present work the stability of 3 different nanoparticles – Silver, Carbon nanotubes, Zinc Oxide have been investigated. These three have been chosen as the representatives of the different classes of nanoparticles – metal, carbon nanotubes and metal oxide respectively. Three popular techniques have been used to investigate into the stability of nanofluids – Dynamic Light Scattering, UV-vis spectrophotometer and Zeta Potential and their results have been compared. Also, the effect of sonication time and addition of SDS (sodium dodecylsulfate) as surfactant have been investigated to see how they affect the stability of a nanofluid. The issue of measurement of thermal conductivity has been dealt with including a review of the different methods that have been used to measure the thermal conductivity and the establishment of the correct technique to use the KD2 Pro to see how stability of a nanofluid affects its thermal conductivity. The Carbon nanotubes have been found to be the most stable of all the nanofluids that have been used. Zinc Oxide is the least stable of all. The spectrophotometer technique gives the best estimate of the stability of a nanofluid. Also, thermal conductivity has been found to be a function of size and concentration of the nanoparticles, and it increases as the particles agglomerate to form clusters; however it decreases as the particles become too large as they begin to settle down and that decreases the concentration of the nanoparticles in the base fluid.

CHAPTER 1: INTRODUCTION

1.1 Introduction

Nanofluids can be defined as the suspension of nanoparticles in a base fluid (such as water, ethylene glycol etc.). A nanoparticle can be defined as a quasi-zero dimensional object in which all characteristic linear dimensions are of the nano-size order of magnitude (Gubin et. al. 2005). Nanofluids are very promising fluids especially in fields involving heat transfer due to their anomalously high thermal conductivity (Choi, 1995). The thermal conductivity of a nanofluid containing some volume fraction of nanoparticles is found to be higher than the thermal conductivity of a fluid containing the same volume fraction of millimetre or micrometer sized particles (Eastman et. al. 2001, Patel et. al. 2003). Owing to their property of enhancement of thermal conductivity, the engineering applications of nanofluids range from the automotive industry and medical sciences to power plants and computers and electronics (Wong and Leon, 2009). The concept of nanofluids is not an absolutely new concept as the method of improving the properties of the fluids using suspended solid particles can be traced back to J.C.Maxwell's theoretical work. (Maxwell, 1873). But the particles that were used back then were millimetre or micrometer sized and such suspensions bear the following major disadvantages:

(1) The particles settle rapidly forming a layer on the surface and reducing the heat transfer capacity of the fluid.

(2) If the circulation rate of the fluid is increased, sedimentation is reduced, but the erosion of the heat transfer devices, pipelines etc. increases rapidly.

(3) The large size of the particles tends to clog the flow channels, particularly if the cooling channels are narrow.

(4) The pressure drop increases in the fluid considerably.

(5) Finally, conductivity enhancement based on particle concentration is achieved (i.e., the greater the particle volume fraction is, the greater the enhancement – and greater the problems (1) - (4) as indicated above. (Das et al. 2006).

However, modern day technology has helped in the synthesis of particles of nanometre size. The materials made of nanometre-sized particles fabricated on the atomic or molecular demonstrate either new or enhanced physical properties that are not exhibited by the material in bulk. These properties include the thermal, mechanical, optical, magnetic and electrical properties. This uniqueness in the properties has been attributed to the high surface area/volume ratio of the nanostructured materials. As a consequence of this, research and development in the field of nanophase materials has drawn considerable attention (Duncan and Rouveray, 1989). With more and more research being devoted to the synthesis of nanoparticles and nanofluids there is a hope that the solution to the aforementioned problems (1) - (4) can be found.

Even though there are numerous industries where nanofluids find applications, automobile, electronics, power, bio-medical to name a few, there are still many challenges strewn in the path of nanofluids being used commercially as an effective heat transfer medium. This is mainly due to three reasons. Firstly, the properties of

nanofluids have been very difficult to understand and even more difficult to model. It is because there are a number of parameters that have to be studied associated with the nanoparticles and also the base fluid such as the particle size, temperatures, pressure, specific heat, thermal conductivity, viscosity and the interaction of the particles with the fluid medium. Secondly, it's a field that involves interdisciplinary knowledge and hence relatively more difficult. (Edward T. Foley and Mark C. Hersam, 2006). Thirdly, even though nanofluids are expected to remain stable due to vigorous Brownian motion of the suspended nanoparticles (Hwang et al., 2006, Keblinski et al., 2002), this is not the case. The nanoparticles agglomerate and form clusters and this reduction in the stability is a hindrance not only because it may cause clogging and abrasion of channels but also because it leads to decrease in the thermal conductivity improvement (Hong et al., 2006). Contrary to this theory, however, is another theory according to which aggregation is a more likely cause for the enhancement of thermal conductivity of nanofluid (Gharagozloo and Goodson, 2010). Thus there is no agreement between the various research groups about the relation of particle agglomeration and stability and the various thermo physical properties of nanofluids.

Since Choi's work in 1995, the published work regarding nanofluids has grown at an average rate of 32 percent per year for the past five years. The term nanofluid was originally coined in the thermal science community and therefore heat transfer and thermal science journals comprise a significant fraction of the articles which discuss nanofluids. Much of the research that has been done on nanofluids pertains to the thermal properties while only a small fraction (estimated at 5% (based on a 2012 Google scholar search) is focussed on synthesis, stability, antibacterial activity, photo-catalytic properties, and a few other miscellaneous topics (Taylor et al., 2013).

1.2 Objectives

This work is aimed at studying the stability of nanofluids. As is evident from the above discussion that very less research has been done in this area and the research is contradictory and inconclusive. It is apparent that different systems of nanoparticles and base fluids behave differently and extensive investigation is required to understand the exact mechanics and formulate theories that justify and explain the different behaviours. How particle agglomeration affects the various properties of interest such as thermal conductivity for different nanoparticles and base fluids is still a conundrum and unless it is solved, the use of nanofluids in various flow based cooling applications shall remain questionable.

It is also important to define the term stability. Stability can be discussed under two headings: particle agglomeration and particle settling. While it seems obvious that particle agglomeration and increase in particle size should lead to settling down of the particles and prove to be a hindrance, however in some cases particle aggregation seems to be a likely cause of enhancement of thermal conductivity. If that is the case then there must be an optimum size of particles which could lead to increase in thermal conductivity while allowing the particles to stay suspended and not settling down as a result of aggregation. In that case stability should be defined as keeping the particle size at an optimum fixed value without any further aggregation so that it stays suspended as well as leads to enhancement in the thermal conductivity of the base fluid on addition of nanoparticles.

CHAPTER 2: LITERATURE REVIEW

This chapter consists of a detailed study of nanofluids, the various materials that make up nanoparticles and the base fluids that are used, the methods of synthesis of nanoparticles and nanofluids, the measurement techniques that are used to measure various parameters that are used to study the nanofluids such as stability and thermal conductivity, characterization techniques and a review of the experimental work that has been done by other researchers.

2.1 Nanonofluid preparation and stability

A nanofluid can be defined as a uniform dispersion of solid particles whose diameters are in nanometres (1000 times smaller than micrometres). As compared to the suspensions of micro sized particles, nanofluids offer more advantages as these are more stable and less likely to cause abrasion and clogging in the system. The concept of nanofluids can be explained under the following subheadings.

a) The nanofluid system - It includes the base fluid and the nanoparticles that make up the nanofluid system. Theoretically, any solid nanoparticle that has higher thermal conductivity than the base fluid can be used so that the suspension has an increased net thermal conductivity. The nanoparticles that have been used can be classified as:

1) Metallic particles (Cu, Al, Fe, Au and Ag)

2) Non-metallic particles (Al_2O_3, CuO, Fe_3O_4, TiO_2 and SiC)

3) Carbon nanotube

4) Nanodroplets (Yang and Han, 2006).

In addition to the above materials for nanoparticles, completely new materials and structures, such as materials doped with molecules in their solid-liquid interface structure, may also have desirable characteristics. The base fluids that are commonly used are water, ethylene glycol, oil, acetone, decene. Presently, the use of nanofluids for enhancement of heat transfer is at an experimental stage and cannot be used in any practical heat transfer application. However while choosing nanoparticles and base fluids, the following points must be considered:

(i) The system must be electrically non-conductive

(ii) The system must have high thermal and heat transfer properties.

(iii) The system must have high density and specific heat so that lesser volume of coolant is required to be circulated to provide cooling.

(iv) The system should have low viscosity so that lesser pumping power is exerted.

(v) The system should be non corrosive

(vi) The nanofluid system should be stable.

(vii) No flammability and toxicity. (Li et al., 2009)

b) Preparation of nanofluids - Under this the various methods employed to synthesize a nanofluid shall be discussed. Two kinds of methods have been employed to produce nanofluids. One is a single step method and the other is a two step method. The single step method is where the synthesis of nanoparticles as well as the nanofluid is done in a single step. Argonne laboratory developed a one-step nanofluid production system in which nanoscale vapour from metallic source material can be directly dispersed into low vapour pressure fluids (Eastman et al. 2000). This one step process was developed to overcome the van der Walls forces between the nanoparticles and produce stable suspensions of Cu nanoparticles without any dispersants but a disadvantage of this method is that only low vapour pressure fluids are compatible with the process which limits the application of the process (Li et al., 2009). Another one-step physical process is wet grinding technology with bead mills (Chopkar et al. 2006). One step chemical methods for producing stable metallic nanofluids have been developed using a chemical reduction method (Zhu et al., 2006). Also, Ag-water nanofluids were produced using one step optical laser ablation in liquid (Phuoc et al. 2007). In the one step method of preparation of nanofluids the process of drying, storage, transportation and dispersion of nanoparticles are avoided, so the agglomeration of nanoparticles is minimized and the stability of nanofluids is increased. The disadvantage associated with this method is that it is difficult to produce nanofluids in bulk.

A one step method that was reported in a research (Hwang et al. 2007) is the Modified Magnetron sputtering System. It consists of a vacuum chamber and the vacuum in the chamber was pumped down to $1x10^{-6}$ torr by a diffusion pump. After filling the

chamber with Argon (Ar) gas up to a desired gas pressure, a constant Ar gas flow ranging from 15 to 50 cm^3/min was adjusted. The sputtering Ar gas pressure was fixed to 10^{-2} torr for producing Ag nanoparticles. The target substrate was a rotating drum dipped into the reservoir of silicon oil. The rotational speed was varied from 0 to 10 rpm. The distance between Ag sputtering target and drum was fixed to 8 centimetres. The Ag particles sputtered directly dispersed in the thin film of silicon oil formed on the rotating drum. To avoid the agglomeration of the Ag particles the Oleic acid (1 wt%) is dissolved in the base fluid prior to the sputtering process.

In the two step method for preparing nanofluids the nanoparticles, nanotubes or nanofibers are first produced as a dry powder by physical or chemical methods and then the task of dispersing them in base fluid is carried out separately. This method is commercially more viable as a number of companies supply nanopowders and it is easy to prepare nanofluid in bulk with the two step method. The two step technique is said to work well for oxide nanoparticles as compared to metallic nanoparticles (Ghadimi et al. 2011). The major problem with two step method is aggregation of nanoparticles. It has been shown that particles strongly aggregated before dispersion are still in an aggregated state after dispersion in ethylene glycol and 9 hours of sonication (Kwak and Kim, 2005). Ultrasonic equipment is used to intensively disperse the particles and reduce agglomeration. Apart from that the use of other techniques such as control of pH or addition of surface active agents is made to avoid agglomeration and sedimentation (Das et al. 2006).

c) Stability of nanofluids - The nanoparticles suspended in a base fluid tend to agglomerate and settle down which is a limitation and one of the reasons due to which the nanofluids cannot be used commercially. In the stationary state, the sedimentation velocity of small spherical particles in a liquid follows the Stoke's law.

$$V = \left(\frac{2R^2}{9\mu}\right)(\rho p - \rho l).g \qquad (2.1)$$

where 'V' is the particle's sedimentation velocity; 'R' is the spherical particle's radius, 'μ' is the liquid medium viscosity, 'ρ_p' and 'ρ_l' are the particle and liquid density and g is the acceleration due to gravity. This equation reveals a balance of the gravity, buoyancy force, and viscous drag that are acting on the suspended nanoparticles. According to Eq. (1), the following measures can be taken to decrease the speed of nanoparticles' sedimentation in nanofluids, and henceforth to produce an improvement for the stability of the nanofluids: (1) reducing R, the nanoparticles size; (2) increasing μ, the base fluid viscosity and (3) lessening the difference of density between the nanoparticles and the base fluid ($\rho_p - \rho_l$). Clearly reducing the particle size should remarkably decrease the sedimentation speed of the nanoparticles and improve the stability of nanofluids, since V is proportional to the square of R. According to the theory in colloid chemistry, when the size of particle decreases to a critical size, R_c, no sedimentation will take place because of the Brownian motion of nanoparticles (diffusion) (Ghadimi et al. 2011).

To determine whether Brownian motion would keep the particles suspended or if the particles would sediment depends on the Peclet number. The Peclet number can be defined as follows:

$$Pe = \frac{V.R}{D} \quad (2.2)$$

where ‘v’ is the terminal velocity given by Stoke’s law (eq. 2.1), ‘R’ is the particle radius and ‘D’ is the diffusion coefficient.

$$D = \frac{kBT}{6\pi\eta R} \quad (2.3)$$

where ‘D’ is the diffusion coefficient, ‘k_B’ is the Boltzmann constant, □ is the dynamic viscosity and ‘R’ is the particle radius.

Substituting the values of ‘V’ and ‘D’ from equations 2.1 and 2.3 respectively in equation 2.2, we get the expression for Peclet number as:

$$Pe = \frac{[4\pi(\rho_p - \rho_l)gR^4]}{3k_B}T \quad (2.4)$$

The Péclet number, ‘Pe’, can be interpreted as a ratio of energy, ‘E_{sed}’, gained by a particle with buoyant mass, ‘m’, settling at a distance equal to its radius, ‘R’, in the gravity field, i.e.:

E_{sed} = mgR

$$= \left(\frac{4}{3}\right)\pi(\rho_p - \rho_l)R^3.g.R \quad (2.5)$$

to the thermal energy, E_{therm} = kT. Thus, if Pe >> 1, the effect of the brownian motion is negligible. It follows from equation 2.4 that the critical value of the sphere radius, 'R', i.e. a value that yields Pe = 1, is:

$$R = \sqrt[4]{\left[3kB\frac{T}{4\pi(\rho p \quad \rho l)g}\right]} \tag{2.6}$$

However, smaller nanoparticles have a higher surface energy, increasing the possibility of the nanoparticle aggregation. Thus, the stable nanofluid preparation strongly link up with applying smaller nanoparticles to prevent the aggregation process concurrently (Ghadimi et al., 2011).

The agglomeration of nanoparticles may result in settlement and clogging of microchannels and it also decreases the thermal conductivity of nanofluids thereby defeating the main purpose. It is therefore a key issue and hence needs to be investigated.

2.2 Nanofluid characterization and stability inspection techniques

2.2.1 Characterization of nanofluids

Characterization of nanoparticles once they have been synthesised allows looking into the structure of the nanoparticles and forms an important part of research. Good methods for characterizing nanofluids are critical to a correct understanding of their novel properties. The particle size is a very important factor that needs to be taken

into consideration in the study of nanofluids for the following reasons. Firstly, particle size matters in making nanofluid stable. Dense nanoparticles can be suspended in liquids because the particles have an extremely high ratio of surface area to volume so that the interaction of the particle surface with the liquid is strong enough to overcome differences in density (i.e. the gravity effect is negligible). Secondly, size matters in making nanofluids with novel properties. Thirdly, particle size matters in making nanofluids useful in some applications. Since the size of nanoparticles is similar to that of bio-molecules, nanofluids can be used in bio-medical applications such as drug delivery and nanofluids based control of biological functions (Choi, 2009). Following is a description of the various techniques that are used for the nanofluid characterization.

(1) X-Ray Diffraction Analysis: X-Ray diffraction is a technique that helps in inferring the material of the unknown structure that is being tested. It is a fast technique and works on the principle that when X-rays are directed on the sample, the electrons present in the material scatter the X-rays. This creates a pattern of maxima and minima which can be used to identify the material of the structure being investigated. This technique uses the Bragg's Law that gives the condition for two X-rays to be in phase with each other which is also termed as 'constructive interference'. If the rays are not in phase then destructive interference occurs reducing the intensity of reflected rays to zero. Bragg's Law can be mathematically written as $n\lambda = 2D \sin\theta$. Here 'λ' is the wavelength, 'θ' is the angle through which the X-rays are diffracted, 'D' is the distance between crystal lattice planes. As we can see, for each lattice spacing 'D', the above equation predicts a maximum at diffraction angle 'θ'. An X-

ray diffraction pattern is obtained when the intensity of detected X-rays is plotted as a function of diffraction angle 'θ'. This plot is matched with that of a pure substance hence confirming the characteristic of the sample material. In a two step process of synthesis of nanofluids, once the nanoparticles are prepared they undergo the X-Ray Diffraction Analysis in order to confirm composition of the nanoparticles.

(2) Scanning Electron Microscopy: A scanning electron microscope (SEM) is a type of electron microscope that produces images of a sample by scanning it with a focused beam of electrons. The electrons interact with electrons in the sample, producing various signals that can be detected and that contain information about the sample's surface topography and composition. Accelerated electrons in an SEM carry significant amounts of kinetic energy, and this energy is dissipated as a variety of signals produced by electron-sample interactions when the incident electrons are decelerated in the solid sample. These signals include secondary electrons (that produce SEM images), backscattered electrons (BSE), diffracted backscattered electrons (EBSD that are used to determine crystal structures and orientations of minerals), photons (characteristic X-rays that are used for elemental analysis and continuum X-rays), visible light (cathodoluminescence--CL), and heat. Secondary electrons and backscattered electrons are commonly used for imaging samples: secondary electrons are most valuable for showing morphology and topography on samples and backscattered electrons are most valuable for illustrating contrasts in composition in multiphase samples (i.e. for rapid phase discrimination). X-ray generation is produced by inelastic collisions of the incident electrons with electrons in discrete orbitals (shells) of atoms in the sample. As the excited electrons return to

lower energy states, they yield X-rays that are of a fixed wavelength (that is related to the difference in energy levels of electrons in different shells for a given element). Thus, characteristic X-rays are produced for each element in a mineral that is "excited" by the electron beam. SEM analysis is considered to be "non-destructive"; that is, X-rays generated by electron interactions do not lead to volume loss of the sample, so it is possible to analyse the same materials repeatedly. This technique is useful in finding the size of the nanoparticles before they are suspended in the nanofluid. It is useful in capturing clusters of nanoparticles.

(3) Transmission Electron Microscope: As opposed to a light microscope, the wavelength of illumination that is produced by an energized beam of electrons in TEM increases greatly the resolving capabilities. So, the main use of this technique is to examine the specimen structure, composition or properties in sub-microscopic details. There are essentially three types of lenses used to form the final image in the TEM. These are the condenser, objective, and projector lenses. The mean function of the condenser lens is to concentrate and focus the beam of electrons coming off of the filament onto the sample to give a uniformly illuminated sample. The objective lens and its associated pole pieces is the most critical of all the lenses. It forms the initial enlarged image of the illuminated portion of the specimen in a plane that is suitable for further enlargement by the projector lens. Finally, one uses the projector lens to project the final magnified image onto the phosphor screen or photographic emulsion. It is in the projector lens that the majority of the magnification occurs. Thus total magnification is a product of the objective and projector magnifications. For higher magnifications an intermediate lens is often added between the objective and projector lenses. This lens serves to further magnify the image. The image is then

projected onto either the fluorescent screen or onto the photographic film. This technique is also useful in finding the size of nanoparticles before they are suspended in the fluid.

Both the SEM (Scanning electron microscopy) and TEM (Transmission electron microscopy) can be used to distinguish the shape, size and distribution of dry nanoparticles. However, they cannot show the real situations of nanoparticles while they are suspended in the fluid. Cryogenic electron microscopy (Cryo-TEM, Cryo-SEM) might provide a method to resolve this problem if the microstructure of nanofluids is not changed during cryoation (Ghadimi et al. 2011). The following procedure is attributed to the standard SEM/TEM micrographs of nanoparticles:

1). Obtain stable nanofluid in solution form.

2). Drop one drop of the solution on sticky tape of top surface of the SEM specimen holder (carbon grid in case of TEM).

3). Heat in the vacuum oven to dry the liquid drop or dried in the air naturally.

4). Obtain solid particle.

5). Bring into the vacuum chamber of SEM/TEM picture after coating with Au and Pd (Liu et al., 2006).

2.2.2 Stability Inspection

The various methods that can be used for stability inspection are as follows:

(1) UV Vis Spectrophotometer: An UV vis spectrophotometer exploits the fact that the intensity of light becomes different by absorption and scattering of light passing through a fluid. At 200–900 nm wavelength, the UV–Vis spectrophotometer measures the absorption by liquid and is used to analyze various dispersions in the fluid. Typically, suspension stability is resolved by measuring the sediment volume versus the sediment time. However, this method is unsuitable for nanofluid dispersions with a high concentration and especially for CNT solutions. These dispersions are too dark to differentiate the sediment visibly. In this method, the first step is to find the peak absorbance of the dispersed nanoparticles at very dilute suspension by scanning. As the concentration of suspension has a linear relation with absorbance, preparing a standard to fit a linear relation to at least three different dilute concentrations (0.01–0.03%) will be the next step in this method. Relative stability measurement will be followed by preparing the desired concentration of nanofluid and put aside for a couple of days. Whenever it is needed to check the relative stability, the supernatant concentration will be measured by UV–Vis spectrophotometer and the concentration can be plotted against time (Hwang et. al., 2006). Thus, we can find the concentration of a nanofluid this way.

(2) Zeta Potential Test: Zeta potential measurement is one of the most critical tests done to investigate the stability of a nanofluid via a study of its electrophoretic behaviour. The zeta potential (ZP) is a function of the surface charge which develops

when any material is placed in a liquid. It is an index of the magnitude of the electrostatic repulsive interaction between particles. The ZP is commonly used to predict and control dispersion stability (Weiner et al., 1993). A higher value of Zeta potential is an indicator of better stability of suspensions. The Zeta potential is measured by the technique of Electrophoretic Light Scattering (ELS). The values of the Zeta potential (ζ) can be calculated by the Helmholtz-Smoluchowski equation (Hwang et. al., 2006)

$$\zeta = \mu . \frac{U}{\varepsilon} \qquad (2.7)$$

where 'U' is the electrophoretic mobility and 'μ' and 'ε' are the viscosity and the dielectric constant of the liquid in the boundary layer, respectively. According to one study (Hwang et. al. 2006) the measured Zeta potential of the carbon black nanoparticles suspended in water without surfactant prepared by the ultrasonic disruptor was found to be -1.27 mV at pH 7.5. However, with the simple addition of the SDS (1 wt%) the Zeta potential of the CB nanoparticle fluid was significantly reduced to -26.25 mV at the same pH level of 7.5. This indicates that the addition of SDS in CB nanofluid promotes the stabilization.

Another study (Wang et. al., 2009) has reported that the greater the Zeta potential the smaller the particle size. Studies show a definite relation between particle size and the Zeta potential and hence the need for addition of surfactants that increase the (absolute value of) Zeta Potential is justified.

According to another study (Vandsburger, 2009), the typically accepted Zeta potential values are greater than 30.

(3) Sediment photo Capturing: Another method which is easy and uncomplicated is photo capturing. After preparation, some amounts of the suspension is left to be captured by photos after certain intervals of time. A suspension which is less stable is likely to appear clearer than others as the suspended particles settle down (Wei et al. 2009). However this method does not give us an absolute result, it only gives information about the relative stability of nanofluid samples.

(4) Light Scattering Method: The single particle analysis from which the light scattering theory can be approached has been used to visualise polymer molecule structure in solutions or colloidal particles in suspension. The intensity of scattered light for a single particle is related to the particle volume (Ghadimi et al. 2011)

(5) Sedimentation balance method: This is another method to measure the stability of a nanofluid. In this method the tray of a sedimentation balance is immersed in the fresh nanosuspension. The weight of the sediment nanoparticles is measured after some time. The suspension fraction (F_s) of nanoparticles at an accepted time is calculated by the formula $F_s = (W_0 – W)/W_0$ in which W_0 is the total weight of the nanoparticle and W is the weight of the sediment nanoparticles at a certain time (Zhu et al. 2007).

(6) Three Omega Method: The 3ω method is widely used to measure the thermophysical properties of thin films and solid substrates (Jacquot et al. 2002). A sinusoidal electric current with an angular frequency of ω is passed through a thin film metal heater patterned on the solid substrate of interest. The metal heater also acts as a thermometer. Due to the sinusoidal heating at a double the frequency of the input current, the metal temperature also oscillates at an angular frequency of 2ω. Since the electrical resistance of the metal heater is a linear function of temperature, the temperature oscillation can be measured indirectly by measuring the associated 3ω voltage across the metal heater. The amplitude and phase of the temperature oscillation can be used to determine the thermo-physical properties of the substrate since these parameters are related to each other through the solution of the energy equation for the given geometry and set of boundary conditions. (Dong Wook Oh et al. 2008). In this work, the original method is extended for use in the case of heat transfer in parallel through two semi-infinite media. The nanofluid of interest is placed on a quartz substrate on which a thin metal heater is attached.

2.3 Stabilisation techniques

(1) Addition of Surfactant or activator: It is one of the most common methods to avoid sedimentation in nanofluids. The mechanism behind the observed stability enhancement is that the hydrophobic surfaces of the nanoparticles are modified to become hydrophilic or vice versa for non aqueous liquids. Hydrophilic particles are more likely to stay suspended in water for a longer time. A repulsion force between suspended particles is caused by the zeta potential which will rise due to the surface charge of the particles suspended in the base fluid indicating a more stable

suspension. The surfactant added must be adequate enough to counter the Van der Walls force of attraction between the particles. Particle size decreases with the addition of the surfactant which is SDBS (sodium dodecylbenzenesulfonate) according to study (Wang et al. 2009).

Popular surfactants that have been used in literature can be listed as sodium dodecylsulfate (SDS), sodium dodecylbenzenesulfonate (SDBS), salt and oleic acid, cetyltrimethylammoniumbromide (CTAB), dodecyl trimethylammonium bromide (DTAB) and sodium octanoate (SOCT), hexadecyltrimethylammoniumbromide (HCTAB), polyvinylpyrrolidone (PVP) and Gum Arabic (Ghadimi et al., 2011).

(2) pH Control: The stability of an aqueous solution also depends on the pH of the solution. However, the optimum pH is different for different nanoparticles. The optimum pH is where the absolute value of the Zeta potential is the maximum. Lee worked on different pH of nanofluids with Al_2O_3. The experiments indicated that when the nanofluid had a pH of 1.7, the agglomerated particle size was reduced by 18% and when the nanofluid had a pH of 7.66, the agglomeration size was increased by 51% (Lee et al., 2009).

(3) Ultrasonic Vibration: All the above methods aim at changing the surface properties of nanoparticles in order to make the suspensions stable and to suppress forming of clusters. Ultrasonic bath, processor and homogenizer are powerful tools for breaking down the agglomerations as compared to magnetic and high shear stirrer as experienced by researchers (Ghadimi et al. 2011). In another research (Hwang et al. 2007) an experimental study on the homogeneous dispersion of nanoparticles in

nanofluids is presented. The samples differed in their treatments, those which were based on two step method included stirrer, ultrasonic bath, ultrasonic disruptor and high pressure homogenizer as techniques used to stabilise them. Out of these techniques the stirrer, ultrasonic bath, ultrasonic disruptor were found to do a poor performance in de-agglomeration process for the initial particle clusters. However the high pressure homogenizer produced the average diameter of the carbon black and Ag particles of 45 nm and 35 nm respectively, initially the particles had agglomerated to a diameter of 330 nm to 585 nm. Another nanofluid with much smaller nanoparticles was synthesised employing a modified magnetron sputtering system, in which the sputtered nanoparticles were designed to directly mix with the running surfactant - added silicon oil thin film formed on a rolling drum (a one step method). The nanoparticles were homogeneously dispersed and long term stable in the silicon-oil based fluid and the average diameter of Ag nanoparticles was found to be ~ 3nm, indicating that the modified magnetron sputtering system is also an effective one step method to prepare stable nanofluids.

High pressure homogenizer: It consists of two micro-channels dividing a liquid stream into two streams. Both the divided liquid streams were then recombined in a reacting chamber. Here the significant increase in the velocity of pressurized liquid streams in the micro channels resulted in the formation of cavitations in the liquid. The high energy of cavitations was used to break the clusters of nanoparticles.

2.4 Measurement of Thermal Conductivity

This section consists of a brief history of the measurement of thermal conductivity and other properties of water and discussion on the conduction heat transfer and the various methods to measure thermal conductivity of liquids.

The measurement of thermal conductivity of water is very tricky. Water is not a viscous fluid due to which there is always a possibility of setting up of natural convection giving rise to faulty readings. In 1963, the Sixth International Conference on Properties of steam was held in Providence and New York and a panel was elected which came up with the First International Formulation for the viscosity and thermal conductivity of fluid H_2O. In 1968, the seventh conference was held on the properties of steam in Tokyo which authorized the creation of an International Association for

Properties of Steam (IAPS). In the next 15 years IAPS coordinated an active international research program with the goal of obtaining improved formulations for thermo-physical properties of both ordinary and heavy water. In 1974, Eighth International Conference on the properties of steam established a special committee for the purpose of preparing new formulations for viscosity and thermal conductivity of water substance. In 1975, IAPS issued a document “Release on Dynamic Viscosity Of water substance” and in 1977, IAPS issued “Release on thermal conductivity of water substance”. Equations for viscosity and thermal conductivity yield these transport properties as function of temperature. One needs an equation of state to

convert the pressure into density. Both the 1975 and 1977 releases were based on the IFC 68 formulation for Scientific and General Use. In 1979, Ninth International Conference on Properties of steam was held in Munich which empowered executive committee of IAPS to issue, among others, a release on thermodynamic properties of ordinary water substance for the purpose of replacing the IFC 68 Formulation for scientific and General Use and also to issue a release on the thermodynamic properties of heavy water substance. Following recommendations of working group, IAPS amended the 1977 releases in 1982 so as to make them consistent with the Provisional IAPS formulation 1982 for the thermodynamic properties of ordinary water substance for Scientific and General Use which suspended IFC 68 formulation. In 1982 the executive committee of IAPS adopted a Provisional IAPS formulation for thermodynamic properties of Ordinary Water substance for Scientific and General Use and a Provisional IAPS formulation 1982 for the Thermodynamic Properties of Heavy water substance. These formulations were based on fundamental equation for the thermodynamic properties of H_2O developed by Haar, Gallagher & Kell and a fundamental equation for the thermodynamic properties of D_2O developed by Hill, McMillan and Lee. In the period after 1982, it became increasingly evident that some improvements could be made in the formulations for the viscosity and thermal conductivity of Ordinary water substance. While the transport properties adopted in 1975 and 1977 were valid from 0 to 800^0C and up to 100 MPa pressure, the IAPS formulation 1984 is valid in a wider range of temperature and pressure. Using improved methods for statistical analysis of data, Watson and co-workers had noted that the number of terms in the international equation for viscosity could be reduced significantly while also obtaining an improved agreement with the experimental data. Thus it can be seen that the accurate measurement of thermal conductivity has been a

matter of research for decades and a lot of research and effort has been dedicated to it. Also, with the improvement in instruments and statistical techniques, more accurate predictions for the property of thermal conductivity have been reached. (Sengers and Watson, 1986)

Conduction is one of the three modes of heat transfer, the other two being convection and radiation. In reality, there is seldom a process with just one pure mode of heat transfer. However, one mode of heat transfer may be dominant enough that the other modes can be neglected. In conduction, heat is transferred due to molecular vibration. It does not involve any movement of the medium.

The conduction in any medium is guided by the Fourier's Law according to which the direction of heat flow is proportional to the temperature gradient in that direction. Mathematically, it can be expressed as

$$q_x = \frac{Q_x}{A} = -k\left(\frac{dT}{dx}\right) \qquad (2.8)$$

where 'q_x' is the heat flux in the x direction, 'Q_x' is the heat flowing in the x direction, 'A' is the area perpendicular to x through which it flows and 'k' is the constant of proportionality known as the thermal conductivity of the medium. The thermal conductivity is a measure of the capability of a medium to conduct heat, it is always

positive. Hence it is necessary to intrioduce a negative sign because the quantity dT/dx is negative (since the temperature decreases in the direction of heat flow).

From the above, it can be seen that thermal conductivity depends on the material and the temperature of the material. Solid metals have the highest values of thermal conductivity followed by liquid metals, non-metallic solids, non-metallic liquids, insulating materials, non-metallic gases and evacuated insulating materials. Free electrons form the carrier of heat in metallic solids and liquids, electrons and phonons form the carrier of heat in non metallic solids and liquids, atoms and molecules carry heat via conduction in gases (Das et al., 2007). There are two types of conduction:

(a). Steady Conduction: It deals with heat flow under steady conditions where temperatures vary along space coordinates but do not change with time. Examples of steady state conduction include conduction through a slab of uniform thickness or a hollow cylinder or a composite cylinder (Das et al., 2007).

(b). Transient Conduction: In many practical problems of heat flow, the temperatures of a medium vary along both space and time coordinates. These situations are designated as transient or unsteady conduction. Such cases are of immense practical importance. The majority of thermal conductivity measurements in nanofluids are carried out with a transient hotwire method, where the mode of conduction is transient in nature. The simplest type of transient analysis is lumped parameter analysis, whose main assumption is that the temperature of a solid body is a function of time alone nad

not space. It means that the conductivity of the body is so high that the uniform body is at uniform temperature at any instant and heat transfer takes place between the body and the surrounding fluid only by convection. In this case the conduction equation is of no help because it is assumed that the body has an infinitely large thermal conductivity. In most applications, the lumped parameter assumptions are not valid, so analysis has to be carried out with temperature as a function of both space and time. The simple case of one-dimensional transient conduction can be used on geometries such as slab, cylinder, or sphere, which are important in practice (Das et al. 2007).

The various methods used to measure the thermal conductivity are discussed below including the design of apparatus and its fabrication and the experimental procedure. There are two types of methods of measuring thermal conductivity of liquids: Steady-state methods and transient methods. The disadvantages of steady-state methods are that the heat loss cannot be quantified and may give considerable inaccuracy and natural convection may set in which gives higher apparent values of conductivity (Das et al. 2007). The various techniques used to measure the thermal conductivity are as follows:

2.4.1 Transient Hot Wire Method

Principle: It is one of the most widely used methods for the measurement of thermal conductivity. In this method a thin metallic wire is used as both a line heat source and

a temperature sensor. The wire is surrounded by the liquid whose thermal conductivity is to be measured. The wire is then heated by sending a current through it. Now, the higher the thermal conductivity of the surrounding liquid, the lower will be the temperature rise of the wire. This principle is used to measure the thermal conductivity. The experiment lasts for a maximum of 2 to 8 seconds, hence it is very fast, and in such a brief duration, natural convection cannot set in. Hence, in conjunction with advanced electronic data acquisition equipment, the method gives very accurate values of thermal conductivity.

An infinitely long line heat source is suspended vertically in the liquid whose thermal conductivity is to be measured. The method is called transient because heat is supplied suddenly, so that eventually the wire gets heated. The working equation is based on a specific solution of Fourier's law for radial (one dimensional) transient heat conduction with a line heat source at the axis of the cylindrical domain. The thermal conductivity of the liquid is given by the following equation:

$$k = \left[\frac{q}{4\pi (T_2 - T_1)}\right] x \ln(t_2/t_1) \qquad (2.9)$$

where 'q' is the heat liberated per unit time per unit length of the light source in W/m and 'k' is the conductivity of the liquid in W/mK and T_1 and T_2 are the temperatures of the heat source are at times t_1 and t_2 (Das et al. 2007).

Experimental Setup and Procedure: In a typical experimental setup for measuring thermal conductivity of nanofluids by the transient hot wire method a wire is placed along the axis of the cell, which will be surrounded by the liquid whose thermal conductivity is to be measured. As the wire is to be used both for heating and for temperature sensing, the wire material generally chosen is platinum. Platinum has high electrical resistivity [i.e. 1.06×10^{-7} Ω.m (at 20 degree Celsius)] an order of magnitude higher than that of other metals. Also, it has a temperature coefficient of resistance of $0.0003925^{o}C^{-1}$. It is an ideal metal for temperature sensing because of its strictly linear variation of resistance over a large temperature range. The wire is to be used as a line heat source, so that the wire diameter is kept within 100μm. The length of the wire is kept to just a few centimetres, which compared to the wire diameter represents an infinitely long line heat source, assuring one directional (radial) heat transfer (Patel et al. 2003). The platinum wire is 15 cm in length. The surrounding fluid acts as a semi-infinite medium. For this, a cylindrical cavity 2cm in diameter and 15 cm in length is provided, which will be filled with fluid whose thermal conductivity is to be measured. Because the experiment lasts for just 4 to 5 seconds and total quantity of heta going into liquid per second is very small (maximum of 0.75J), the diameter of the container provided is sufficient to assume the liquid to be a thermally semi-infinite medium. The wire is soldered to a copper screw at one end and the copper strip at the other end. Both the screw and the strip are thick enough to provide the least electrical resistance. As the wire has to work simultaneously as line heating source and temperature sensor, it is made an arm of a Wheatstone Bridge circuit. The Wheatstone bridge is balanced before starting the experiment. A variable but stable voltage source is used to supply current. The electrical circuit is connected to the data acquisition system, which is connected to a computer (Das et al., 2007).

The constant-voltage source is connected to the grid lines. All the resistances are measured accurately. The platinum wire is heated by sending current through the Wheatstone bridge for 5 to 10 seconds. Data are acquired for voltage supplied by the voltage source as well as the voltage difference across the bridge at a small time interval (less than 40ms). The measurement cell can be immersed in a constant temperature bath to measure the thermal conductivity at high temperature. The natural log of the time (t) is plotted against the temperature of the wire, which is calculated from the data acquired. The initial portion of the graph, which is a straight line is chosen and its slope $[\ln(t_2/t_1)/(T_2-T_1)]$ is measured to calculate the thermal conductivity from the equation 2.9.

2.4.2 Transient short-hot-wire (SHW) method

Principle: Transient SHW technique is used to measure the thermal conductivity and thermal diffusivity of nanofluids simultaneously (Zhang et al., 2000). Zhang et al. (2000) explained the principle of operation of transient SHW technique in detail. Zhang et al. (2000) explained that (SHW) technique was developed from the conventional transient hot wire method. This technique is also based on the two-dimensional transient heat conduction numerical solution for a short wire of the same length-to-diameter ratio and boundary conditions as those used in the actual measurements. The thermal conductivity of nanofluids in transient SHW technique is calculated by equation 2.2 (Zhang et al. 2000):

Coefficient E is calculated by the least-squares method for a relevant range of Fourier number corresponding to the periods of measurement. Coefficient E is also

determined by the least squares method for time range before the onset of natural convection.

Experimental Setup and Procedure: To explain the working of this method specification of Zhang et al. (2000) are considered. Figure 2.1 shows the schematic of transient SHW cell. The SHW probe is set on the Teflon cap of the cell. A short platinum wire of 9.2 mm length and 97 micrometer diameter (1) is welded at the both ends to 1.5 mm diameter platinum lead wire (3) which is supported by a ceramic circular plate (2) and joined with voltage (5) and current (6) platinum lead wires of 0.5 mm diameter. A pure gold crucible (4) of 50 mm diameter and 120 cm^3 volume is heated with an electric furnace (8) which is outside covered with a thermal insulator (9). The temperatures at the outside wall of crucible are measured with thermocouples (7) to give a feedback signal for the temperature controller. The measurements have to carry at atmospheric pressure and different temperature levels. Platinum wire is welded to the platinum lead terminals. Alumina is used as a coated material which is 99.99% pure. The sputtering time is 6.4 h for Al_2O_3 film thickness of 2 micrometer. Sputtering apparatus provide a thin uniform film on the cylindrical wire. The measuring system of SHW technique is also shown in Figure 2.2. Measuring system is composed of a dc power supply current and voltage measuring system, digital multimeter, power input/output (PI/O) controller and personal computer. A maximum constant current of 1 A with 1.5 mA resolution cab be generated by power supply. When the liquid temperature becomes uniform and constant, a small current of 15 mA, is supplied to the probe for 3 s for the measurement of initial temperature of liquid. The switch is turned on to the dummy circuit. Dummy circuit is having the same resistance as the main circuit including the probe. A heating current of 0.3 to 0.5

A is supplied. When the current becomes stable (after 1 s,), the switch is closed to the main circuit to begin heating the hot wire. In this process, the voltage and current are measured 20 times per sec. All the measurements are carried out automatically using a personal computer.

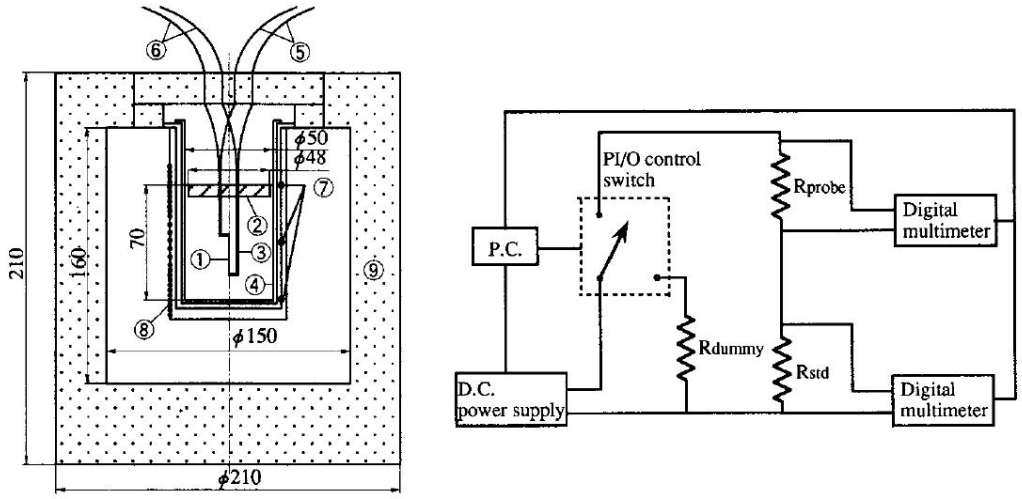

Figure 2.1: Schematic of experimental setup and measurement system by Zhang et al. (2000)

2.4.3 Temperature Oscillation Method

Principle: The principle of measurement of thermal conductivity in this method is based on the propagation of a temperature oscillation inside a cylindrical liquid volume. The measurement of thermal diffusivity and thermal conductivity is based on the energy equation for conduction:

$$\left(\frac{1}{\alpha}\right)\left(\frac{\partial T}{\partial \tau}\right) = \nabla^2 T \qquad (2.10)$$

In the present case this equation is applied with the assumption that the test fluid is isotropic and the thermo physical properties are uniform and constant with time throughout the entire specimen volume (Das et al. 2007).

Experimental Setup and Procedure*:* The experimental setup is shown in figure 2.2. It is a modification of technique used by Czanetzky and Roetzel (1995). The technique requires a specially fabricated test cell (1) which is cooled by cooling water (2) on both of the ends coming from a thermostatic bath (3). An electrical connection provides dc power obtained through a converter (4) to the Peltier element. The temperatures are measured in the test section (discussed later) through a number of thermocouples, and the responses are amplified using an amplifier (5) followed by a filter, which is finally fed to a data acquisition system (6) comprising a card for logging the data measured. The data logger is, in turn, connected to a computer (7). Fluid temperature control is effected by proper adjustment of the cooling water from the thermostatic bath. However, for higher temperatures it is sometimes necessary to increase the input voltage to attain the required temperature level, which is then fine-tuned to the required temperature by controlling the cooling water temperature.

The test section is a flat cylindrical shell. The cell is mounted with its axis horizontal. The frame of the cell is made of poly (oxymethylene), which acts as the first layer of

insulation. The frame consists of the main part with a 40 mm hole that acts as a cavity to hold the test fluid, and two end plates , which sandwich the water cooler and the Peltier element. The hole in the main frame is closed from both sides with disk type reference material 40 mm in diameter and 8 mm thick. The fluid is filled through a small hole in the body of the cell. Temperatures are measured at three locations: at the interface of the Peltier element and the reference layer, at the interface of the reference layer and the test fluid and at the central axial plane of the test fluid. For this purpose, Ni-CrNi thermocouples 0.1mm in diameter were used at the interfaces and those 0.5 mm in diameter were used at the central plane for stability considerations. The thermocouples at the interface are put in a small groove and welded at the tip, whereas the thermocouple at the center is hung from the wall. The central position of the thermocouple is ensured before placing the end reference plates. This is done through a precision measurement instrument. The entire cell is insulated. The temperature of the reference material is oscillated periodically by two Peltier elements (40mm * 40mm) from both ends. The temperature oscillations in this element are controlled to obtain two objectives:

(1). The oscillation amplitude is adjusted to keep it small (on the order of 1.5K) within the test fluid to retain constant fluid properties and to avoid natural convection and not allow amplitude to be decreased so much that the accuracy of the measurement was affected.

(2). The smaller amplitude and accurate adjustment of the mean temperature of oscillation ensures that for the conducting fluid, the test is made at the temperature selected (Das et al. 2007).

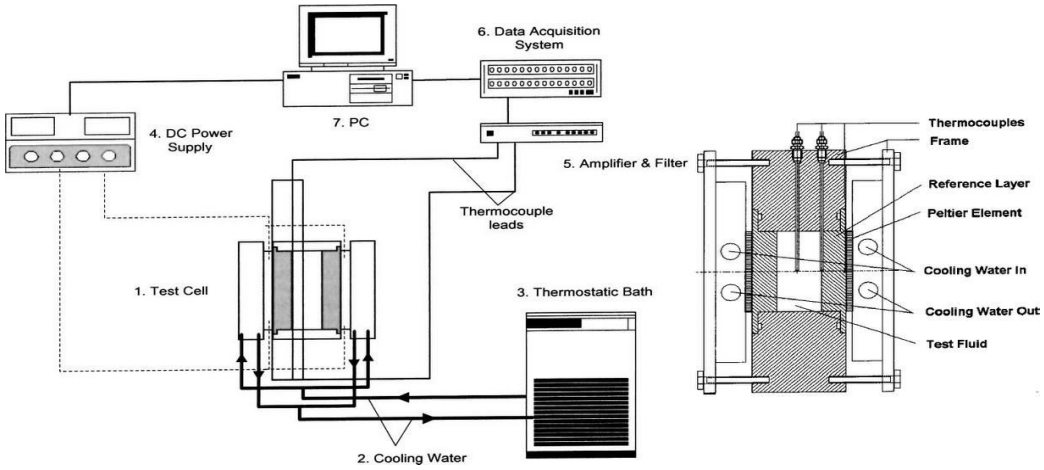

Figure 2.2: Schematic of experimental setup and test cell by Das et al. 2003

2.4.4 Steady-state parallel-plate method

Principle: This method is used to measure the thermal conductivity of nanofluids, this method requires very small amount of liquid sample. Wang et al. (1999) used this method to measure the thermal conductivity of Al_2O_3 and CuO nanofluids. Figure 3.5 shows the experimental setup. Fluid sample is placed between two parallel round copper plates. The surface of the fluid sample is slightly higher than the lower surface of upper plate. Any gas bubbles are avoided when fluid sample is filled into the cell. The cross-sectional area of the upper plate is 9.552 cm^2. Both the copper plates are separated by three small glass spacers. Each glass spacer is of 0.9652 mm in thickness and a total surface area of 13.76 mm^2. Liquid cell is housed in a larger aluminium cell

to control the temperature of liquid cell. The top copper plate is centred and away from the inside wall of the aluminium cell. There is a hole of 0.89 mm diameter is drilled in aluminium cell and copper plates. Temperature is measured by inserting E-type thermocouples (nickel–chromium/copper– nickel) into these holes. Because the thermal conductivity of copper is much higher than the thermal conductivity of the liquid, thermocouples provide temperatures at the surfaces of the plates. Total 14 thermocouples are used. At the time of experiment heater 1 gives the heat flux from upper plate to lower plate. Uniformity in temperature of the lower copper plate is maintained by heater 4. Heaters 2 and 3 are used to increase the temperature of the aluminium cell to that of the upper plate to eliminate radiation and convection losses from the upper copper plate. The temperature difference between the inside wall of the aluminium cell and upper copper plate is less than 0.05^{o}C, during all measurements. The uniformity of temperature in the top and the bottom plates is better than 0.02^{o}C. The difference of temperature between the two copper plates varies from 1 to 3^{o}C. All the heat supplied by heater 1 flows between both the copper plates. The overall thermal conductivity across the two copper plates, adding the effect of the three glass spacers, can be calculated by the one-dimensional heat conduction equation:

$$K = \frac{(P.X_g)}{(a_c \Delta T)} \qquad (2.11)$$

where X_g=0.9652mm, a_c=9.552 mm^2. Thermal conductivity of nanofluids is calculated by equation 2.12:

$$K_{nf} = \frac{K a_t - K_s a_g}{a_t - a_g} \qquad (2.12)$$

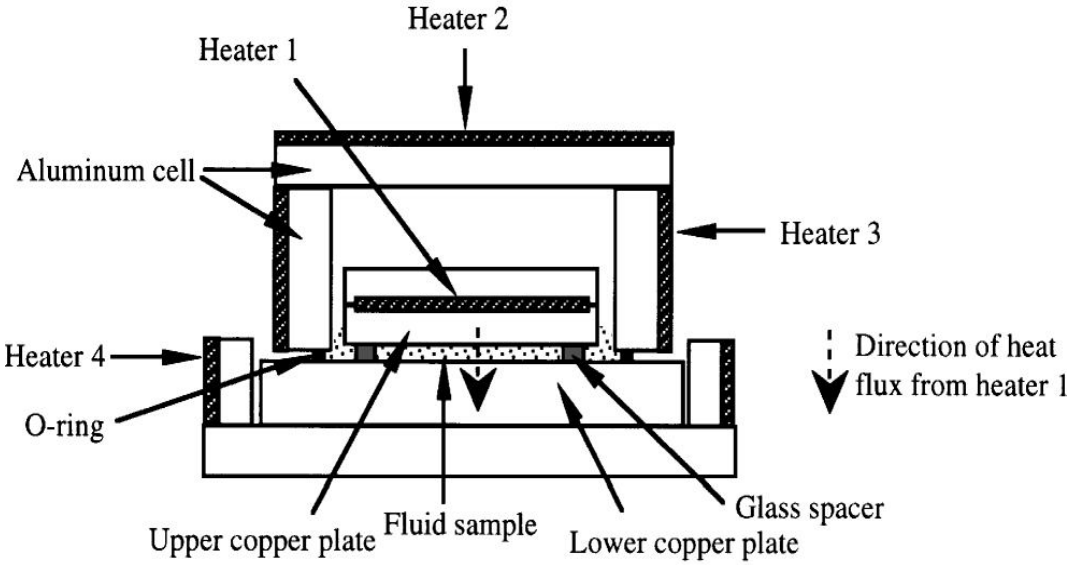

Figure 2.3: Schematic Of Experimental setup by Wang et al. (1999)

CHAPTER 3: AN EXPERIMENTAL INVESTIGATION INTO THERMAL CONDUCTIVITY AND STABILITY OF NANOFLUIDS

The study presents an investigation into the stability and thermal conductivity of nanofluids. The nanoparticles dealt here were of three kinds: silver nanoparticles, zinc oxide and carbon nanotubes. As already discussed, the nanoparticles can be broadly classified as metals, metal oxides and carbon nanotubes. The nanoparticles chosen for the present study are representatives of each category of nanoparticles. Also, since the present study involves measurement of thermal conductivity with KD2 Pro, this chapter involves a section on KD2 Pro and the correct technique that was reached by trial and error to measure the thermal conductivity of nanofluids with this instrument. The section lists the precautions that must be taken while measuring thermal conductivity and the results of the thermal conductivity measurement of water using the different set up. This chapter is therefore divided into four sections, the first section deals with measurement of thermal conductivity with KD2 Pro and the next three sections deal with silver, carbon nanotubes and zinc oxide.

3.1 Measurement with KD2 Pro

The KD2 Pro is a handheld device used to measure thermal properties. It consists of a handheld controller and sensors that can be inserted into the medium one wants to measure. The single-needle sensors measure thermal conductivity and resistivity;

while the dual-needle sensor also measures volumetric specific heat capacity and diffusivity (KD2 Pro Manual).

Specifications

Operating Environment:

Controller: 0 to 50 °C

Sensors: -50 to +150 °C

Power: 4 AA cells

Battery Life: At least 500 readings in constant use or 3 years with no use (battery drain in sleep mode < 50 uA)

Case Size: 15.5 cm x 9.5 cm x 3.5 cm

Display: 3 cm x 6 cm, 128 x 64 pixel graphics LCD

Keypad: 6 key, sealed membrane

Data Storage: 4095 measurements in flash memory (both raw and processed data are stored for download)

Interface: 9-pin serial

Read Modes: Manual and Auto Read

Sensors:

(1). 60 mm (small) single-needle (KS-1):

Size: 1.3 mm diameter x 60 mm long

Range: 0.02 to 2.00 W/(m· K) (thermal conductivity)

50 to 5000 °C·cm/W(thermal resistivity)

Accuracy (Conductivity): ± 5% from 0.2 - 2 W/(m· K)

±0.01 W/(m· K) from 0.02 - 0.2 W/(m· K)

Cable length: 0.8 m

(2). 100 mm (large) single-needle (TR-1):

Size: 2.4 mm diameter x 100 mm long

Range: 0.10 to 4.00 W/(m· K) (thermal conductivity)

25 to 1000 °C·cm/W (thermal resistivity)

Accuracy (Conductivity): ±10% from 0.2 - 4 W/(m· K)

±0.02 W/(m· K) from 0.1 - 0.2 W/(m· K)

Cable length: 0.8 m

(3). 30 mm dual-needle (SH-1):

Size: 1.3 mm diameter x 30 mm long, 6 mm spacing

Range: 0.02 to 2.00 W /(m· K) (thermal conductivity)

50 to 5000 °C·cm/W (thermal resistivity)

0.1 to 1 mm^2/s (diffusivity)

0.5 to 4 $mJ/(m^3K)$ (volumetric specific heat)

Accuracy: (Conductivity) ± 10% from 0.2 - 2 W/(m· K) ±0.01 W/(m· K) from 0.02 - 0.2 W/(m· K)

(Diffusivity) ±10% at conductivities above 0.1 W/(m· K)

(Volumetric Specific Heat) ±10% at conductivities above 0.1 W/(m·K)

Cable length: 0.8 m

Choosing a Sensor

The KD2 Pro comes with three separate sensors, each of which is designed for measurements in specific sample types.

KS-1

The small (60 mm long, 1.3 mm diameter) single needle KS-1 sensor measures thermal conductivity and thermal resistivity. It is designed primarily for liquid samples and insulating materials (thermal conductivity < 0.1 W (W/m· K)). The KS-1 sensor applies a very small amount of heat to the needle which helps to prevent free convection in liquid samples. However, the small size of the needle and typically short heating time make the KS-1 a poor choice for granular samples such as soil and powders where contact resistance can be an important source of error. In insulating materials, the errors from contact resistance become negligible making the KS- 1 sensor a good choice.

TR-1

The large (100 mm long, 2.4 mm diameter) single needle TR-1 sensor measures thermal conductivity and thermal resistivity. It is designed primarily for soil, concrete, and other granular or solid materials where an appropriate sized hole can be easily drilled or a pilot pin can be inserted (in the case of uncured concrete). The relatively large diameter and typically longer heating time of the TR-1 sensor minimize errors from contact resistance in granular samples or solid samples with pilot holes. The TR-1 needle heats the sample significantly more than the KS-1 sensor, which allows it to measure higher thermal conductivity samples (see specifications), but means that you should not measure liquid samples with the TR-1 sensor. The large diameter of the

TR-1 is more robust than the KS-1, meaning that it is less likely to be damaged by normal usage conditions in soil or other solid materials.

SH-1

The dual needle SH-1 sensor measures volumetric heat capacity, thermal diffusivity, thermal conductivity, and thermal resistivity. The SH-1 is compatible with most solid and granular materials, but should not be used in liquids due to the large heat pulse and possible resulting free convection in liquid samples.

Taking a Measurement

The following steps are taken to make a measurement with a KD2 Pro:

1. Attach appropriate sensor then turn on the KD2 Pro.

2. Properly insert the sensor into the material to be measured

3. When the KD2 Pro turns on, you should be in the Main Menu. If not, press the Menu key until you arrive there. Press Enter to begin the measurement.

4. An icon will appear on the left and right side of the screen. The icon at left indicates the type of sensor connected. The circular icon indicates that a reading is underway. It will change to a thermometer icon to indicate whether the measurement is currently in heating or cooling mode; when the thermometer is rising, heat is applied to the needle, and when it is falling, heat is off. A progress bar shows the elapsed time.

5. When the progress bar has fully darkened, the results are displayed as follows:

Figure 3.1: KD2 Pro screen

On the left side of the screen are three measured values:

Thermal Properties Reading - The calculated thermal measurement.

Starting Temperature - The initial temperature prior to any heating or cooling.

Err Value- The err value is the relative goodness of fit or relative error for the data set. It is a measure of how well the model fits the data (the Theory chapter of this manual describes the model that is fit to the data). If the model fits the data perfectly, then err = 0.0000. The purpose of displaying this reading is to indicate possible problems with the data. A good data set will give err values below 0.0100, except at very low thermal conductivity (e.g. insulation materials). If the err value is unusually large, discard the data, wait fifteen minutes and take another reading.

Precautions to be taken while measuring thermal conductivity of liquids with KD2 Pro

1) Keep the temperature of the sample as constant as possible during the measurement. The measurement is made by heating a needle that is placed in the sample and monitoring either the temperature of that needle or a second needle adjacent to the heater. The heat input is made as small as possible to avoid thermally driven redistribution of moisture in the sample. The temperature change from heating may therefore be only a few tenths of a degree. Sample temperature changes during

the measurement period degrade the data and make it difficult for the inverse calculation to find the correct values for the thermal properties. The algorithms in the KD2 Pro are several orders of magnitude less sensitive to these errors than the conventional approach (plotting temperature vs. log time during heating and looking for a linear portion of the graph) but there can still be errors if the temperature changes too rapidly during a measurement. To minimize these sources of error:

2) In the laboratory, allow samples and sensors to come to temperature equilibrium before the measurement starts. Fifteen to twenty minutes is a reasonable rule of thumb.

3) Avoid convection in liquid samples: The KD2 Pro KS-1 sensor is specifically designed to measure thermal conductivity/resistivity of liquid samples. However, measuring thermal properties of liquids is difficult, and great care must be taken for accurate and repeatable results. For an accurate measurement of thermal properties of a liquid sample, the sample must be absolutely still in relation to the KS-1 sensor. Convection, or bulk movement of the sample, will result in error in the thermal properties measurement. Error from convective heat exchange is often very large, rendering the thermal properties measurement useless, and must be avoided. Convective heat exchange in fluids can be broken down into two categories: forced and free convection. Forced convection occurs when the fluid is agitated or mixed by mechanical forces. Free convection may occur when a body of higher or lower temperature is inserted into a fluid. The temperature difference between the body and fluid creates density gradients in the fluid, and these density gradients cause the fluid to mix. From a practical standpoint certain steps can be taken to minimize both forced

and free convective heat exchange. To eliminate forced convection, the fluid sample and the sensor must be absolutely still during the measurement. Even minute vibrations in the sample are often enough to compromise the thermal properties measurement. Some common sources of vibrations found in the laboratory that have been shown to affect thermal properties measurement in liquids and must be avoided include:

a) Vibration from computer fans that are near the measurement apparatus

b) Vibration from people moving around the lab

c) Vibration from other laboratory equipment

d) Vibration from HVAC (Heating, Ventilating, and Air Conditioning) systems.

If sources of vibration are present in laboratory, it may be necessary to place the sample on a vibration isolation table to prevent errors from convection. Another common strategy is to configure the KD2 Pro in auto mode and make measurements overnight after turning off the HVAC system and any other lab equipment that might cause vibrations. This was followed while testing the thermal conductivity in the present study.

The KD2 Pro KS-1 sensor is specially designed to add a very small amount of heat to the sample during measurement and thereby minimize problems with free convection. In high viscosity liquids (e.g. oils, glycerin), free convection is generally not an issue. However, in low viscosity liquids like water or aqueous solutions, there are several important steps that aid in accurate measurements.

a) When dealing with low viscosity liquid samples, the duration of the read time should be minimized to minimize the amount of heat added to the sample.

b) The default read time for the KS-1 sensor is 1 minute. If one is measuring in low viscosity liquids, this read time should be used. However for low viscosity liquids such as water, the read time of 30 seconds was used.

c) In liquid samples, the KS-1 sensor needle should be oriented vertically during the measurement to help prevent free convection. The heat transfer by free convection can be described by

$$g_H = \frac{\left\{0.54\,\rho\, D_H \sqrt[4]{\left[\frac{g\, d^3\, \Delta T}{T\, \mu\, D_H}\right]}\right\}}{d} \qquad (3.1)$$

where g_H is the heat conductance (mol m^{-2} s^{-1}), 'ρ' is the molar density of the fluid (mol/m^3), D_H is the thermal diffusivity of the fluid (m^2/s), g is gravitational acceleration (m/s^2), d is the characteristic dimension of the object placed in the fluid (m), ΔT is the temperature difference between the bulk fluid and the object inserted into it, T is temperature (K), and μ is the kinematic viscosity of the fluid (m^2/s) (KD2 Pro Manual).

Examining eq. 3.1, we see that the heat conductance is inversely related to the characteristic dimension (d) of the probe inserted into the fluid. For this discussion, the needle probe can be accurately described as a cylinder. For a cylinder with its axis parallel to the fluid flow, the characteristic dimension is its length. For a cylinder with its axis perpendicular to the fluid flow, the characteristic dimension is its diameter. Keeping in mind that the heat conductance by free convection is inversely proportional to the

characteristic dimension, inserting the needle into the fluid vertically will greatly reduce convective heat transfer, and result in more accurate measurement of thermal conductivity.

Again from eq. 3.1, we discover that the heat conductance by free convection is proportional to the temperature difference between the fluid and the object inserted into it. Hence, free convection can be decreased by limiting the heating of the needle.

Further examination of eq. 3.1 shows us that the heat conductance is inversely proportional to the kinematic viscosity of the fluid. So, thermal conductivity measurements in more viscous (thicker) fluids are less affected by free convection. More viscous fluids such as castor oil (μ = 1.0 X 10^{-3} m^2/s @ 20C) and glycerol (υ = 7.4 X 10^{-4} m^2/s @ 20C) are unaffected by free convection during the thermal conductivity measurement, and are easy to measure with the KS-1 needle without further precautions. However, in low viscosity fluids such as water (υ = 8.9 X 10^{-7} m^2/s @ 20C) free convection is difficult to prevent. With careful experimental technique, it is possible to measure the thermal conductivity of water and aqueous solutions with the KS-1 sensor, but fluids with viscosities lower than that of water cannot be measured accurately.

The KS-1 sensor should be used in high power mode in liquids. The sensor must be configured in low power mode to prevent free convection.

It is very important to take the above precautions in order to obtain accurate readings. The final setup for the accurate measurement of thermal conductivity was obtained after a period of trial and error. The initial setup consisted of a test tube stand in which the test tube was housed as shown in figure 3.2. The test tube is covered by a leak

proof cap through which the needle (KS1) of the KD2 Pro passes. The needle is clamped to fix it and so that it stays still as any kind of movement of the needle is undesirable and may lead to incorrect reading as discussed earlier. The diameter of the test tube is 2.2 cms as measured by a Vernier Callipers. According to the KD2 Pro manual, the needle should be surrounded by a 1.5 cm thickness of the medium while taking the measurement. In this case the needle is surrounded by 1.1 cm of the fluid around it. In this method, the readings were taken once every hour over a period of 24 hours. The results are plotted as shown in figure 3.4. The blue curve shows the readings obtained by this method. It can be seen that the readings are fluctuating during the day when the laboratory is occupied by people and other instruments and fans are operating and this leads to forced convection. The readings become much more stable at around 8 by when all other instruments are turned off and the KD2 Pro is put on the auto mode to take the readings. Also, the recorded thermal conductivity value at night stays at around 0.535 which is much lower than the thermal conductivity of water at room temperature. The thermal conductivity of water at the temperature of 27 degree Celsius is 0.6 (Young, Hugh D. 1992). The reasons for inaccurate readings with this method are as follows:

1) In this method the diameter of the test tube is less than 3 centimetres due to which the heat from the needle is conducted by the air that comes in contact with the surface of the test tube.

2) The needle maybe misaligned and may not be vertical.

3) Air bubbles at the top of the test tube are likely to be formed which may result in incorrect measurement of thermal conductivity.

Due to the factors above, the thermal conductivity as recorded by this method is less than the actual thermal conductivity of water at the room temperature.

The second method for the measurement of thermal conductivity is an improvement upon the previous method. The set up is as shown in figure 3.3. In this method, water was filled in a sample jar which is inverted. The KD2 Pro needle is fixed in place by making a slot for it on a flat piece of wood. The needle passes through a hole in the sample jar. The cap of the jar has a thin rubber flap on the inside that does not allow fluid to leak when the jar is put upside down. The readings taken with this method are also plotted on the graph shown in figure 3.4 in the red curve. The readings fluctuate during the day when there are vibrations present but during the night when the KD2 Pro is put on the auto mode, the readings show the thermal conductivity as 0.605 which is very close to the thermal conductivity of water at room temperature. In the second method, the problems associated with the first method have been minimised and accurate values for the thermal conductivity of water are obtained.

In order to get true values of thermal conductivity for nanofluids, the second method was followed in the present study. The samples were prepared during the day and the thermal conductivity was measured at night by leaving KD2 Pro in auto mode.

The measurement of thermal conductivity of liquids such as water is a tricky issue and it becomes even more difficult to measure conductivity at temperatures higher than 40 degree Celsius when convection sets in and its effect becomes more dominant. The transient methods are considered to be one of the most efficient methods to measure thermal conductivity but it is very important that all the necessary precautions are taken because even a very slight disturbance can result in a faulty measurement. The

steady state methods are not considered as efficient because of the setting of convection. The problems associated with the measurement of thermal conductivity of fluids especially water and less viscous fluids can be one of the possible reasons of why there is a difference in the data collected by various group of researchers. There is no standard technique that has been used for the measurement of thermal conductivity and this could be one of the causes of discrepancy in the literature associated with the thermal conductivity of nanofluids.

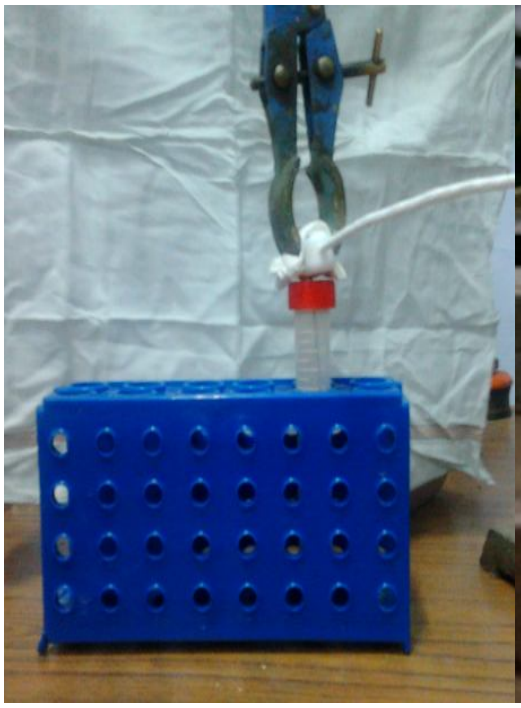

Figure 3.2: Test tube diameter 2.2 cms

Figure 3.3: Container diameter 5 cms

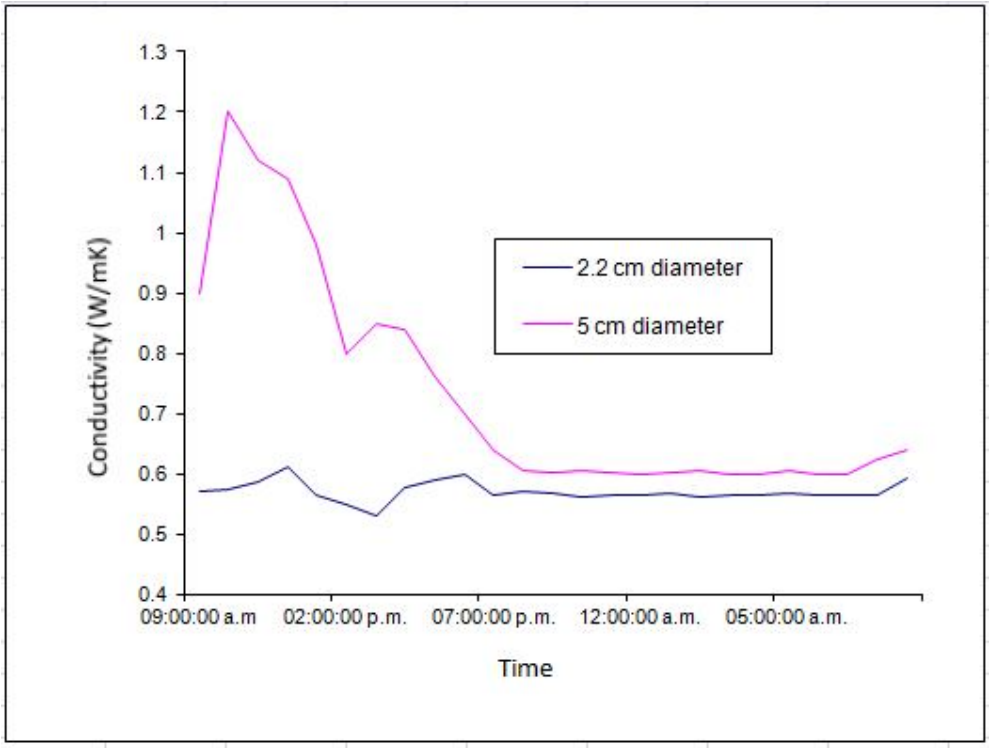

Figure 3.4: Thermal conductivity of water measured by the two techniques over a period of 24 hours. The above figure gives the plot of conductivity (W/mK) vs. time.

From the above plot it can be seen that the readings fluctuate during the day when there are disturbances around the KD2 Pro such as the HVAC system, fans and human presence. The readings are stable after 7:00 p.m. when there are no disturbances. The readings are quite accurate for the second case when the diameter of the container is 5 cm. In the first case where the diameter is 2.2 cm, the thermal conductivity measured is much lower due to effect of air. From the results, we can safely conclude that the best way to measure the thermal conductivity is by using the first method and measuring thermal conductivities at night when the sample is left undisturbed.

3.2 Silver Nanoparticles

This section presents results from an investigation into the stability and conductivity of nanofluids. Aqueous solution of colloidal silver nanoparticles was used to prepare nanofluids with water as the base fluid. Different concentrations were considered to study stability and conductivity. Sonication was used as a means to disperse nanoparticles in the aqueous solution and the sonication time was varied for different concentrations. The stability of the nanofluids obtained was tested using three popular techniques – Dynamic Light Scattering (or DLS) technique, Zeta Potential technique and the UV-vis spectrophotometer. The results of the three stability inspection techniques as measured over a period were plotted on the graph. Since the main interest in the study of nanofluids lies in the enhancement of thermal conductivity, thermal conductivity values have been measured which show how the stability of nanofluids affects the thermal conductivity. From the data collected, it can be seen that the thermal conductivity is a function of particle size as well as the concentration of the nanofluid.

The aim of the present study is to investigate the various methods of stability inspection and check if their results are in good agreement with each other or not and also the relationship between the conductivity and stability of a nanofluid. The stability of a nanofluid can be described by two phenomenon, particle clustering and particle settling. While particle settling is absolutely undesirable as it lowers the concentration of the nanofluid and hence its conductivity also decreases, particle clustering may not be an undesirable phenomenon because the clustering may lead to

better conductivity of the nanofluid (Gharagozloo and Goodson, 2010). This paper is also an attempt to understand how these two phenomenons affect the conductivity.

3.2.1 Experiments

For the purpose of experiment, colloidal solution of silver nanoparticles was purchased from Reinste Nanoventures. The nanoparticle size was 10 nm and the concentration of the aqueous solution was 0.1mg/ml. The study of stability and its effect on thermal conductivity of nanofluid is done under three headings:

a). Stabilisation techniques : These include investigation into different measures taken to enhance the stability of the nanofluid and prevent them from aggregate them or to reverse the aggregation that has already taken place. Techniques that have been reported in literature include the ultrasonic vibration in the nanofluid, addition of surfactants, variation of pH etc. For this study we have used ultrasonic vibration in order to de-agglomerate silver particles.

b). Stability Inspection techniques: These include investigation into stability of a nanofluid by using different techniques such as Dynamic Light Scattering (popularly known as DLS), UV-vis spectrophotometer, Zeta Potential, Sediment photo capturing, Sedimentation Balance Method. For this study we have used DLS, UV-vis spectrophotometer and Zeta Potential.

c). Measurement of thermal conductivity: The thermal conductivity can be measured using the Three Omega Method, Hot plate method or Transient Hot wire

method as reported in the literature. For this study the Transient Hot Wire set-up has been used to measure the thermal conductivity of the nanofluid.

3.2.1.1) Study of effect of Ultrasonic Vibration on the silver nanofluid

In order to study the effect of ultrasonic vibration on nanofluids, two concentrations by weight were considered, 0.5% and 1%. For each concentration the sonication time was varied as 0, 2, 4, 6 hours. The DLS and Zeta potential techniques were used to inspect the stability of the resulting eight samples over a period of 10 days. Oscar Ultrasonic processor was used to sonicate the nanofluid [Fig. 3.5].

Figure 3.5: Oscar Ultrasonic Processor

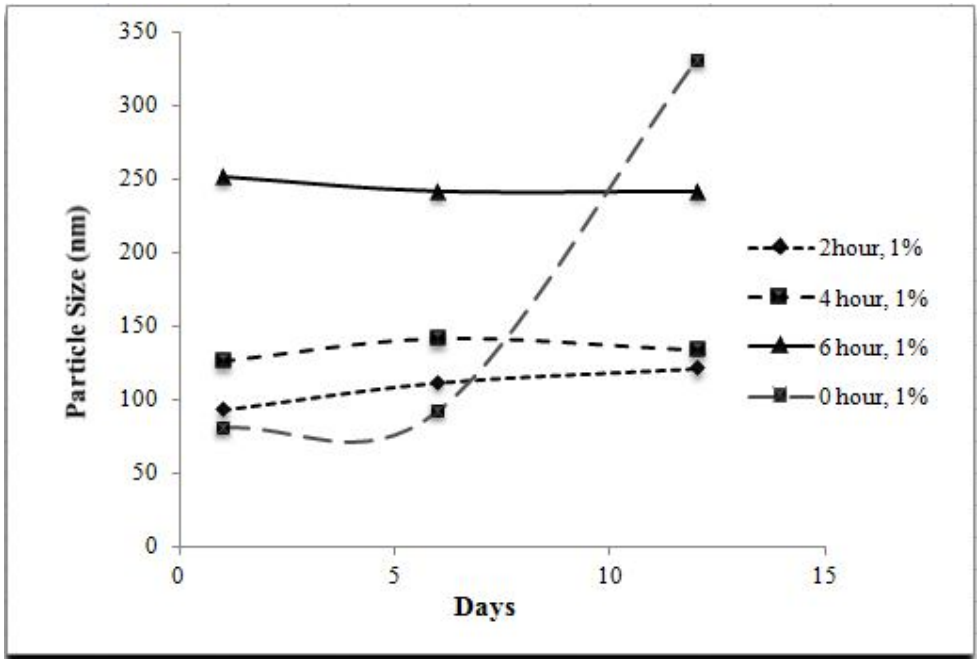

Figure 3.6: Effect of sonication on particle size for 1% concentration

Figure 3.6 shows the effect of ultrasonic vibration on nanofluids over a period of 12 days. The concentration of the samples was 1% and the samples were sonicated for 0hours, 2 hours, 4 hours and 6 hours. From the graph it is seen that sonication has resulted in an aggregation of nanoparticles for the silver aqueous colloid initially. The snapshots of the DLS results for the silver samples are shown in Appendix A.

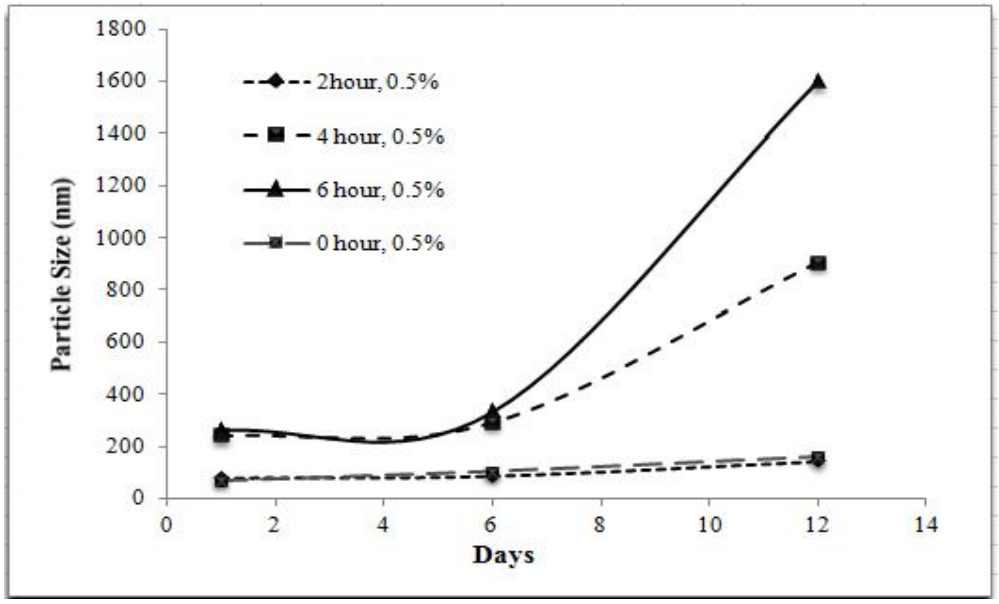

Figure 3.7: Effect of sonication on particle size for 0.5% concentration

Figure 3.7 shows the effect of ultrasonic vibration on nanofluids over a period of 12 days. The concentration of the samples was 0.5% and the samples were sonicated for 0hours, 2 hours, 4 hours and 6 hours. From the graph it is seen that sonication has resulted in an aggregation of nanoparticles for the silver aqueous colloid and the trend is seen over the entire period of 12 days. The aggregation is more than it is in 1% concentration. One reason for the increase in aggregation at a lower concentration could be that the energy absorbed during sonication per unit mass of the nanofluid is more at a lower concentration. The snapshots of the DLS results for the silver samples are shown in Appendix A.

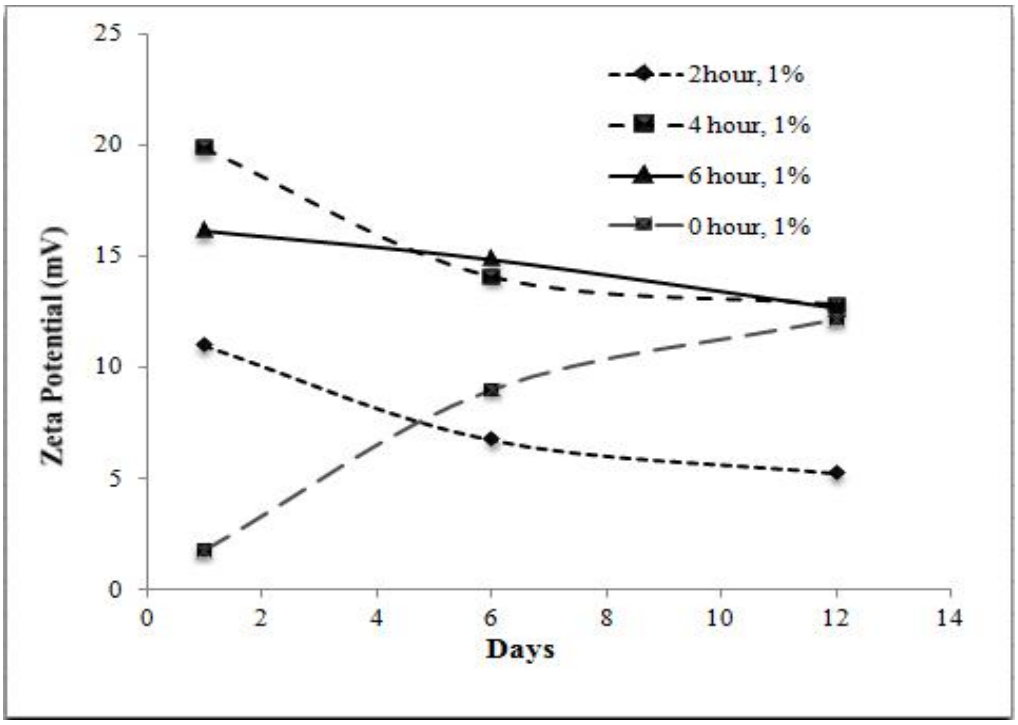

Figure 3.8: Effect of sonication on Zeta Potential values for 1% concentration

The Zeta Potential values have also been plotted for both concentrations as shown in figures 3.8 and 3.9. The Zeta Potential values fall down over time for all samples except for the unsonicated samples for which the Zeta Potential values increase at both concentrations. At both concentrations, the Zeta Potential values are highest for the samples that have been sonicated for 4 hours and 6 hours. However according to DLS values the particle size has increased for higher sonication. Thus we see that the DLS results are not consistent with the Zeta Potential results.

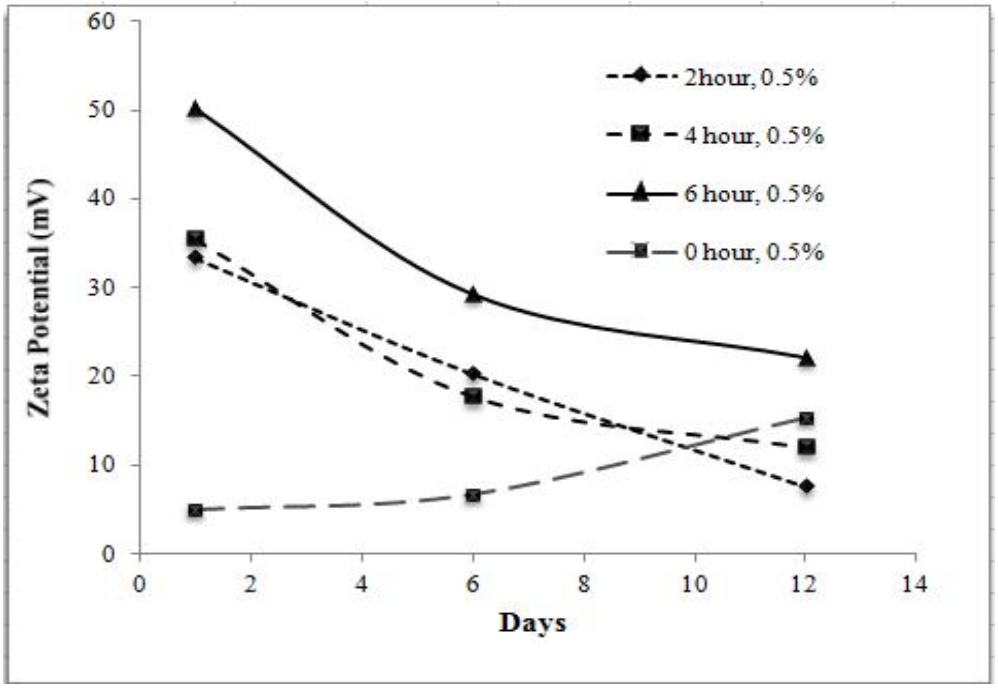

Figure 3.9: Effect of sonication on Zeta Potential values for 0.5% concentration

From the above 4 graphs related to DLS and Zeta Potential, it can be seen that while Zeta Potential values are better with greater sonication time (showing better stability), the particle size has grown with greater sonication (less stable). Another method of UV-vis spectrophotometer was used to understand how sonication affects the concentration of the samples so that we could get a clear picture of the effect of sonication.

In order to get more clarity about whether the stability increases or decreases with sonication, a third method, UV-vis spectrophotometer was also used. 5 samples were made and kept under observation for twelve days. The stability inspection was done using a spectrophotometer. Three of the samples were unsonicated and their concentrations were 0.5%, 1% and 2% by weight (figures 3.10, 3.11 and 3.12 respectively). The fourth sample was sonicated for thirty minutes and its concentration was 0.5% by weight (figure 3.13). The fifth sample was sonicated for 6 hours and its concentration was 1% by weight (figure 3.14). The height of peak of the graph is directly proportional to the concentration of the nanofluid. The peak for silver nanoparticles lies at around 400 nm. There may be a shift in the peak depending on the size of the particles. If the particle size lowers the peak shifts towards the left and if it increases the peak shifts towards the right.

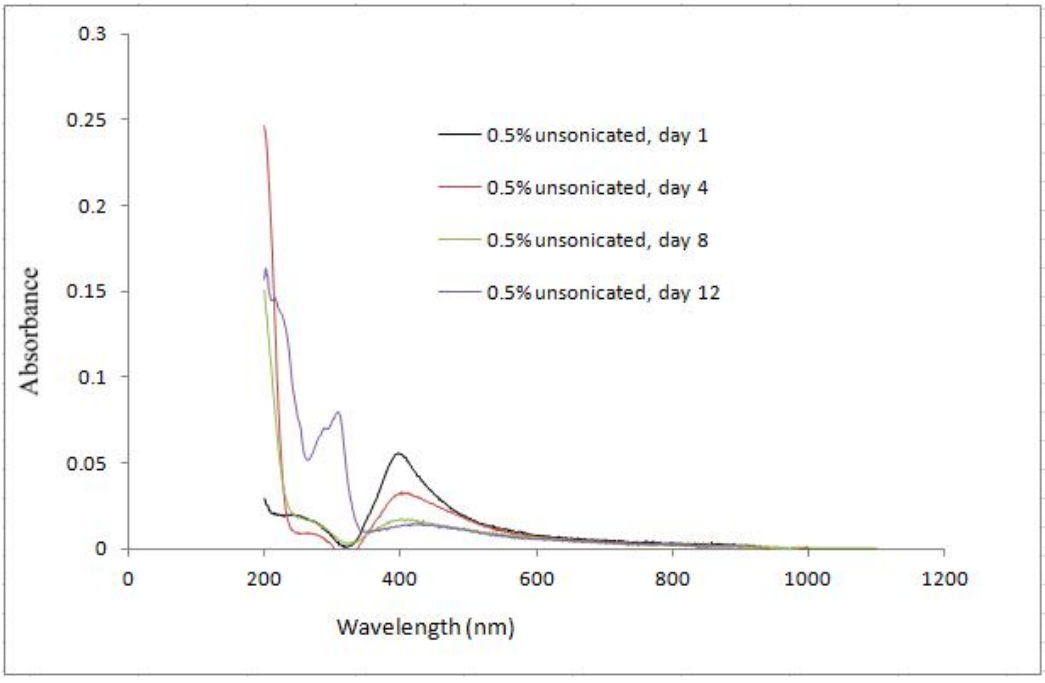

Figure 3.10: Unsonicated silver sample 0.5% concentration over a period of 12 days

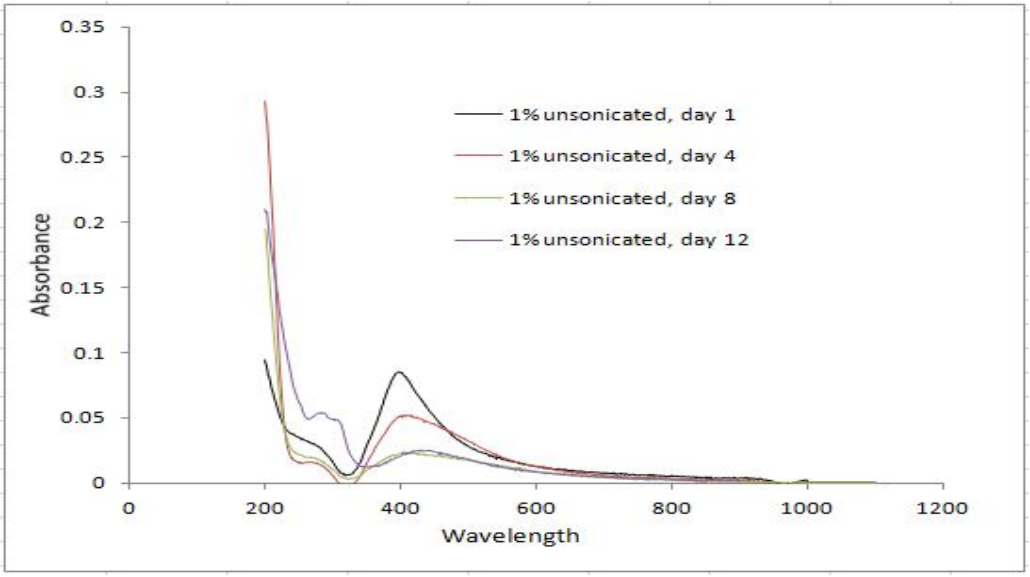

Figure 3.11: Unsonicated silver sample 1% concentration over a period of 12 days

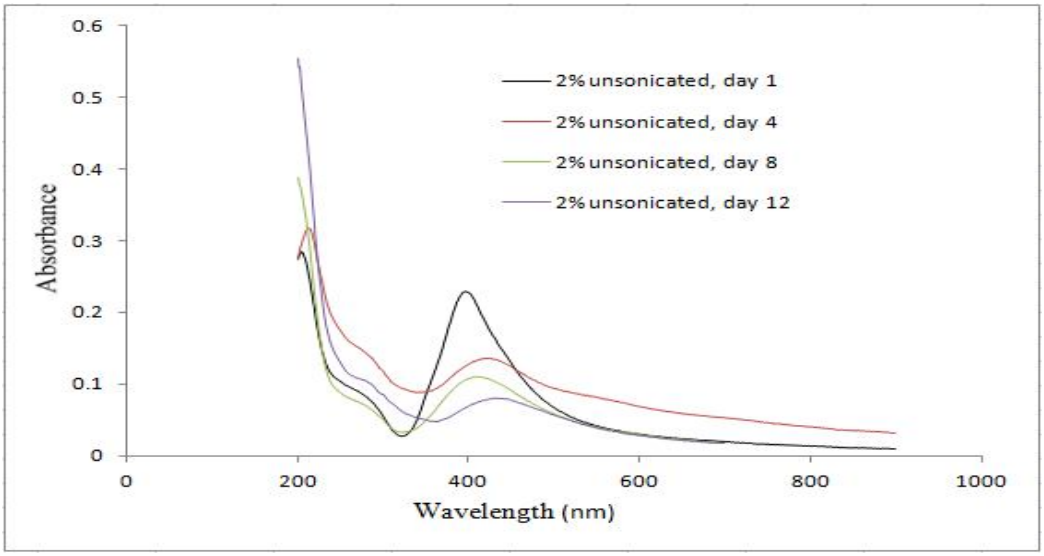

Figure 3.12: 2% unsonicated silver, spectrophotometer results

Figures 3.10, 3.11 and 3.12 show the UV- vis spectrophotometer results for concentrations of 0.5%, 1% and 2% respectively. Since the absorbance values on the graph are directly proportional to the concentrations of the samples according to the Beer Lambert law, it can be seen from the graph that in all cases the concentrations fall to approximately 30 percent of the original concentration in a period of 15 days. This makes the unsonicated samples unstable for long term use as they settle down easily.

The next two graphs are for two samples that were sonicated for 30 minutes (0.5% concentration) and 6 hours (1% concentration).

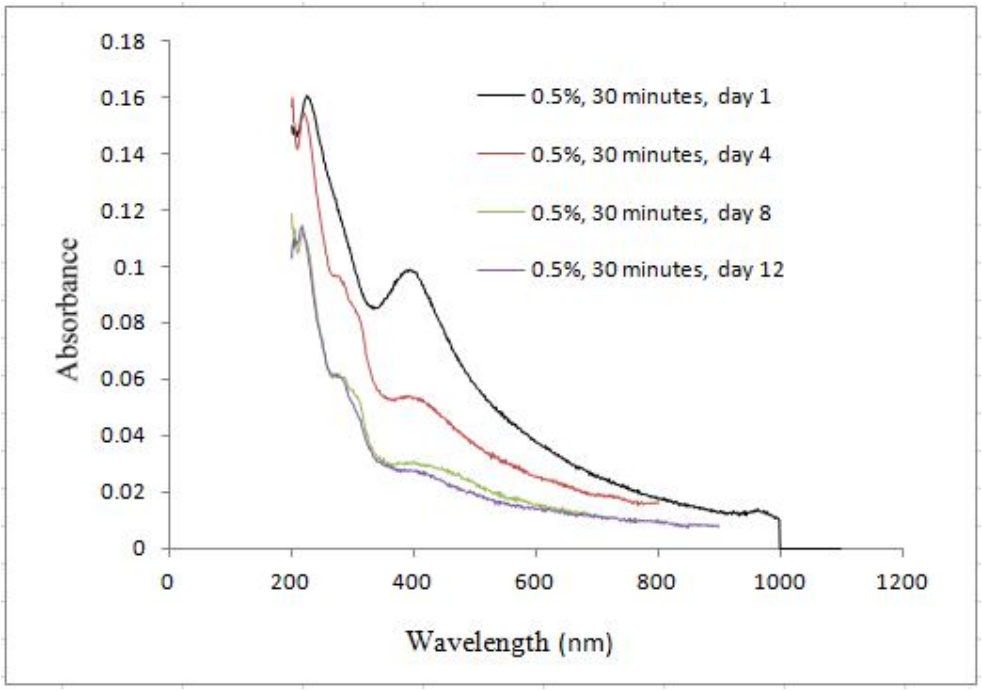

Figure 3.13: 0.5% concentration, 30 minutes sonicated

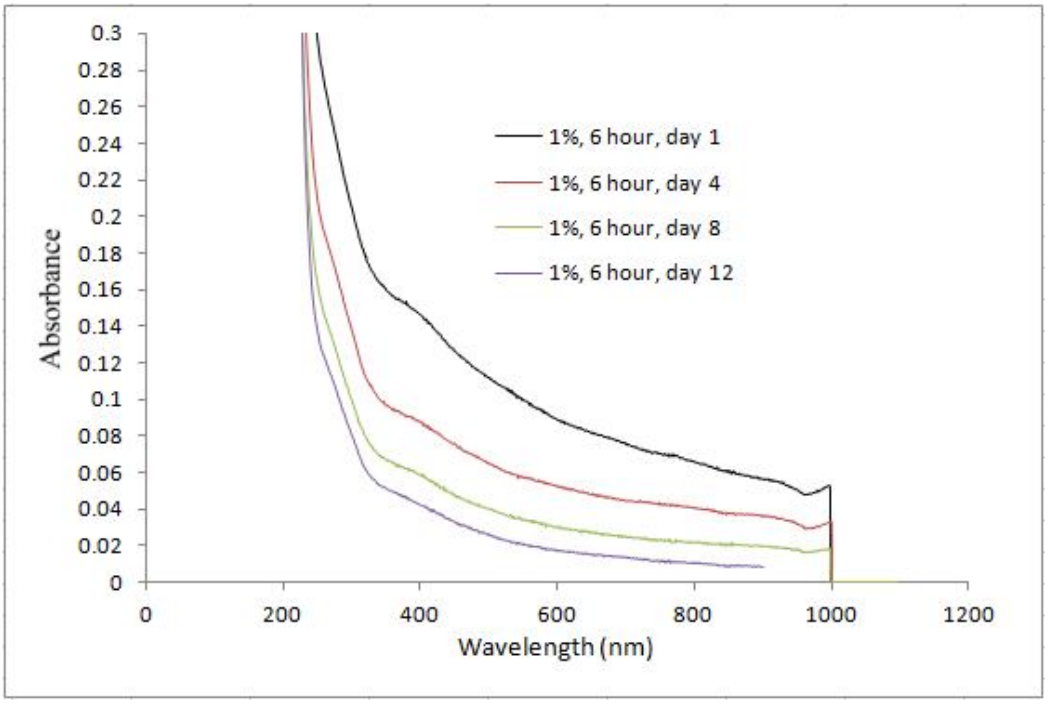

Figure 3.14: 1% concentration, 6 hours sonicated

On comparing figures 3.10 and 3.13 for 0.5% concentration, it can be seen that sonication has resulted in an improved concentration of the nanofluid on day 1, even though it has resulted in clustering and agglomeration of the particles but the particles stay suspended for a longer period. Similar conclusions can be drawn from the comparison of figure 3.11 and figure 3.14. This can also be deduced from the higher values of Zeta Potential from the samples that have been sonicated for a longer period. Thus Zeta Potential and UV-vis spectrophotometer results are in good agreement with each other.

Another observation from figures 3.13 and 3.14 is that even though the initial concentration of sonicated samples is higher than that of the unsonicated samples but the final concentration of the sonicated samples still remains almost 30 percent of the

initial concentration. Thus, even though sonication has improved the stability, however it is only a temporary effect.

3.2.1.2) Study of effect of particle size and concentration on the thermal conductivity of silver nanofluid

In order to study the effect of particle size and concentration on thermal conductivity of silver nanofluid, three samples of different concentrations were prepared. The concentrations were 0.5%, 1% and 2% by weight. The particle size was measured with DLS (figure 3.15) and concentration was measured with UV-vis spectrophotometer (figures 3.10, 3.11 and 3.12). The conductivity was also measured over a period of 12 days (figure 3.16). It can be seen that as the particle size increases the conductivity increases as well and it shows a peak value at a certain particle size. However when the particle size becomes too large, the conductivity values fall down. KD2 pro was used to measure the thermal conductivity. The instrument utilises the transient hot wire method for the measurement of conductivity.

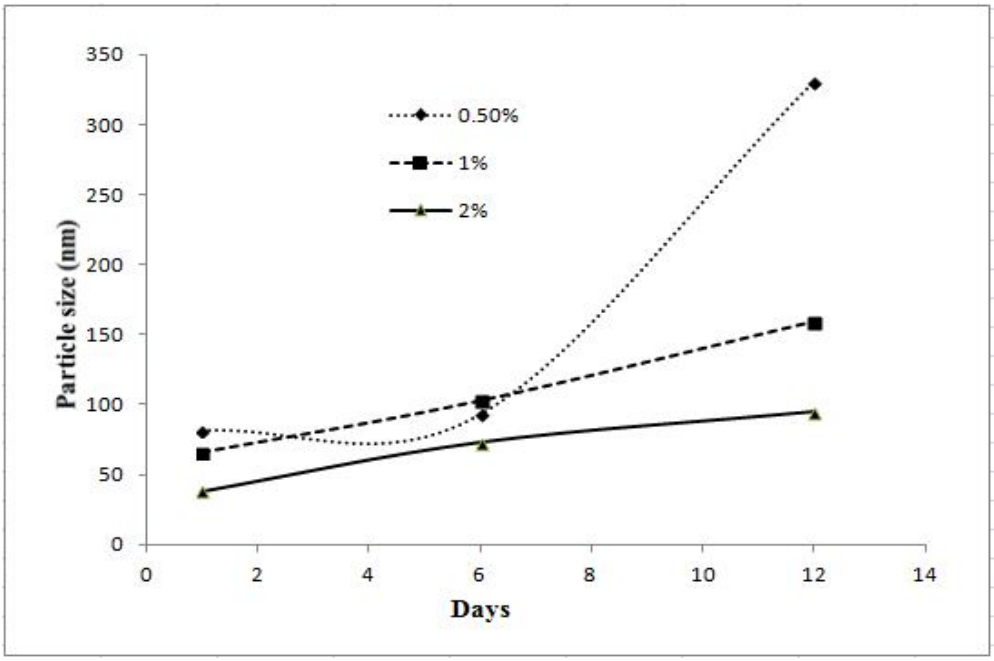

Figure 3.15: DLS results showing particle size for three concentrations

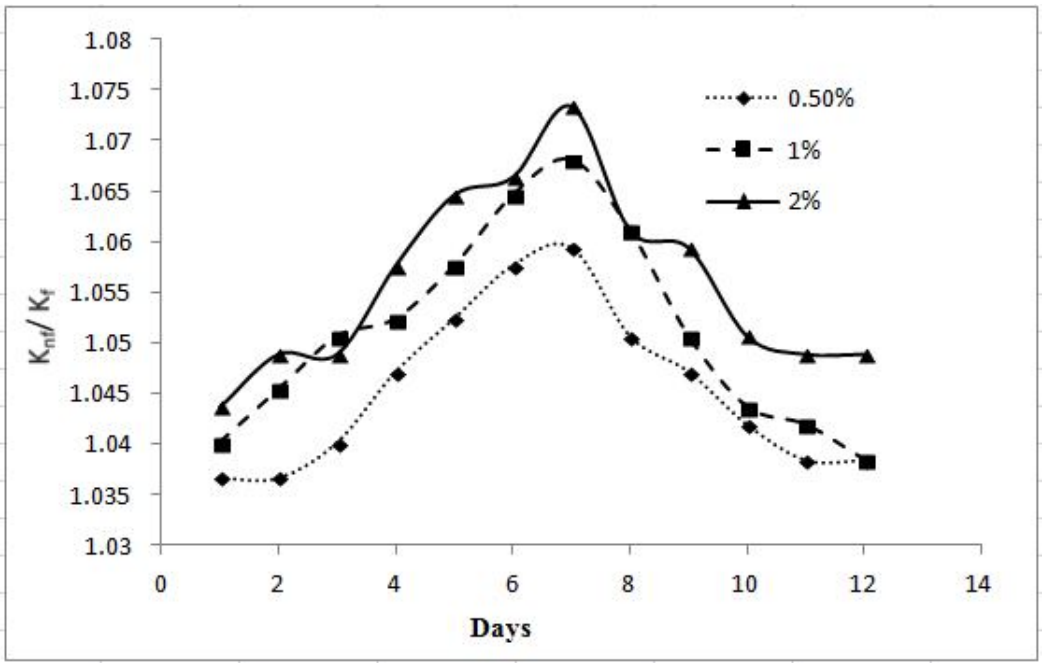

Figure 3.16: Thermal Conductivity for three concentrations

3.2.2 Results and Discussion for Silver nanoparticles

The following conclusions can be drawn from the experiments and graphs for silver nanoparticles:

1). Dynamic Light Scattering results are inadequate while measuring the stability of the fluid. The Zeta Potential values are in good agreement with the stability results shown by the UV-vis spectrophotometer. Higher values of Zeta Potential are very well in accordance with the higher absorbance value shown in the spectrophotometer results. The Zeta Potential values increase with the sonication time, however there is an anamolous aggregation of particles due to sonication which needs to be investigated. This aggregation is more at lower concentration which maybe due to the fact that at lower concentrations more energy per unit mass is absorbed by the nanoparticles.

2). Even though the sonicated samples stay suspended for a longer period of time than the unsonicated samples but in a period of 12 days, the final concentration is nearly 30 percent of the initial concentration in all cases whether sonicated or not. Thus, sonication is only a temporary solution.

3). The thermal conductivity of the sample rises once the particles begin to agglomerate, however as the particle size goes beyond a certain value, the conductivity begins to decrease.

The snapshots of the DLS results for the silver samples are shown in Appendix A

3.3 Carbon nanotubes

3.3.1 Experiments

Carbon nanotubes are one of the most interesting of all the nanoparticles that have been encountered by researchers. Not only these show a very high enhancement in thermal conductivity, these have been shown to be highly stable with the addition of surfactants such as SDS (sodim dodecylsulfate). The Carbon nanotubes were purchased from Reinste Nanoventures and were obtained as a sheet which was then grinded and made into a powder. In the investigation of stability of Carbon nanotubes SDS was added in various (five) concentrations to 2 concentrations of the nanofluid, thus making 10 samples in all. The water-CNT-SDS was sonicated for 3 hours to make the sample homogeneous. The stability of the nanofluid was tested using UV-vis spectrophotometer over a period of 22 days. The following graphs show the results for the 10 samples. The graphs are accompanied by an explanation of the results. The two concentrations of CNT were 0.025% and 0.01%. The concentration of SDS was varied as 5, 15, 50, 100, 200 times that of the CNT concentration.

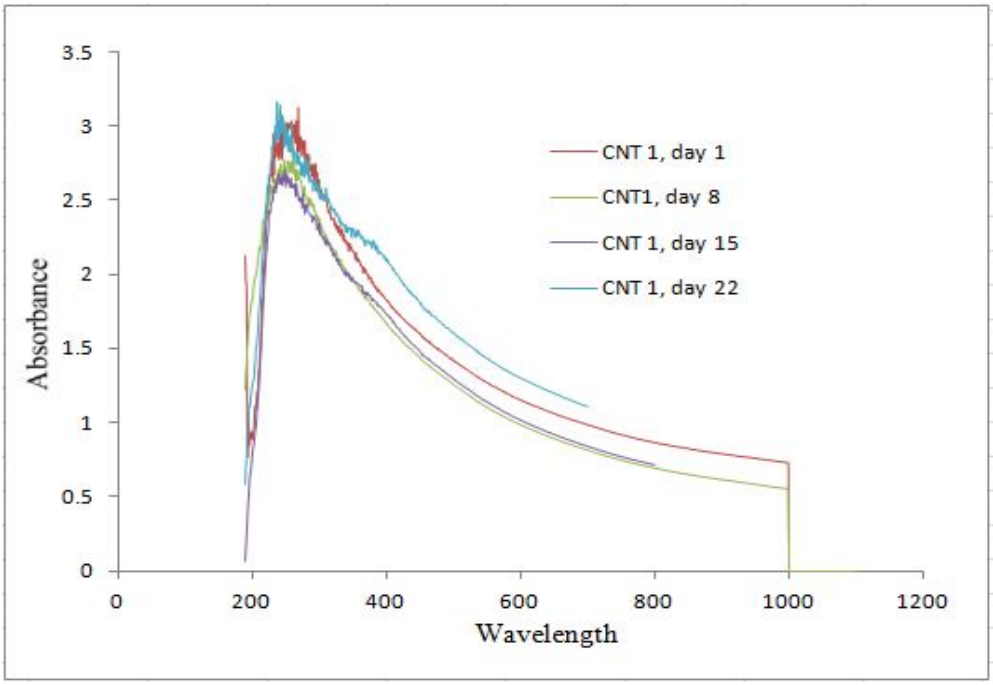

Figure 3.17: CNT sample1, Spectrophotometer results over a period of 22 days

Sample Details and observations:

The sample CNT 1 contains CNT: 0.025%, SDS: 0.125% (5 times CNT). The sample was sonicated for 3 hours after adding CNT and SDS to the base fluid (DI water). The red curve shows peak absorbance of over 3 on day 1 and the blue curve shows peak absorbance of over 3 on day 22. The concentrations have decreased in the first 15 days, however on day 22, the concentration has increased again. The sample has shown good stability over a long period of time.

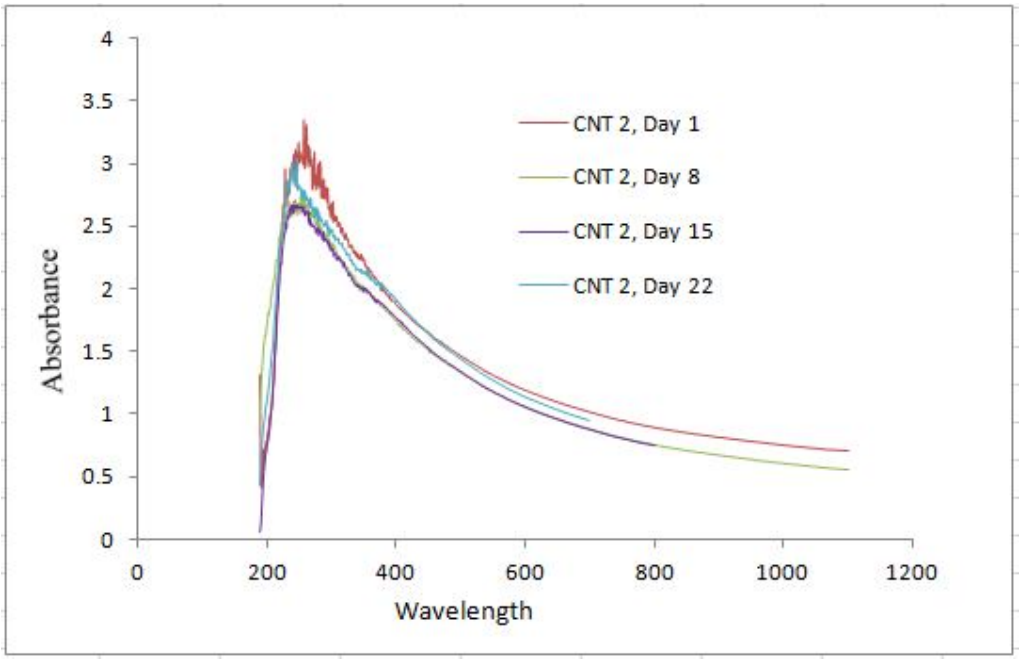

Figure 3.18: CNT sample 2, spectrophotometer results over a period of 22 days.

Sample Details and Observations:

The sample CNT 2 contains CNT: 0.025%, SDS: 0.375% (15 times CNT). The sample was sonicated for 3 hours after adding CNT and SDS to the base fluid (DI water). The red curve shows peak absorbance of over 3 on day 1 and the blue curve shows peak absorbance of around 3 on day 22. The concentrations have decreased in the first 15 days, however on day 22, the concentration has increased again. The increase has not been as much as in CNT 1(Figure 3.17). The sample has shown good stability over a long period of time.

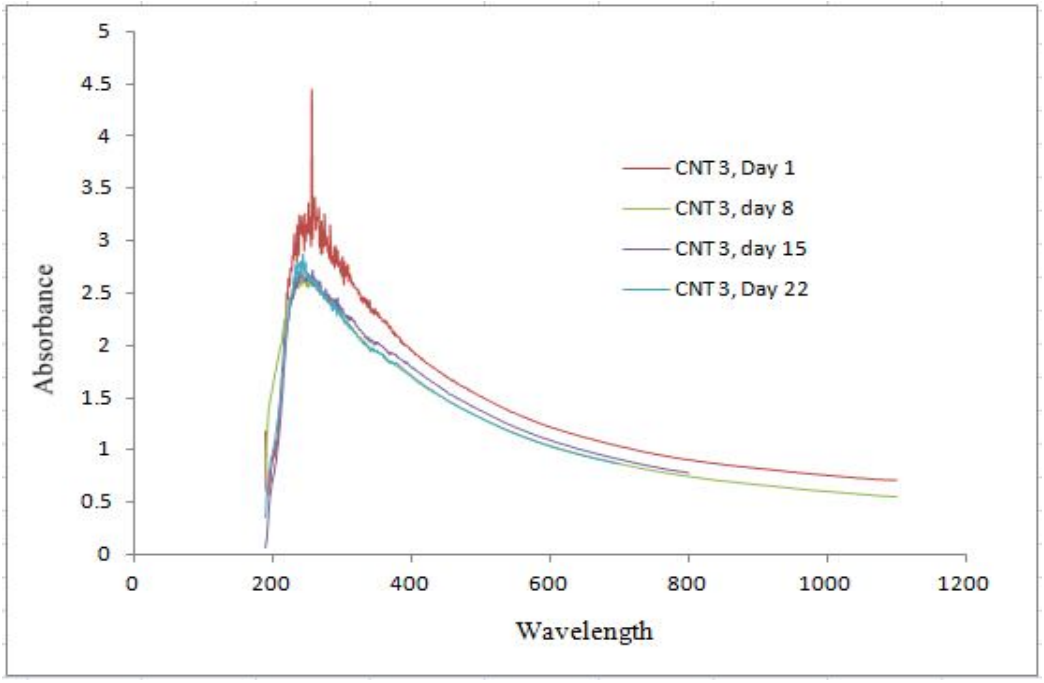

Figure 3.19: CNT sample 3, spectrophotometer results over a period of 22 days

Sample Details and Observations:

The sample CNT 3 contains CNT: 0.025%, SDS: 1.25% (50 times CNT). The sample was sonicated for 3 hours after adding CNT and SDS to the base fluid (DI water). The red curve shows peak absorbance of over 3 on day 1 and the blue curve shows peak absorbance of around 3 on day 22. The concentrations have decreased in the first 15 days, however on day 22, the concentration has increased again. The increase has not been as much as in CNT 2 (Figure 3.18). The sample has shown good stability over a long period of time.

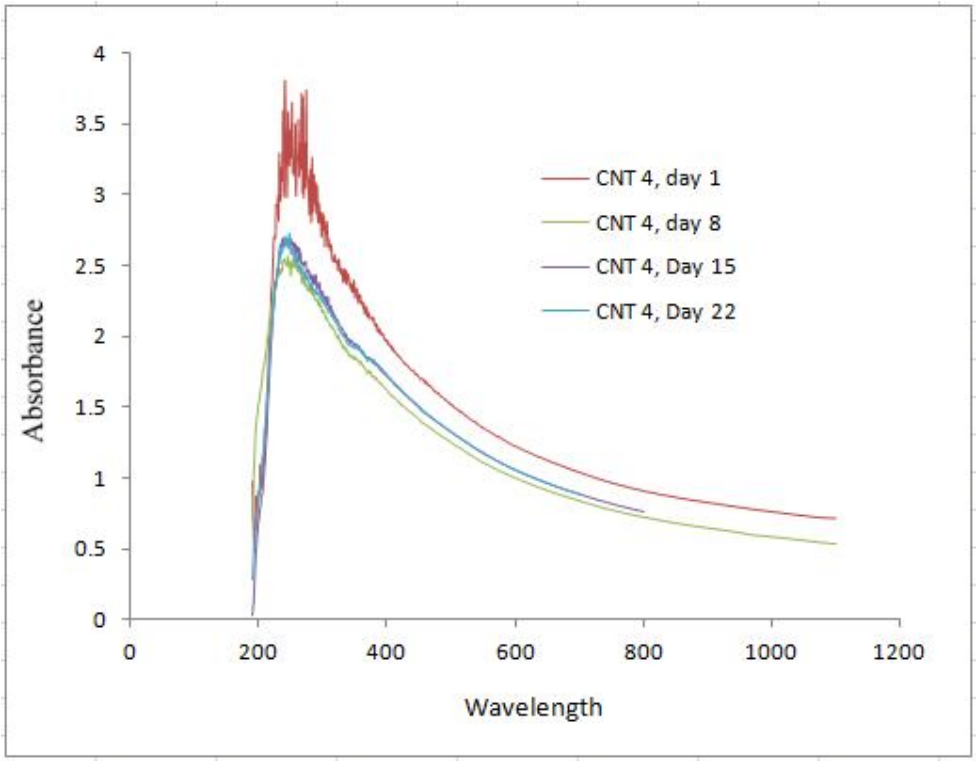

Figure 3.20: CNT sample 4, spectrophotometer results over a period of 22 days

Sample Details and Observations:

The sample CNT 4 contains CNT: 0.025%, SDS: 2.5% (100 times CNT). The sample was sonicated for 3 hours after adding CNT and SDS to the base fluid (DI water). The red curve shows peak absorbance of over 3.5 on day 1 and the blue curve shows peak absorbance of around 2.7 on day 22. The concentrations have decreased in the first 15 days, however on day 22, the concentration has increased again. The increase has not been as much as in CNT 3 (Figure 3.19). The sample has shown good stability over a long period of time.

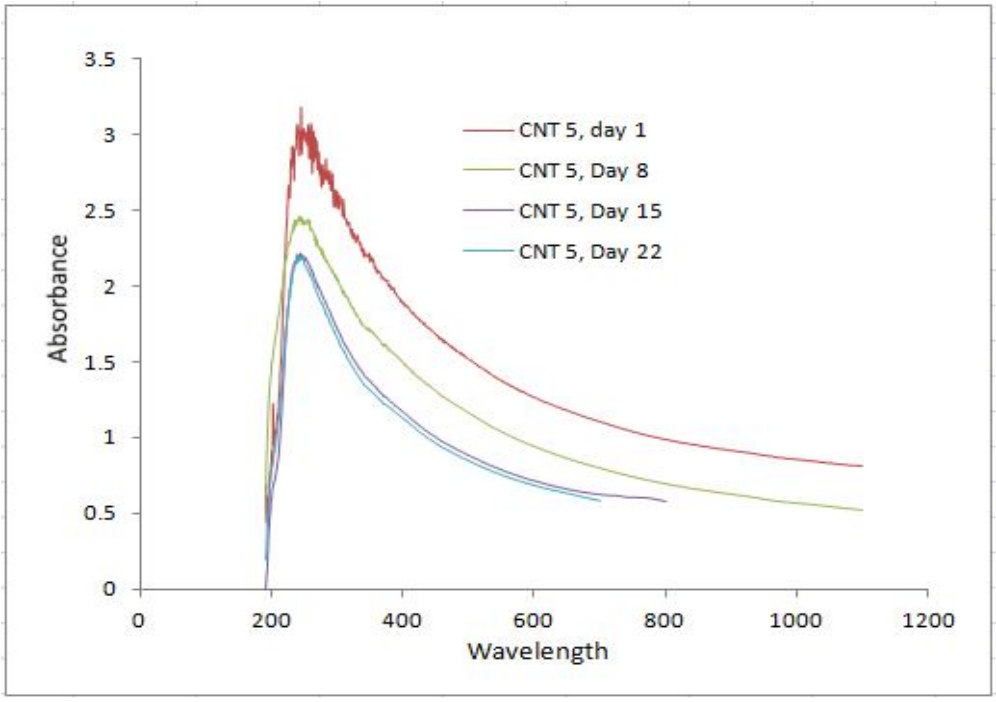

Figure 3.21: CNT sample 5, spectrophotometer results over a period of 22 days

Sample Details and Observations:

The sample CNT 5 contains CNT: 0.025%, SDS: 5% (200 times CNT). The sample was sonicated for 3 hours after adding CNT and SDS to the base fluid (DI water). The red curve shows peak absorbance of over 3.5 on day 1 and the blue curve shows peak absorbance of around 2.7 on day 22. The concentrations have decreased throughout the 15 days. The increase has not been as much as in CNT 4 (Figure 3.20). The sample has shown good stability over a long period of time however the stability is not as good as with the lower concentrations of CNT.

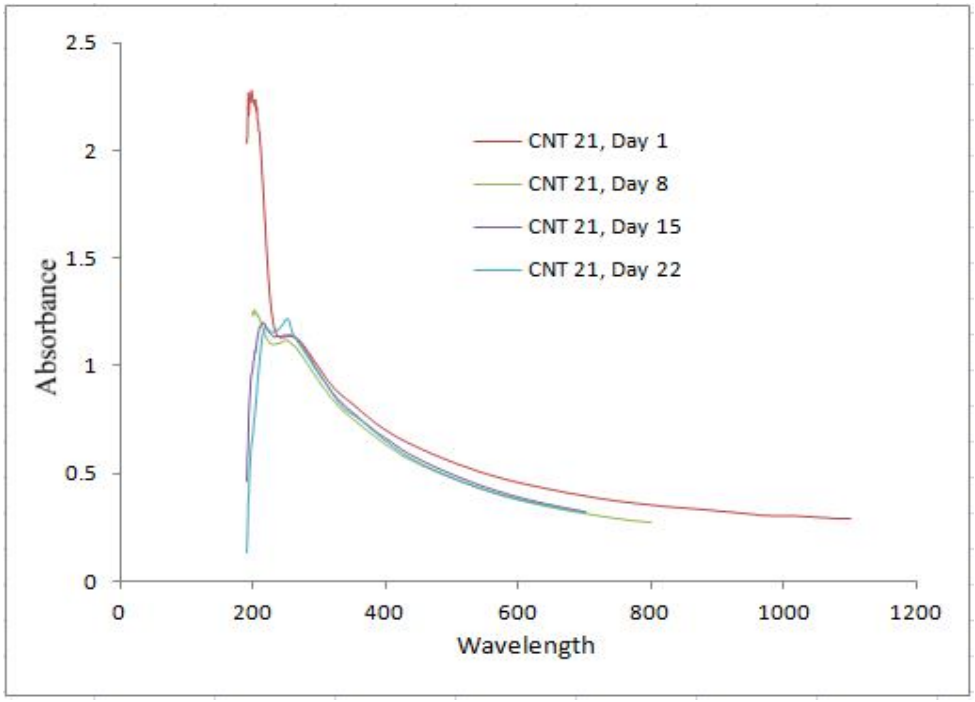

Figure 3.22: CNT sample 21, spectrophotometer results over a period of 22 days

Sample Details and Observations:

The sample CNT 21 contains CNT: 0.01%, SDS: 0.05% (5 times CNT). The sample was sonicated for 3 hours after adding CNT and SDS to the base fluid (DI water). The red curve shows peak absorbance of around 1.2 on day 1 and the blue curve shows peak absorbance of around 1.25 on day 22. The concentrations have decreased throughout the 15 days. However it has shown an increase on 22nd day. The sample has shown good stability over the period.

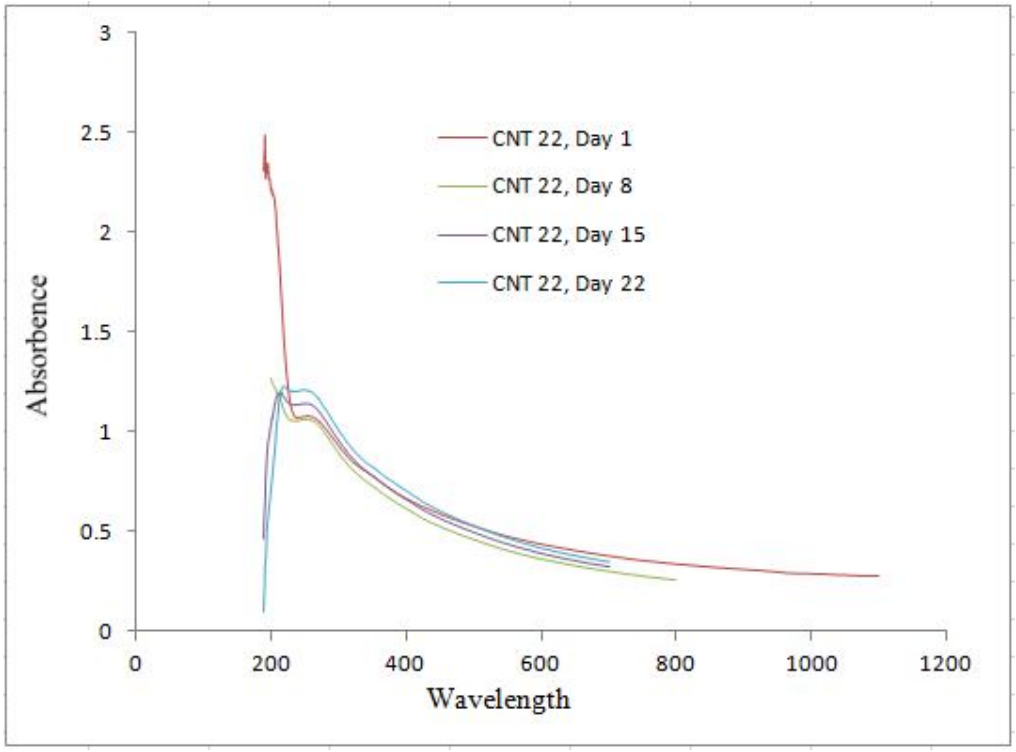

Figure 3.23: CNT sample 22, spectrophotometer results over a period of 22 days

Sample Details and Observations:

The sample CNT 22 contains CNT: 0.01%, SDS: 0.15% (15 times CNT). The sample was sonicated for 3 hours after adding CNT and SDS to the base fluid (DI water). The red curve shows peak absorbance of around 1.1 on day 1 and the blue curve shows peak absorbance of around 1.25 on day 22. The concentrations have decreased throughout the 15 days. However it has shown an increase on 22nd day. The sample has shown good stability over the period.

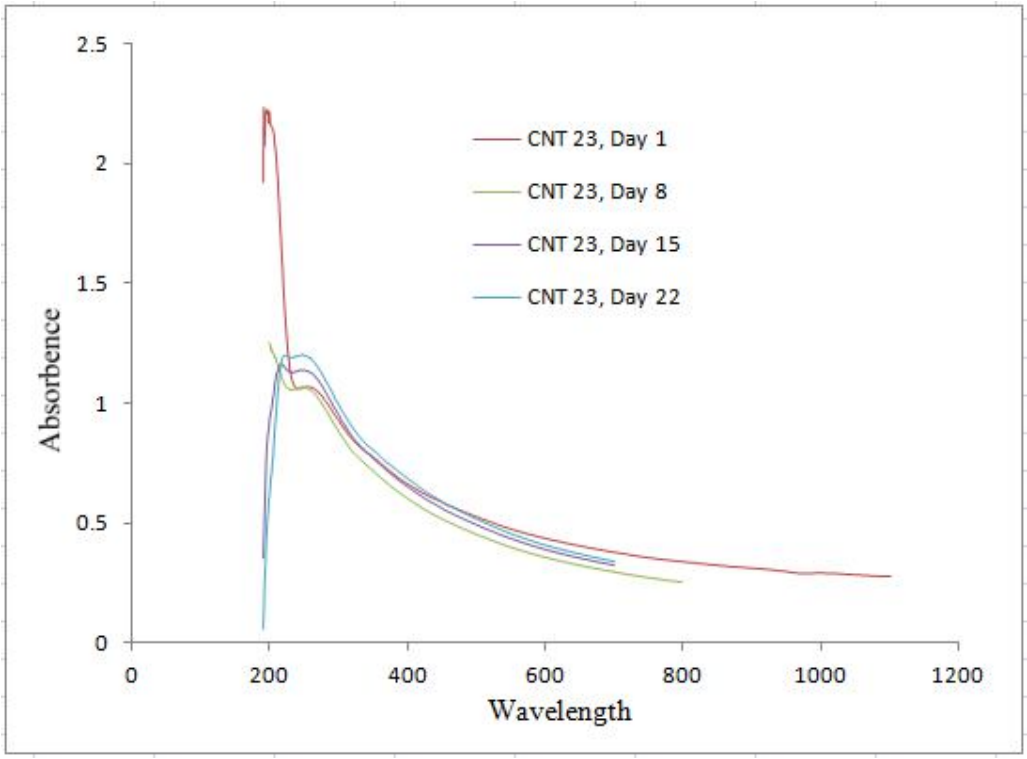

Figure 3.24: CNT sample 23, spectrophotometer results over a period of 22 days

Sample Details and Observations:

The sample CNT 23 contains CNT: 0.01%, SDS: 0.5% (50 times CNT). The sample was sonicated for 3 hours after adding CNT and SDS to the base fluid (DI water). The red curve shows peak absorbance of around 1.1 on day 1 and the blue curve shows peak absorbance of around 1.25 on day 22. The concentrations have decreased throughout the 15 days. However it has shown an increase on 22nd day. The sample has shown good stability over the period.

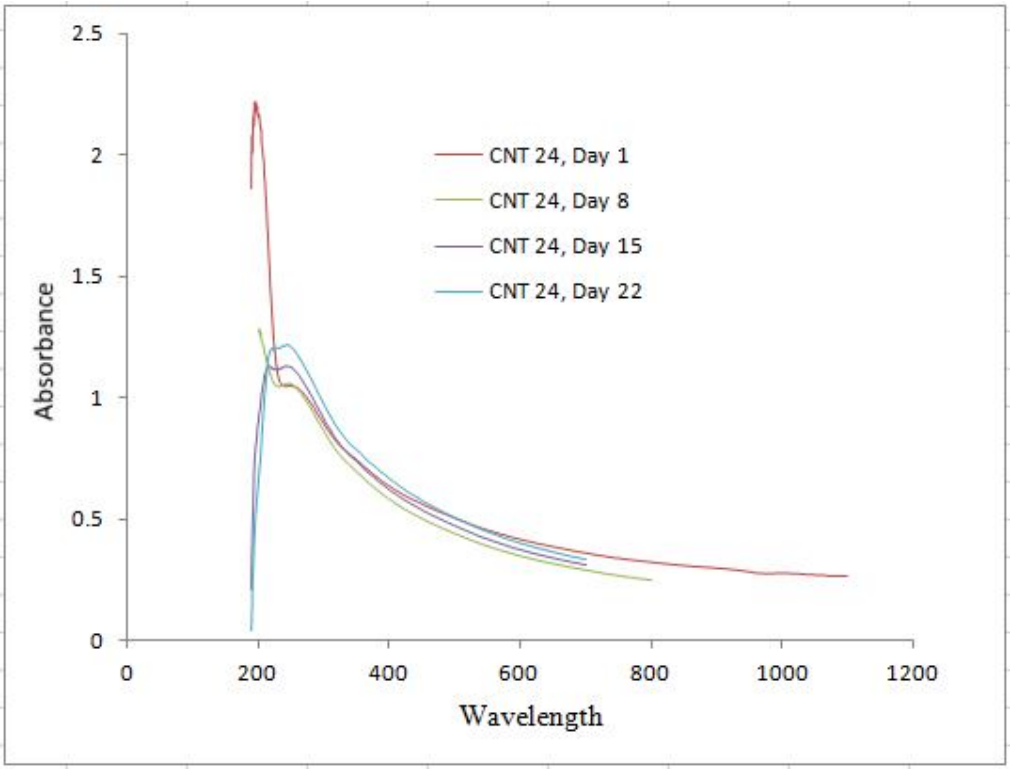

Figure 3.25: CNT sample 24, spectrophotometer results over a period of 22 days

Sample Details and Observations:

The sample CNT 24 contains CNT: 0.01%, SDS: 1% (100 times CNT). The sample was sonicated for 3 hours after adding CNT and SDS to the base fluid (DI water). The red curve shows peak absorbance of around 1.1 on day 1 and the blue curve shows peak absorbance of around 1.25 on day 22. The concentrations have decreased throughout the 15 days. However it has shown an increase on 22nd day. The sample has shown good stability over the period.

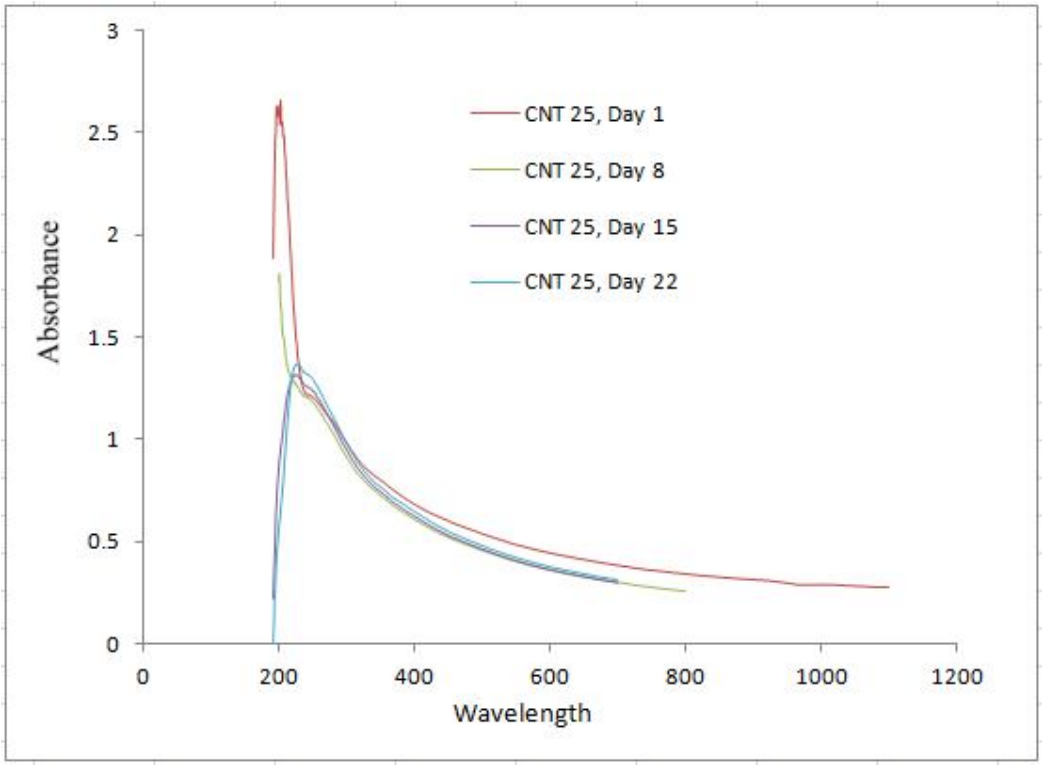

Figure 3.26: CNT sample 25, spectrophotometer results over a period of 22 days

Sample Details and Observations:

The sample CNT 24 contains CNT: 0.01%, SDS: 2% (200 times CNT). The sample was sonicated for 3 hours after adding CNT and SDS to the base fluid (DI water). The red curve shows peak absorbance of around 1.3 on day 1 and the blue curve shows peak absorbance of around 1.4 on day 22. The concentrations have decreased throughout the 15 days. However it has shown an increase on 22nd day. The sample has shown good stability over the period.

3.3.2 Results and Discussion for Carbon Nanotubes

The following conclusions can be reached based on the UV-vis-spectrophotometer graphs for carbon nanotubes.

1). Carbon nanotubes show excellent results with the addition of SDS as surfactant. The settling that occurs initially stabilises after a period of time and there is an increase in the concentration of CNT samples after a period of time. This is an anomalous behaviour that has not been reported in any literature that we have come across so far. A possible explanation to the phenomenon is that after a certain period of time, the settled nanoparticles diffuse back into the liquid and stay suspended. Carbon nanotube is already one of the most exciting of al the nanoparticles and this phenomenon where the setlled nanoparticles diffuse back into the liquid make it even more useful and interesting.

3.4 Zinc Oxide

A lot of research has been done on oxide of metals to understand how these are excellent conductors of thermal energy and the enhancement in thermal conductivity. The Zinc Oxide was purchased from Reinste Nanoventures. The size of the purchased nanoparticles in the powder was 10 nm. To investigate into the stability of zinc oxide, five samples were prepared by adding SDS as surfactant, each sample had different concentration of SDS, and the concentration of Zinc oxide was same. The stability of the nanofluid was tested using UV-vis spectrophotometer over a period of 22 days.

Also, another study was done on Zinc Oxide to see the effect of sonication time and concentration on the particle size of Zinc Oxide. 3 different concentrations of Zinc Oxide were prepared and each concentration was sonicated for two different sonication times. In all, 6 samples were prepared DLS results were obtained. The DLS results are shown in the section 4.4.2.

3.4.1 Effect of SDS on ZnO stability

The following graphs show the results for 5 ZnO samples. The graphs are accompanied by an explanation of the results. The concentration of ZnO was 0.01%. The concentration of SDS was varied as 5, 15, 50, 100, 200 times that of the ZnO concentration.

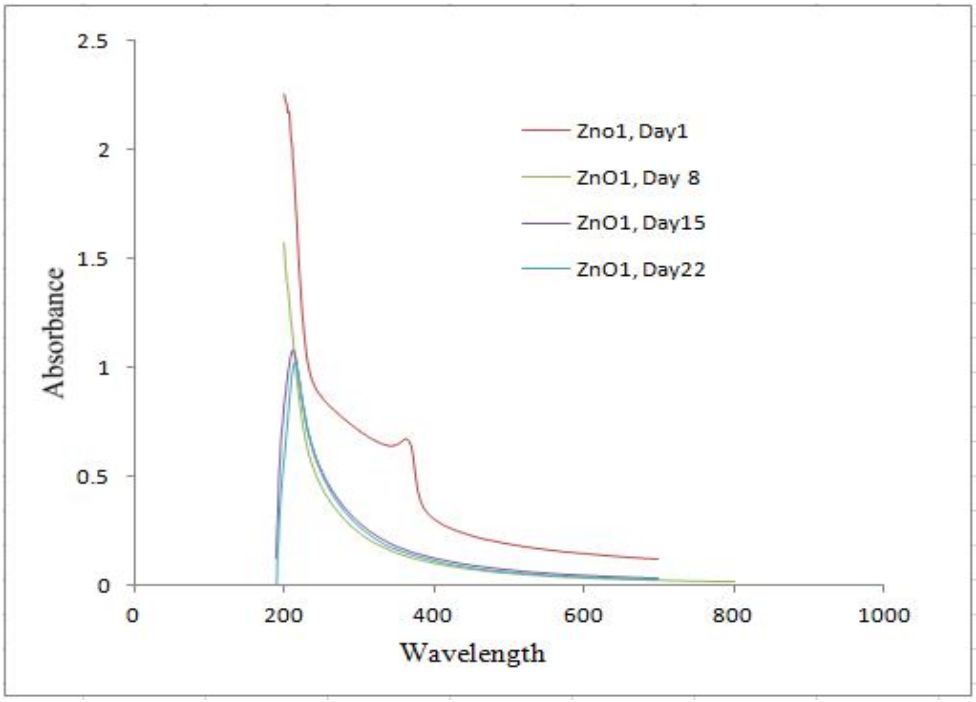

Figure 3.27: ZnO sample 1, spectrophotometer results over a period of 22 days

Sample Details and Observations:

The sample ZnO 1 contains ZnO: 0.01%, SDS: 0.05% (5 times ZnOT). The sample was sonicated for 3 hours after adding ZnO and SDS to the base fluid (DI water). The red curve shows peak absorbance of around 0.7 on day 1 and the blue curve shows absorbance on day 22. This curve does not show any peak. The concentrations have decreased throughout the 22 days. The sample is not stable and has in fact fallen down to the minimum level in a period of 8 days.

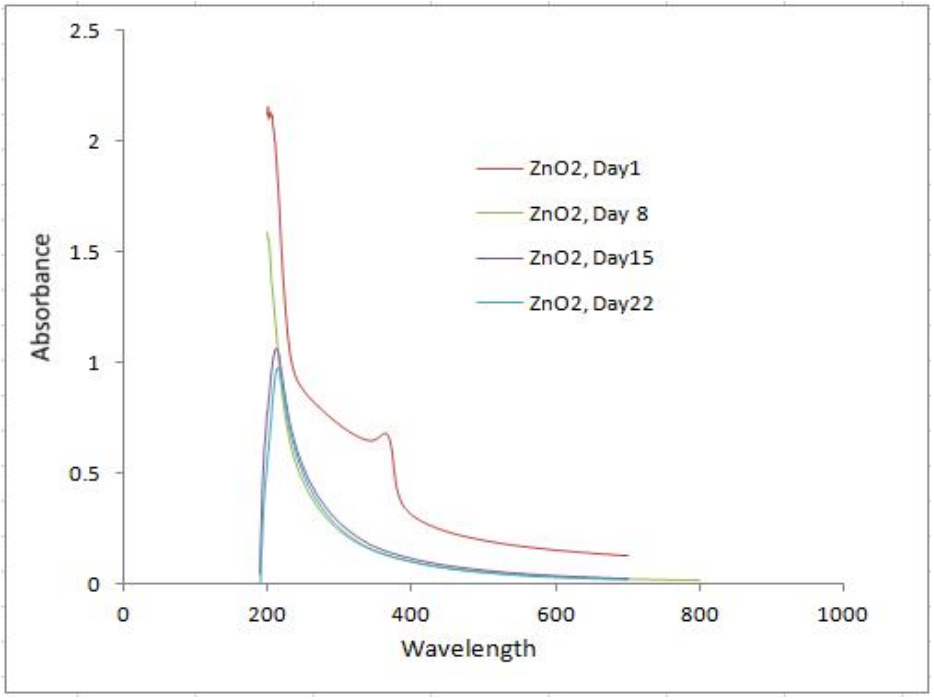

Figure 3.28: ZnO sample 2, spectrophotometer results over a period of 22 days

Sample Details and Observations:

The sample ZnO 2 contains ZnO: 0.01%, SDS: 0.15% (15 times ZnOT). The sample was sonicated for 3 hours after adding ZnO and SDS to the base fluid (DI water). The red curve shows peak absorbance of around 0.7 on day 1 and the blue curve shows absorbance on day 22. This curve does not show any peak. The concentrations have decreased throughout the 22 days. The sample is not stable and has in fact fallen down to the minimum level in a period of 8 days.

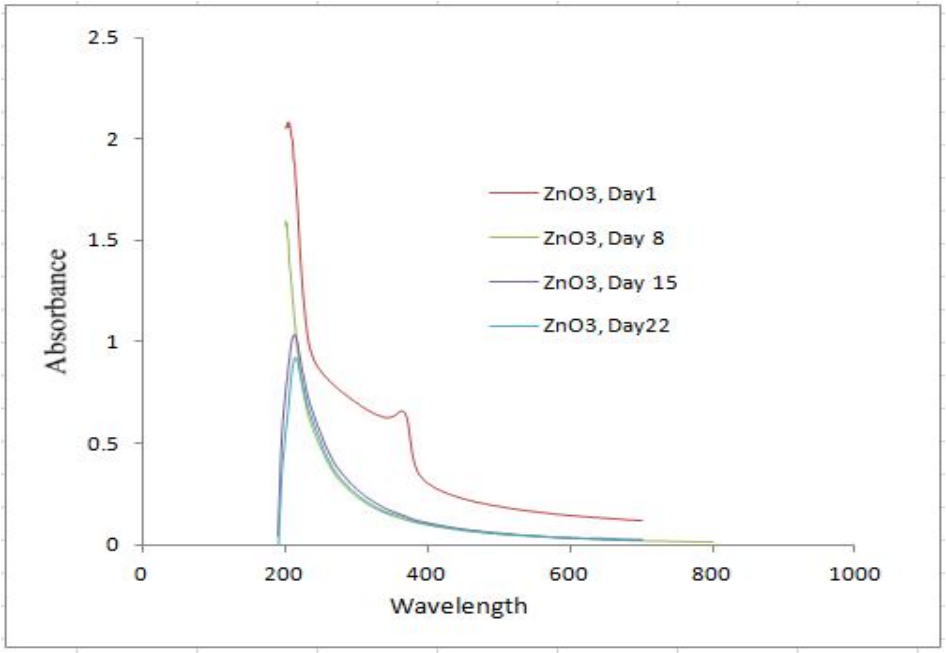

Figure 3.29: ZnO sample 3, spectrophotometer results over a period of 22 days

Sample Details and Observations:

The sample ZnO 3 contains ZnO: 0.01%, SDS: 0.5% (50 times ZnOT). The sample was sonicated for 3 hours after adding ZnO and SDS to the base fluid (DI water). The red curve shows peak absorbance of around 0.7 on day 1 and the blue curve shows absorbance on day 22. This curve does not show any peak. The concentrations have decreased throughout the 22 days. The sample is not stable and has in fact fallen down to the minimum level in a period of 8 days.

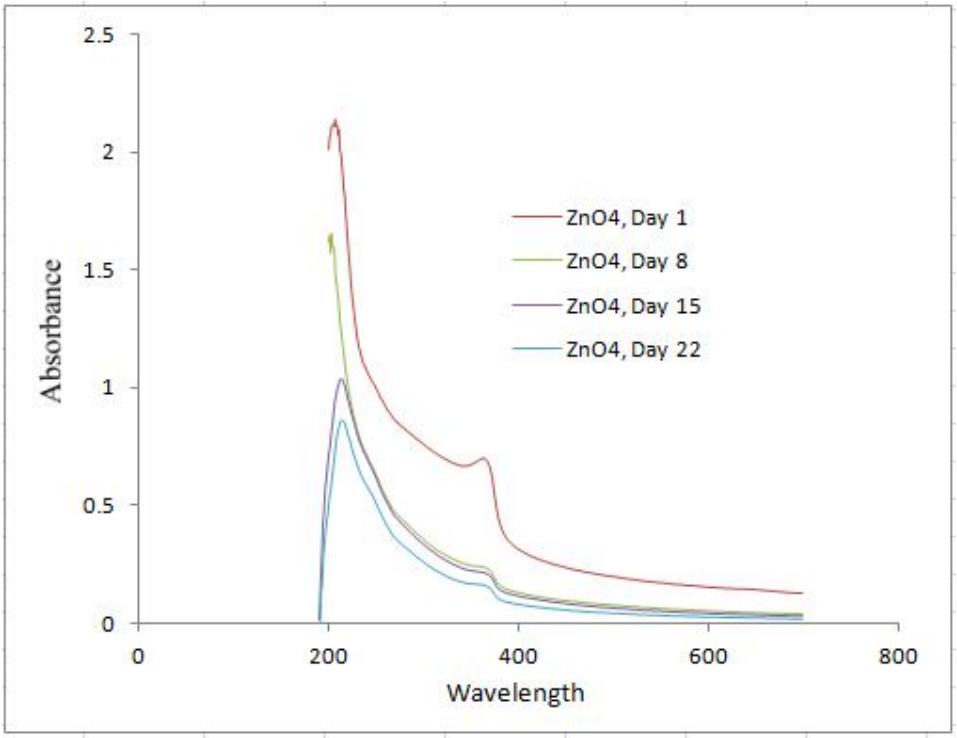

Figure 3.30: ZnO sample 4, spectrophotometer results over a period of 22 days

Sample Details and Observations:

The sample ZnO 4 contains ZnO: 0.01%, SDS: 1% (100 times ZnO). The sample was sonicated for 3 hours after adding ZnO and SDS to the base fluid (DI water). The red curve shows peak absorbance of around 0.7 on day 1 and the blue curve shows absorbance on day 22. This curve shows a peak. The concentrations have decreased throughout the 22 days. The sample is not stable and has settled down, however the settling is not as bad as in the first three cases.

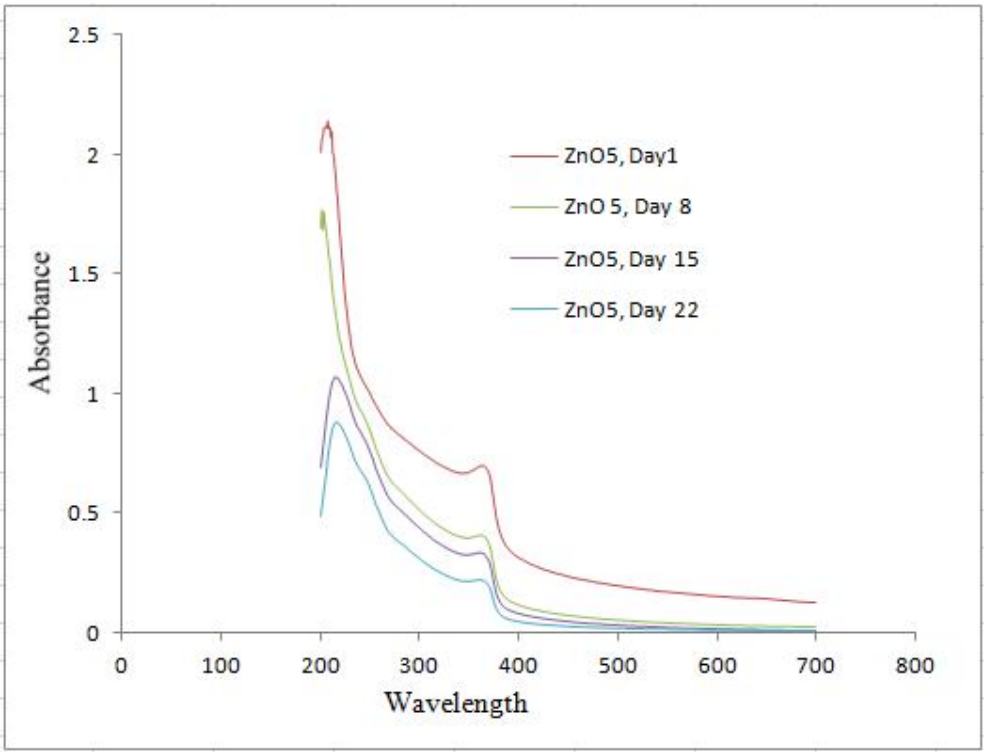

Figure 3.31: ZnO sample 5, spectrophotometer results over a period of 22 days

Sample Details and Observations:

The sample ZnO 5 contains ZnO: 0.01%, SDS: 2% (200 times ZnO). The sample was sonicated for 3 hours after adding ZnO and SDS to the base fluid (DI water). The red curve shows peak absorbance of around 0.7 on day 1 and the blue curve shows absorbance on day 22. This curve shows a peak. The concentrations have decreased throughout the 22 days. The sample is not stable and has settled down, however the settling is not as bad as in the first three cases and it has shown better stability than sample 4.

3.4.2 Effect of sonication time on ZnO particle size

Two different concentrations of Zinc Oxide were prepared and the concentrations were sonicated for two different sonication times. In all, 4 samples were prepared DLS results were obtained. The concentrations were taken as 0.01%, 0.02% and 0.03%. The sonication times were 2.5 hours and 6 hours. The following results were obtained as shown in table 3.1. The percentage of SDS was 0.4% in all samples.

Concentration (percentage)/ Time of sonication (hours)	0.02%	0.03%
2.5 hours	311.5 nm	348.3 nm
6 hours	359.6 nm	351.3 nm

Table 3.1: Effect of sonication time and concentration on particle size

The snapshots of the above DLS results have been added to the appendix.

In the next section we discuss the spectrophotometer and DLS results obtained from Zinc Oxide.

3.4.3 Results and Discussion for Zinc Oxide

1). Zinc Oxide nanoparticles have shown the least stability. At lower concentrations of SDS the particles settle down very soon, however, at higher concentrations of SDS the settling is slower but it is still huge and renders it unsuitable for use in practical applications.

2). The effect of sonication on ZnO is also not clear. The particle sizes have remained the same inspite of increase in sonication period. The particle size has remained in the range of around 300-400 nm in all cases.

List of Symbols

D : Diffusion Coefficient

D_H : Thermal diffusivity

d: Characteristic dimension

E_{sed} : Energy gained by a particle settling at a distance equal to its radius

E_{therm} : Thermal energy of the particle

g : Acceleration due to gravity

g_H : Heat Conductance

k: Thermal conductivity

k_B : Boltzmann Constant

m: Mass of particle

Pe : Peclet Number

q_x : Heat flux in x-direction

Q_x : Heat flowing in x-direction

R : Radius of spherical particle

T: Temperature

U: Electrophoretic mobility

V: Terminal velocity of a particle settling down in a fluid

Greek Symbols:

Δ : Difference

ε : Dielectric Constant

ρ: Density

□: Dynamic viscosity

μ: Kinematic viscosity

ζ : Zeta Potential

Subscripts:

B : Boltzmann

p : particle

l : liquid

x : x-direction

REFERENCES

Choi S.U.S., 2009, Journal of Heat Transfer, Vol 131.

Chopkar M., Das P.K., Manna I., 2006, Synthesis and characterization of nanofluid for advanced heat transfer application, Scr Mater, 55, PP 549-552.

Das S.K., Choi S.U.S., Patel H.E., 2006, Heat Transfer in Nanofluids – A review, Heat Transfer Engineering, Vol. 27 no. 10.

Dong Wook Oh, Jain A., Eaton J.K., Goodson K.E., Lee J.S., 2008, Thermal conductivity measurement and sedimentation detection of aluminium oxide nanofluids by using the 3-omega method, International Journal of heat and fluid flow 29, 1456-1461.

Eastman J.A., Choi S.U.S., Li S., Yu W., Thomson L.J., 2011, Anomalaously increased effective thermal conductivities of ethylene glycol based nanofluids containing copper nanoparticles, Appl. Phys Lett, 78, PP 718-720.

Foley E.T., Hersam M.C., 2006, assessing the need for nanotechnology education reform in the United States, Nanotechnology Law & Business Volume 3 No. 4.

Ghadimi A., R.Saidur, Metselaar H.S.C., 2011, A review of nanofluid stability properties and characterization in stationary conditions, International Journal of Heat and Mass transfer 54, 4051-4068.

Gharagozloo P.E., Goodson K.E., 2010, Aggregate fractal dimensions and thermal conduction in nanofluids, J. Appl. Phys. 108 (7).

Hong K.S., Hong T.K., 2006, Thermal conductivity of Fe nanofluids depending on the cluster size of nanoparticles, Appl. Phys. Lett. 88 (3) 1-3.

Hwang Y., Lee J.K., Lee C.H., Jung Y.M., Cheong S.I., Lee C.G., Ku B.C., Jang S.P., 2007, Stability and thermal conductivity characteristics of nanofluids, Thermochimica Acta 455, 70-74.

Hwang Y., Lee J.K., Lee Jong-Ku, Jeong Young-Man, Cheong Seong-ir, Ahn Young-Chull, Soo H. Kim, 2008, Production and dispersion stability of nanoparticles and nanofluids, Powder technology 186, 145-153.

J.V. Sengers and J.T.R. Watson, Improved International Formulations for the Viscosity and thermal conductivity of water substance, 1986.

Keblinski P., Prasher R., Eapen J., 2008, Thermal Conductance of nanofluids: is the controversy over?, J Nanopart RES 10: 1089-1097.

Kwak K., Kim C., 2005, Viscosity and thermal conductivity of copper oxide nanofluid dispersed in ethylene glycol, Korea-Aust. Rheol J., 17(2), pp 35-40.

L. Vandsburger, 2009, Synthesis and covalent surface modification of carbon nanotubes for preparation of stabilized nanofluid suspensions, M-Eng, Mc Gill University (Canada).

Lee K., Hwang Y., Cheong S., Kwon L., Kim S., Lee J., 2009, Performance evaluation of nanolubricants of fullerene nanoparticles in refrigeration mineral oil, Curr Appl Phys. 9 (2, Suppl. 1), e128-e131.

Li Y., Zhou J.E., Tung S., Schneider E., Xi S., 2009, A review on development of nanofluid preparation and characterization, powder Technol. 196(2), 89-101.

Liu M.S., Lin M.C.C., Tsai C.Y., Wang C.C, 2006, Enhancement of thermal conductivity with copper for nanofluids using Chemical reduction Method, int. J. Heat Mass Transfer, 49, pp 3028-3033.

Maxwell J.C. 1873, A treatise on electricity and magnetism.

Phuoc T.X., Soong Y., Chyu M.K., 2007, Synthesis of Ag-deionized waternanofluids using multi beam laser ablation in liquids, opt. laser engg., 45, pp1099-1106.

Wang X.-J., Zhu D.-S.Yang S., 2009, Investigation of pH and SDBS on enhancement of thermal conductivity in nanofluids, Chem Phys. Lett. 470 (1-3), 107-111

X. Wei, H. Zhu, T. Kong, L. Wang, Synthesis and thermal conductivity of Cu_2O nanofluids, Int. J. Heat Mass Transfer 52 (19-20), 4371-4374.

Yang B., Han Z.H., 2006, Thermal conductivity enhancement in water in FC72 nanoemulsion fluids, volume 88, issue 26, pages 261914-261914(3).

Zhu H., Zhang C., Liu S., Tang Y., 2006, Effect of nanoparticle clustering and alignment on Thermal Conductivities of Fe_3O_4 aqueous nanofluids, Appl. Phys. Lett., 89, p. 023123.

Y. Hwang, H.S.Park, J.K.Lee, W.H. Jung, Thermal Conductivity and Lubrication characteristics of nanofluids, Current Applied Physics 6SI (2006) e67-e71.

P.Keblinski, S.R. Phillpot, S.U.S. Choi, J.A. Eastman, Mechanisms of heat flow in suspensions of nano-sized particles (nanofluids), International Journal of Heat and Mass Transfer 45 (2002) 855-863.

Robert Taylor, Sylvan Coulombe, Todd Otanian, Patrick Phelan, Andrey Gunawan et al. Journal of Applied Physics, Small particles big impacts: A review of the diverse applications of nanofluids.

APPENDIX A

The following are the snapshots of the DLS results of the silver samples along with the sample description (section 3.2).

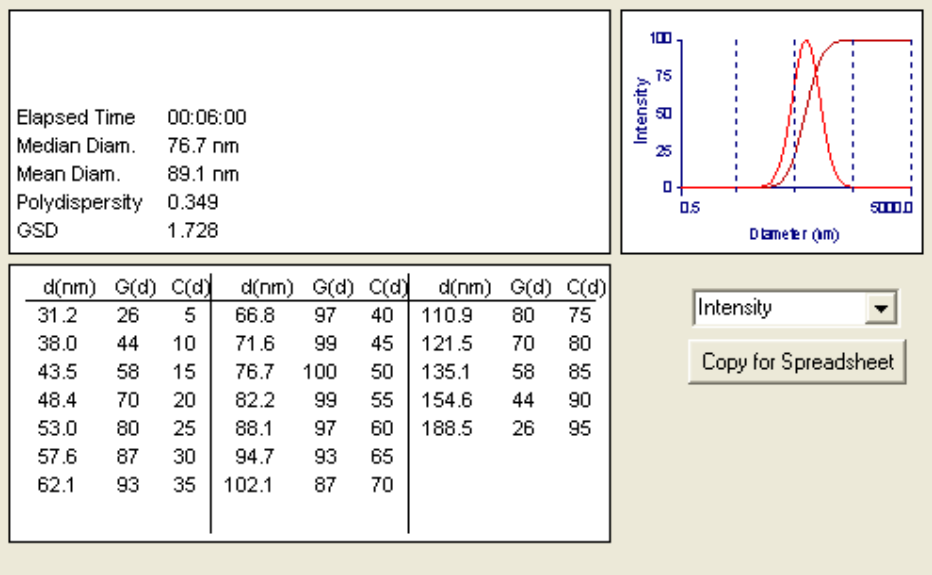

d(nm)	G(d)	C(d)	d(nm)	G(d)	C(d)	d(nm)	G(d)	C(d)
31.2	26	5	66.8	97	40	110.9	80	75
38.0	44	10	71.6	99	45	121.5	70	80
43.5	58	15	76.7	100	50	135.1	58	85
48.4	70	20	82.2	99	55	154.6	44	90
53.0	80	25	88.1	97	60	188.5	26	95
57.6	87	30	94.7	93	65			
62.1	93	35	102.1	87	70			

Figure A1: 0.5% concentration, 2 hour sonication, day 1

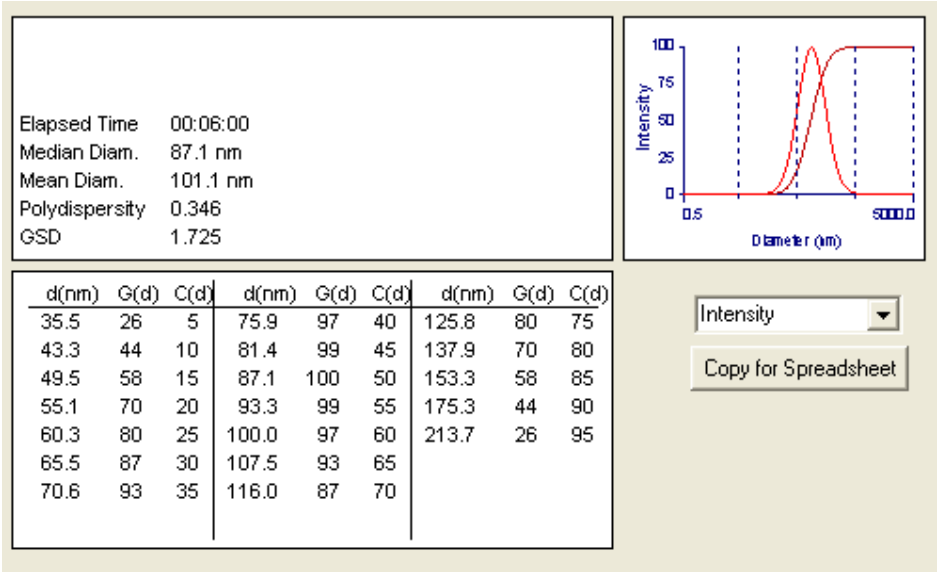

Figure A2: 0.5% concentration, 2 hour sonicated, day 6

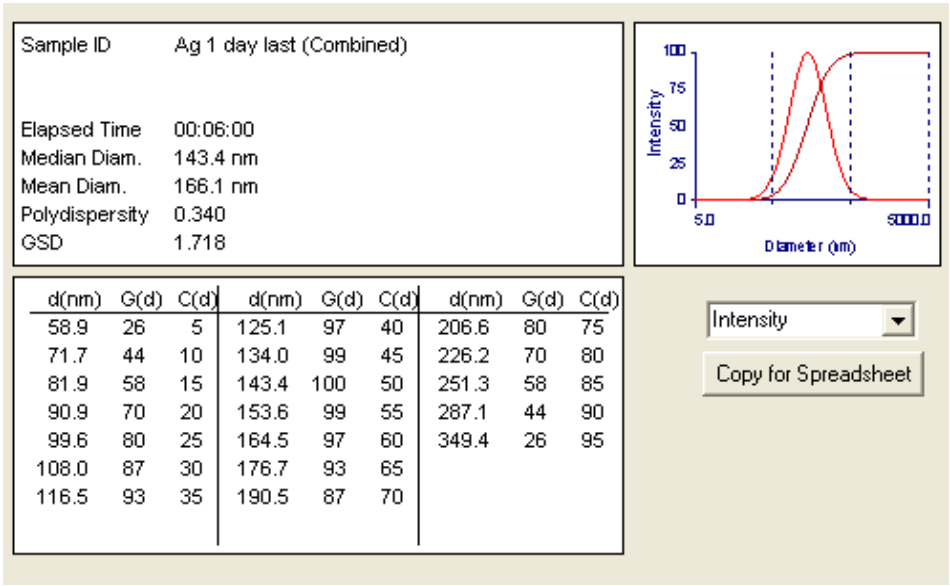

Figure A3: 0.5% concentration, 2 hour sonicated, day 12

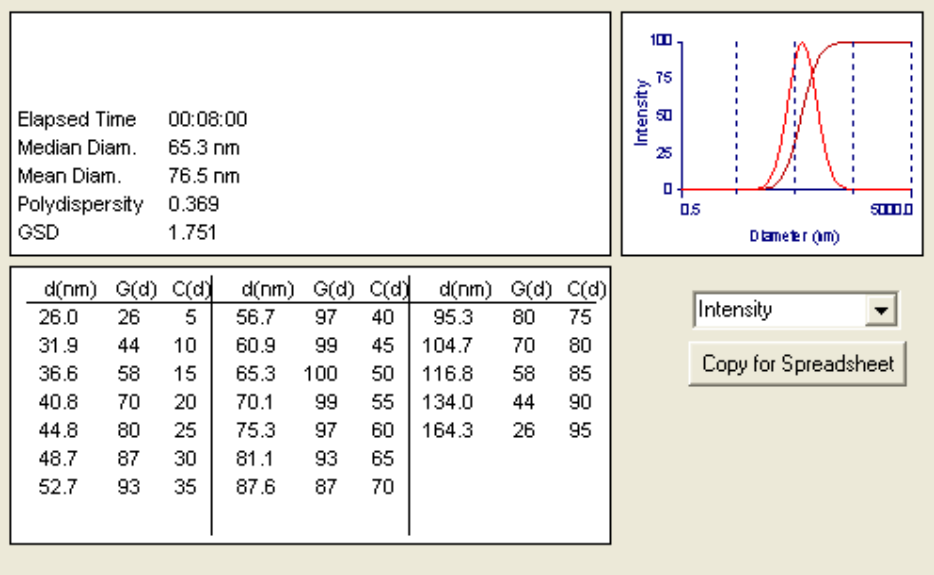

Figure A4: 0.5% concentration, 0 hour sonicated, day 1

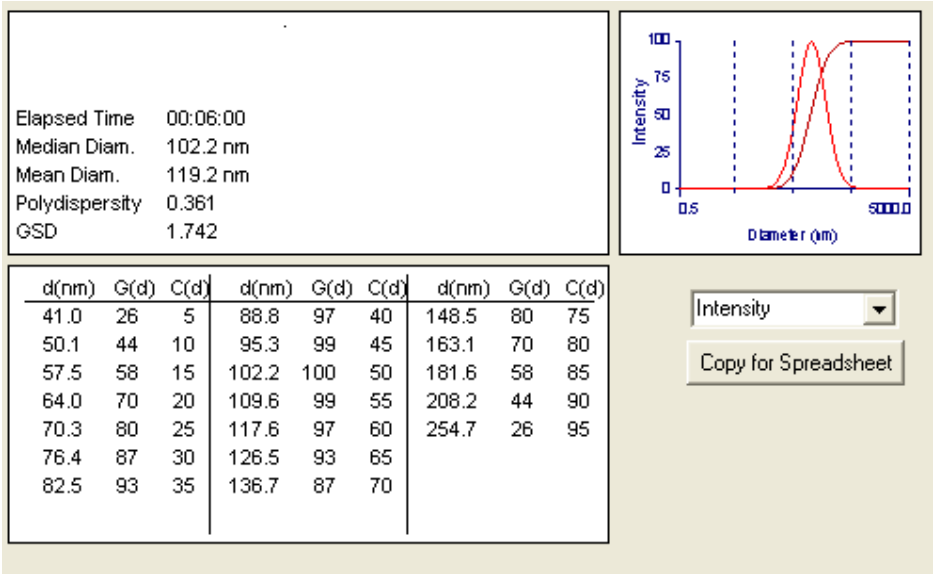

Figure A5: 0.5% concentration, 0 hour sonicated, day 6

Sample ID	Ag 7 day last (Combined)
Date - Time	Apr 13, 2013 16:43:55
Operator ID	parveer
Elapsed Time	00:06:00
Median Diam.	157.5 nm
Mean Diam.	183.9 nm
Polydispersity	0.364
GSD	1.746

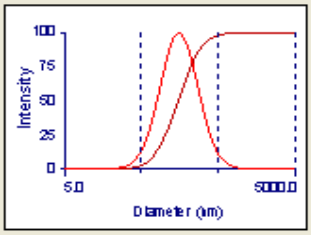

d(nm)	G(d)	C(d)	d(nm)	G(d)	C(d)	d(nm)	G(d)	C(d)
63.0	26	5	136.8	97	40	229.3	80	75
77.1	44	10	146.8	99	45	251.8	70	80
88.4	58	15	157.5	100	50	280.5	58	85
98.5	70	20	169.0	99	55	321.7	44	90
108.2	80	25	181.3	97	60	393.9	26	95
117.6	87	30	195.2	93	65			
127.1	93	35	210.9	87	70			

Intensity

Copy for Spreadsheet

Figure A6: 0.5% concentration, 0 hour sonicated, day 12

Elapsed Time	00:06:00
Median Diam.	239.2 nm
Mean Diam.	276.1 nm
Polydispersity	0.333
GSD	1.709

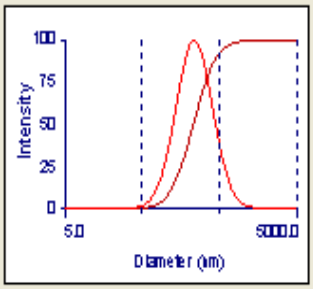

d(nm)	G(d)	C(d)	d(nm)	G(d)	C(d)	d(nm)	G(d)	C(d)
99.1	26	5	208.9	97	40	343.2	80	75
120.4	44	10	223.6	99	45	375.6	70	80
137.3	58	15	239.2	100	50	416.7	58	85
152.3	70	20	255.9	99	55	475.4	44	90
166.7	80	25	273.9	97	60	577.5	26	95
180.6	87	30	294.0	93	65			
194.6	93	35	316.7	87	70			

Intensity

Copy for Spreadsheet

Figure A7: 0.5% concentration, 4 hour sonicated, day 1

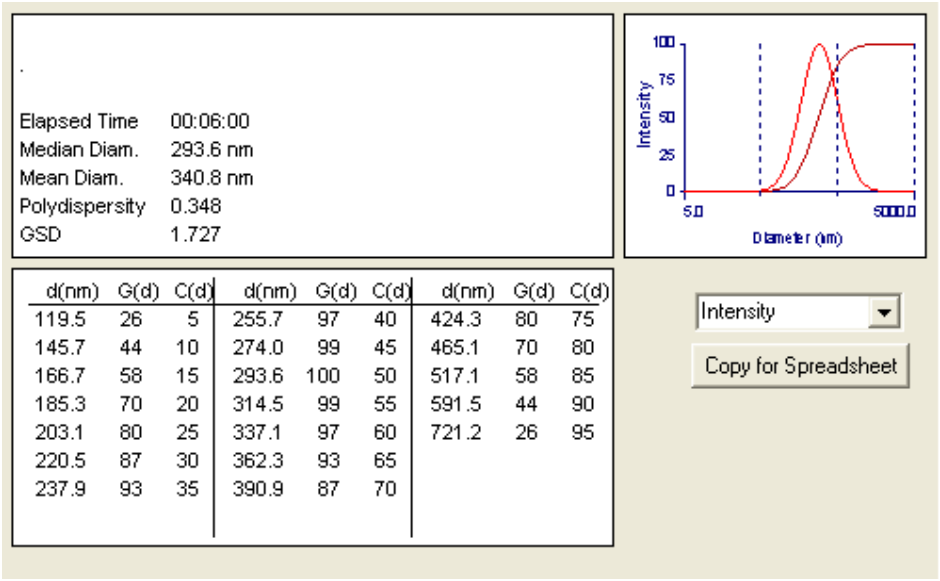

Figure A8: 0.5% concentration, 4 hour sonicated, day 6

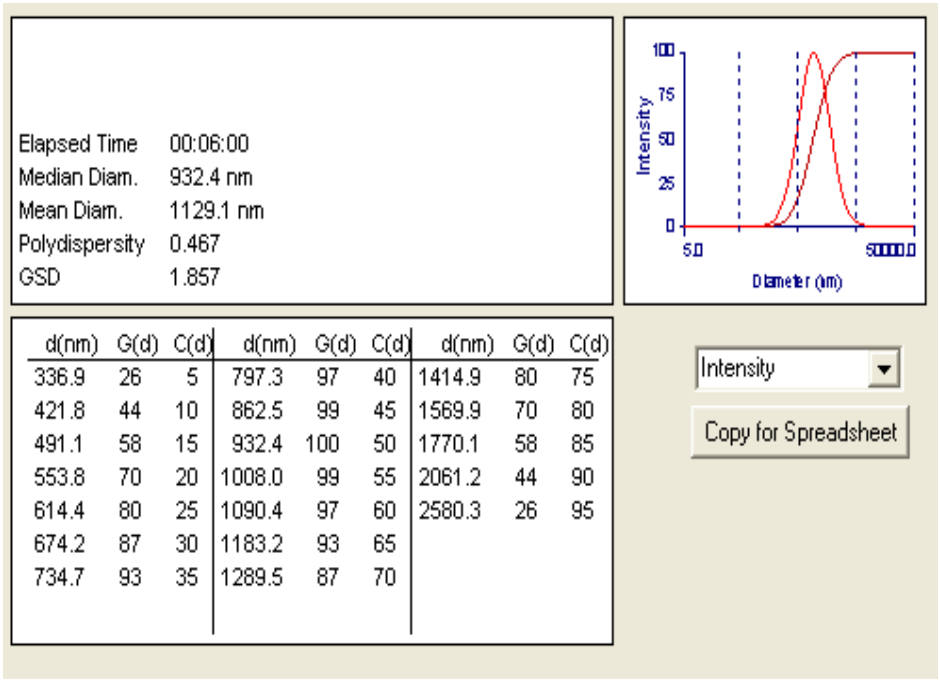

Figure A9: 0.5% concentration, 4 hour sonicated, day 12

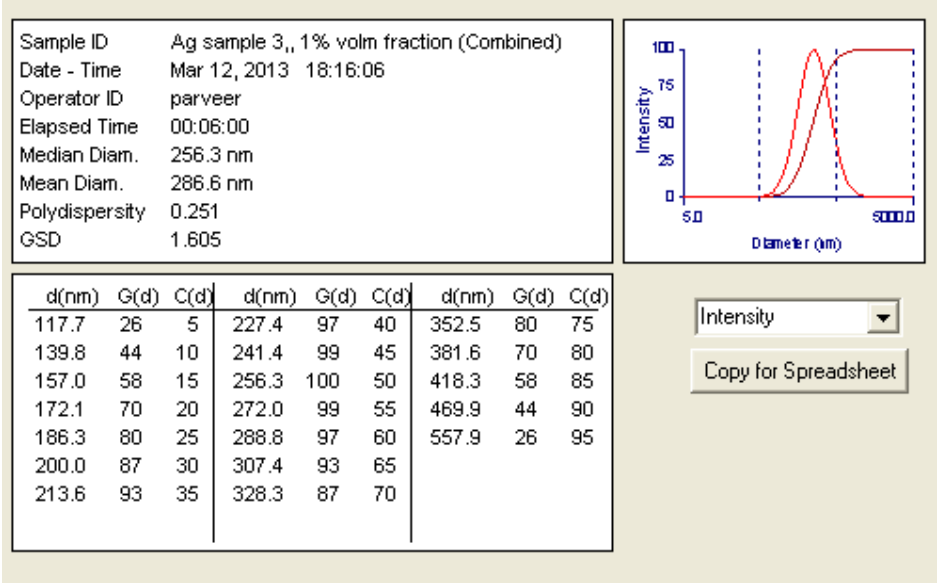

Sample ID	Ag sample 3,, 1% volm fraction (Combined)
Date - Time	Mar 12, 2013 18:16:06
Operator ID	parveer
Elapsed Time	00:06:00
Median Diam.	256.3 nm
Mean Diam.	286.6 nm
Polydispersity	0.251
GSD	1.605

d(nm)	G(d)	C(d)	d(nm)	G(d)	C(d)	d(nm)	G(d)	C(d)
117.7	26	5	227.4	97	40	352.5	80	75
139.8	44	10	241.4	99	45	381.6	70	80
157.0	58	15	256.3	100	50	418.3	58	85
172.1	70	20	272.0	99	55	469.9	44	90
186.3	80	25	288.8	97	60	557.9	26	95
200.0	87	30	307.4	93	65			
213.6	93	35	328.3	87	70			

Figure A10: 0.5% concentration, 6 hour sonicated, day 1

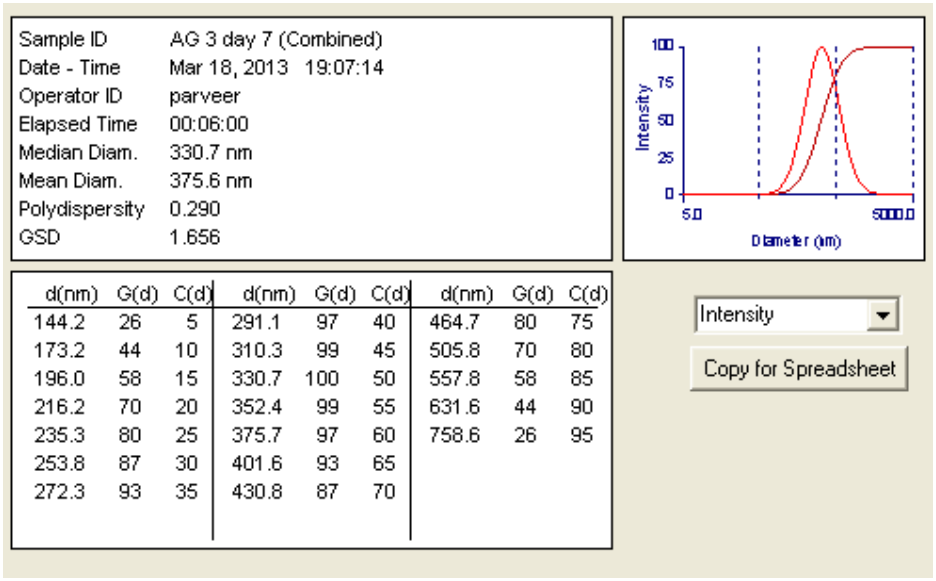

Sample ID	AG 3 day 7 (Combined)
Date - Time	Mar 18, 2013 19:07:14
Operator ID	parveer
Elapsed Time	00:06:00
Median Diam.	330.7 nm
Mean Diam.	375.6 nm
Polydispersity	0.290
GSD	1.656

d(nm)	G(d)	C(d)	d(nm)	G(d)	C(d)	d(nm)	G(d)	C(d)
144.2	26	5	291.1	97	40	464.7	80	75
173.2	44	10	310.3	99	45	505.8	70	80
196.0	58	15	330.7	100	50	557.8	58	85
216.2	70	20	352.4	99	55	631.6	44	90
235.3	80	25	375.7	97	60	758.6	26	95
253.8	87	30	401.6	93	65			
272.3	93	35	430.8	87	70			

Figure A11: 0.5% concentration, 6 hour sonicated, day 6

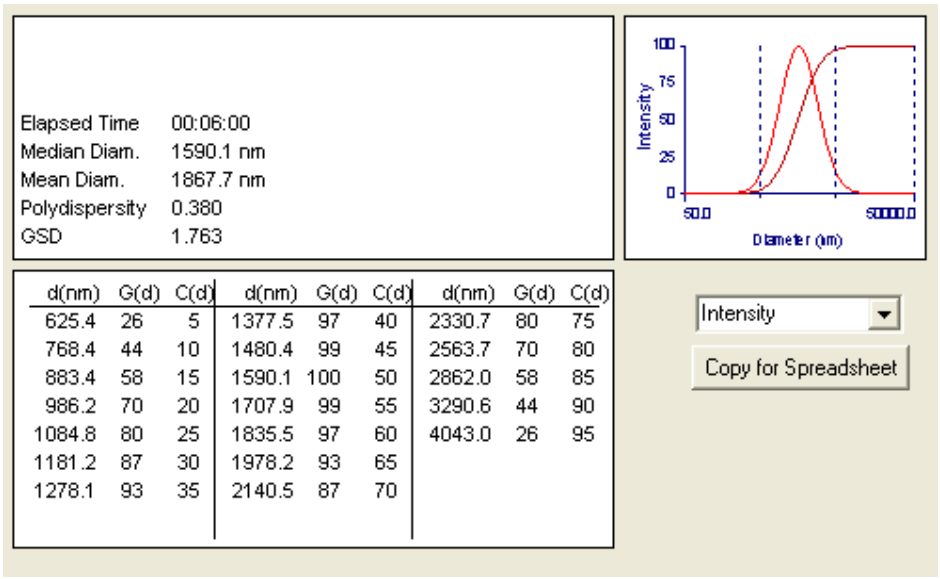

Figure A12: 0.5% concentration, 6 hour sonicated, day 12

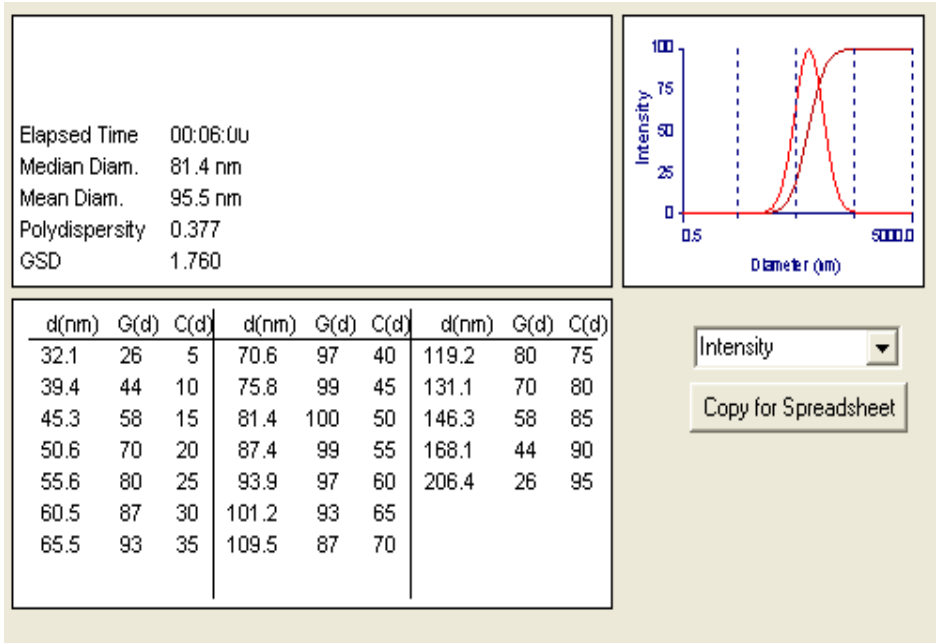

Figure A13: 1% concentration, 0 hour sonicated, day 1

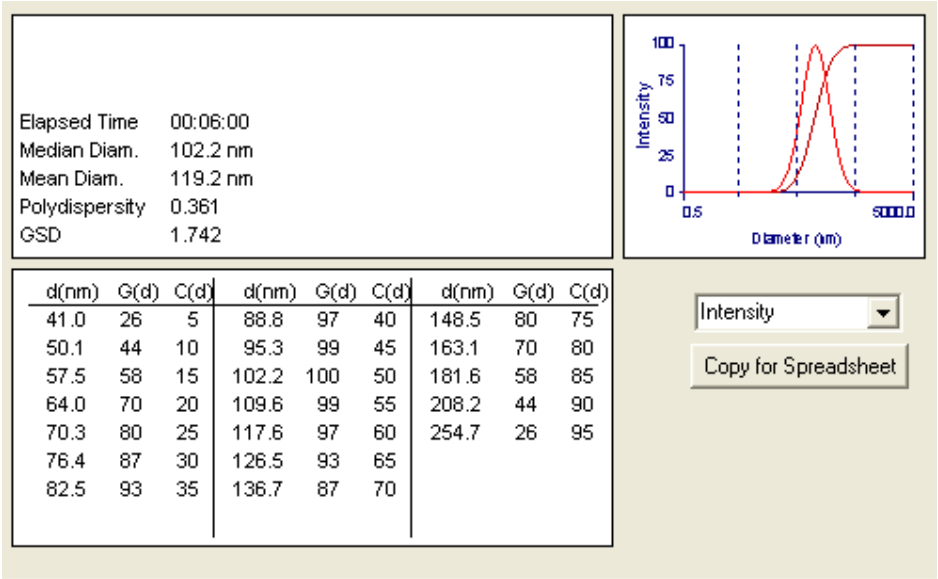

Figure A14: 1% concentration, 0 hour sonicated, day 6

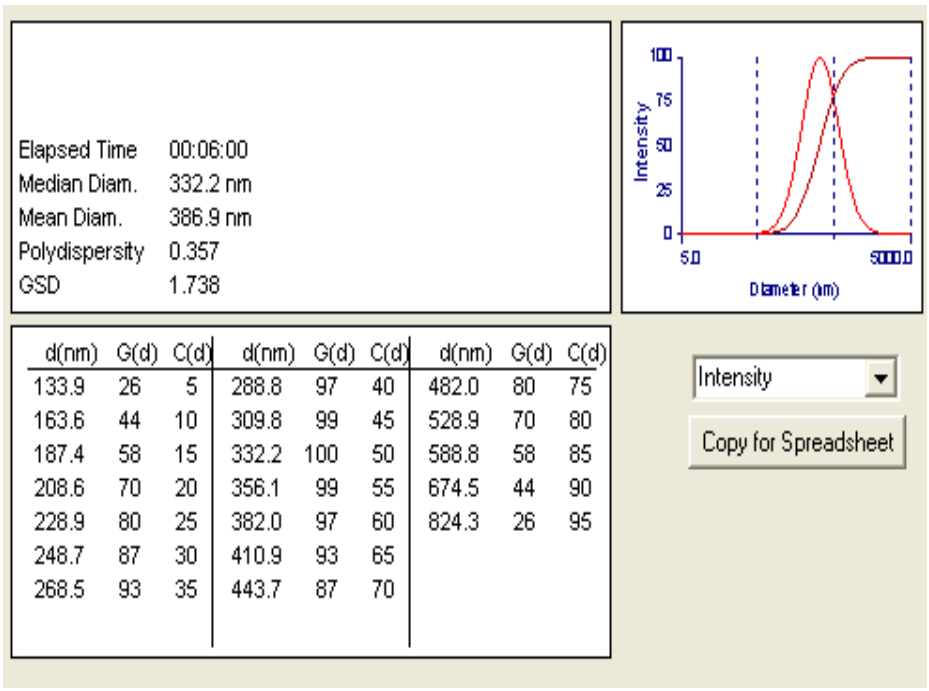

Figure A15: 1% concentration, 0 hour sonicated, day 12

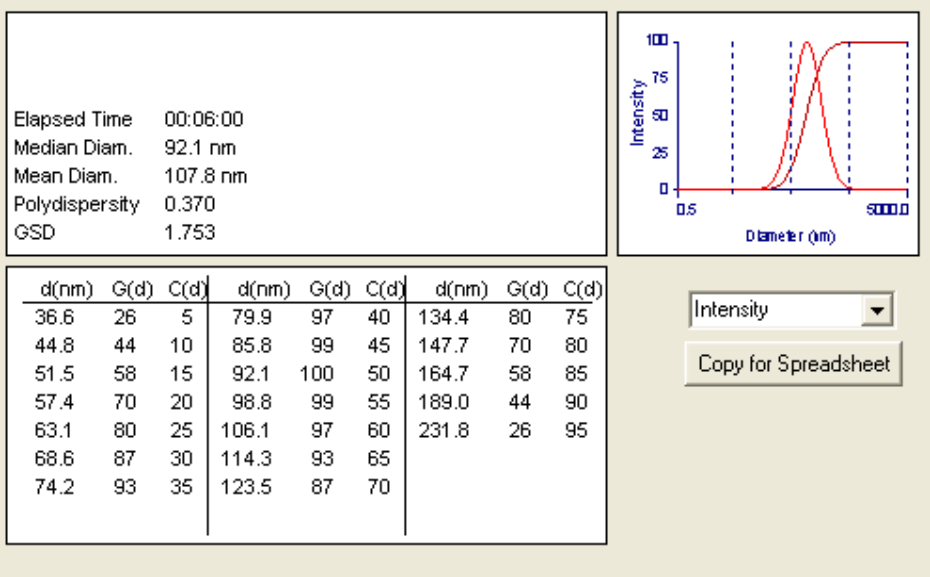

Figure A16: 1% concentration, 2 hour sonicated, day 1

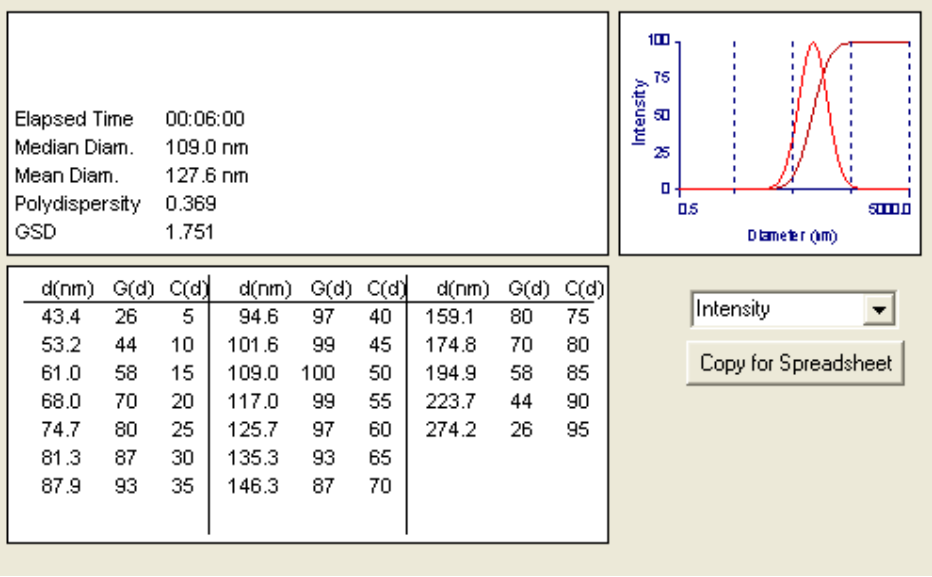

Figure A17: 1% concentration, 2 hour sonicated, day 6

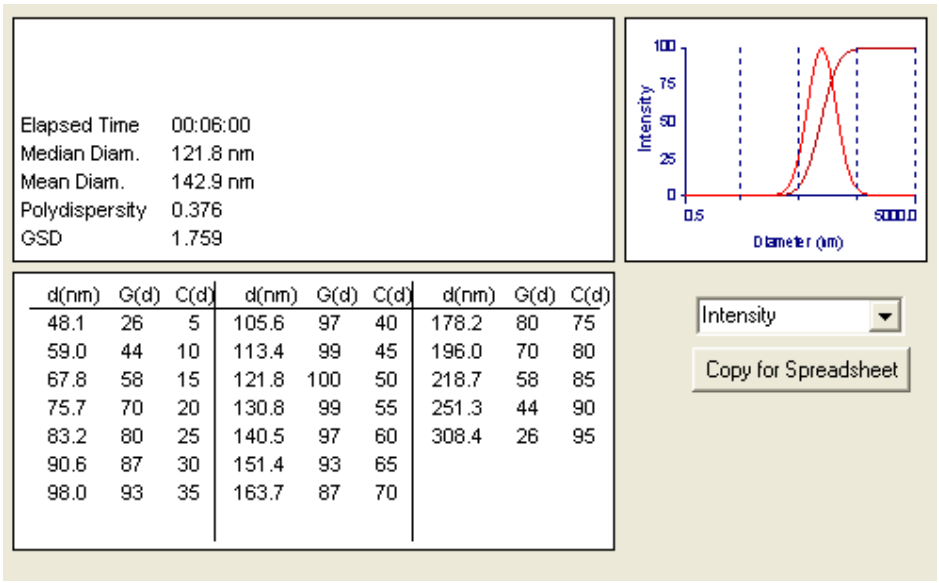

Figure A18: 1% concentration, 2 hour sonicated, day 12

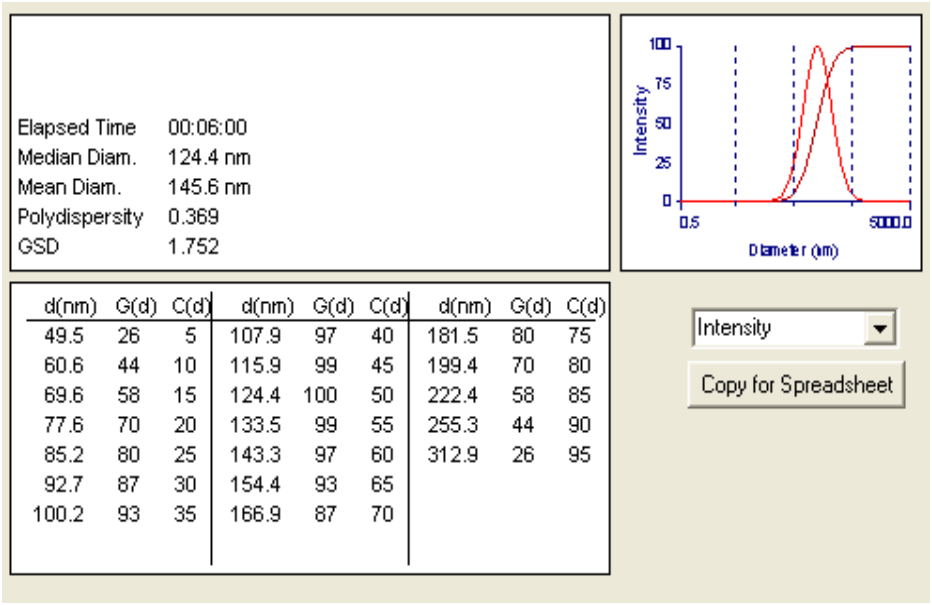

Figure A19: 1% concentration, 4 hour sonicated, day 1

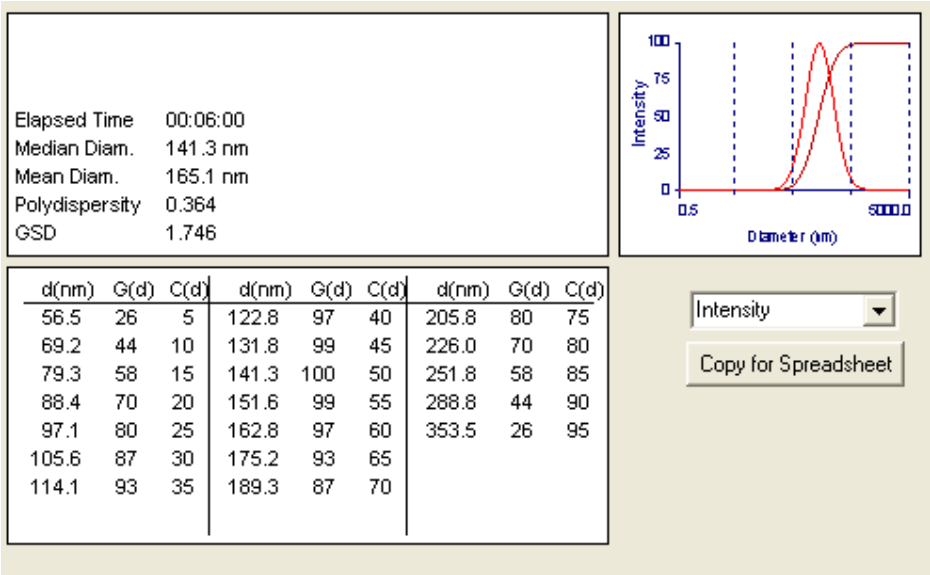

Figure A20: 1% concentration, 4 hour sonicated, day 6

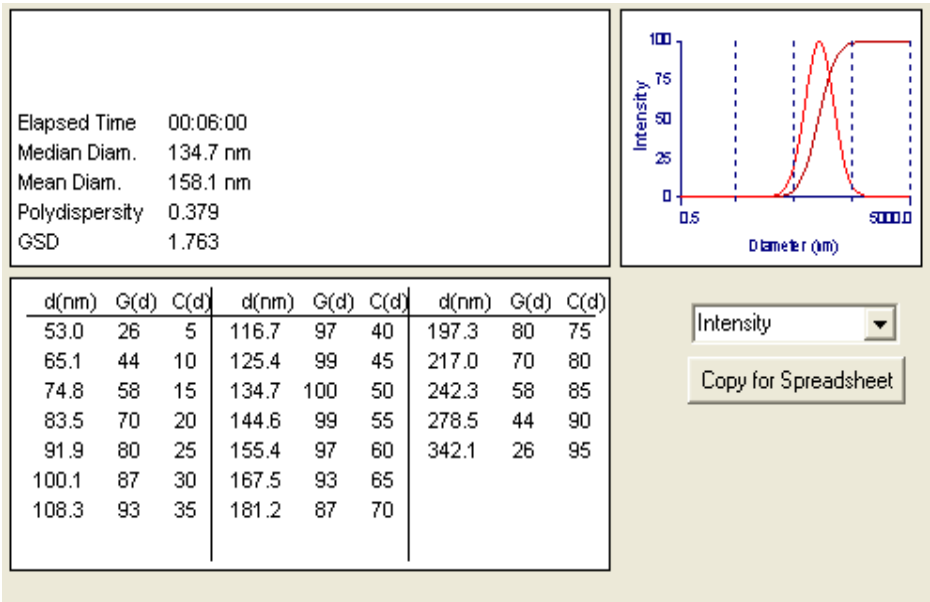

Figure A21: 1% concentration, 4 hour sonicated, day 12

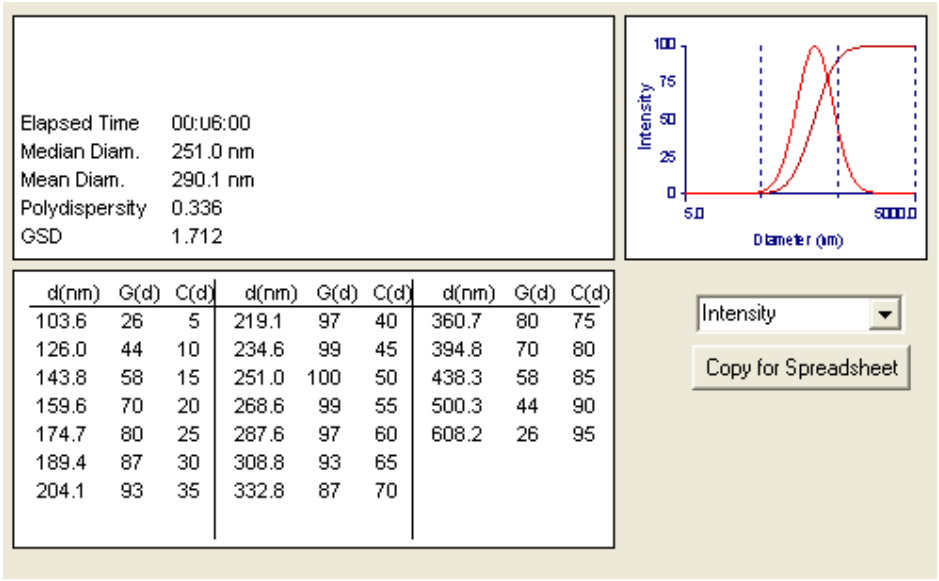

Figure A22: 1% concentration, 6 hour sonicated, day 1

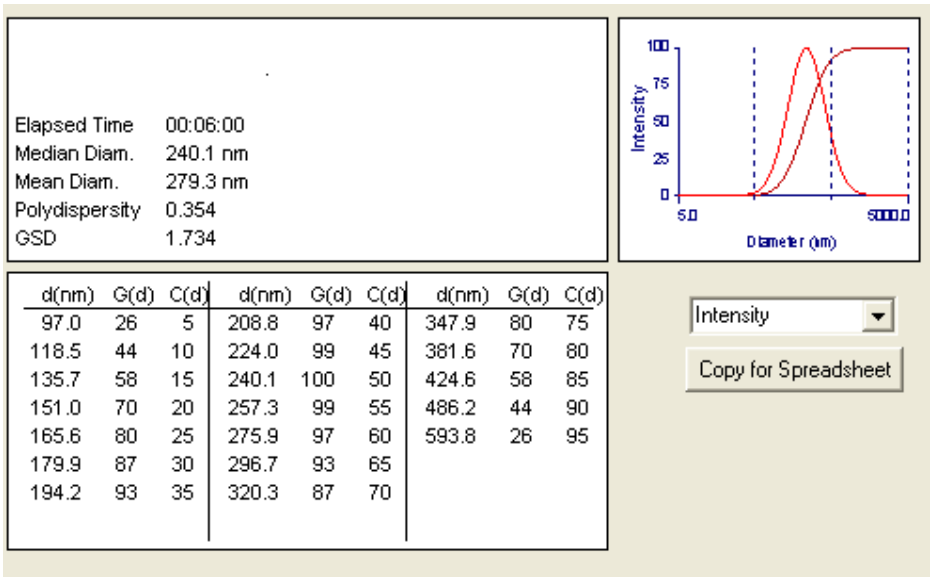

Figure A23: 1% concentration, 6 hour sonicated, day 6

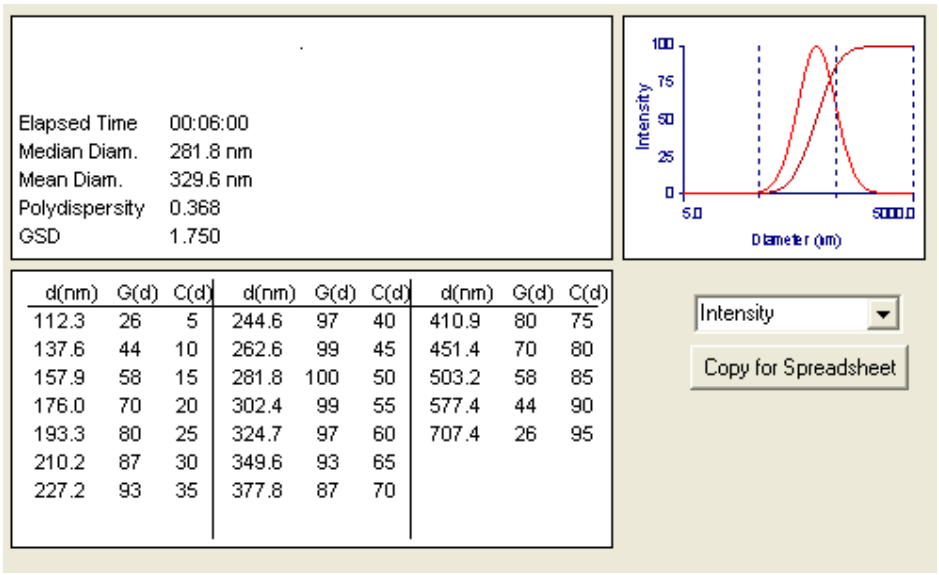

Figure A24: 1% concentration, 6 hour sonicated, day 12

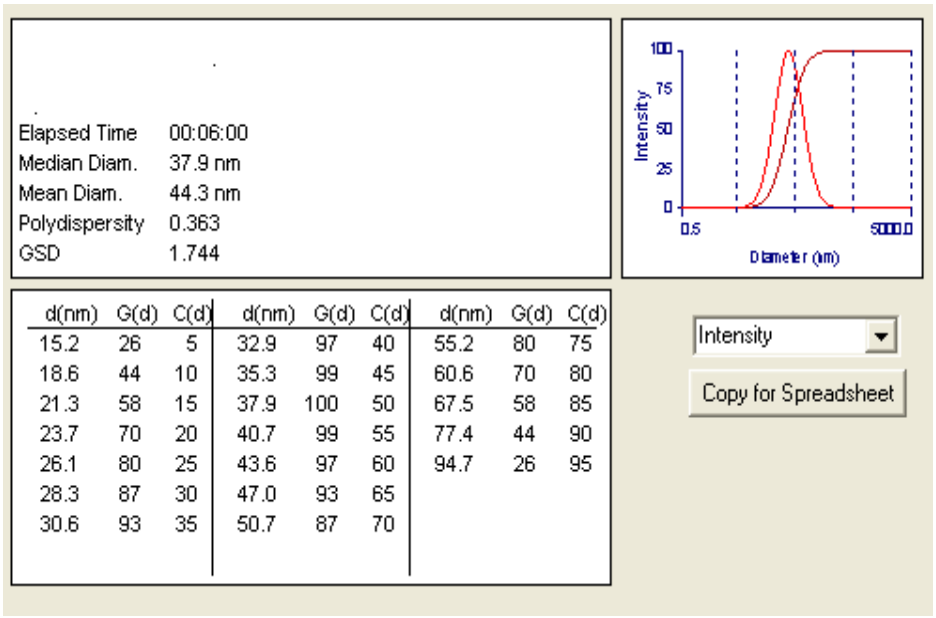

Figure A25: 2% concentration, unsonicated, day 1

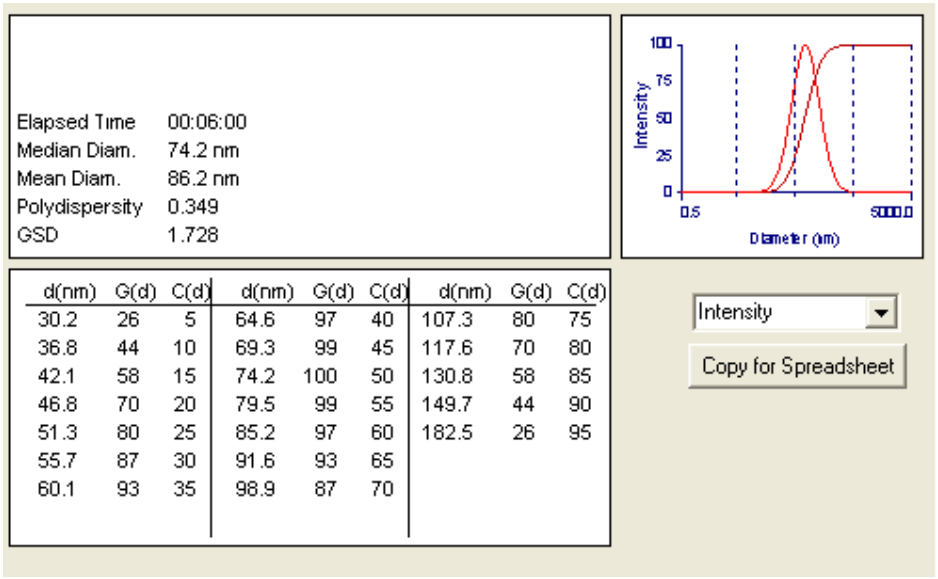

Figure A26: 2% concentration, unsonicated, day 6

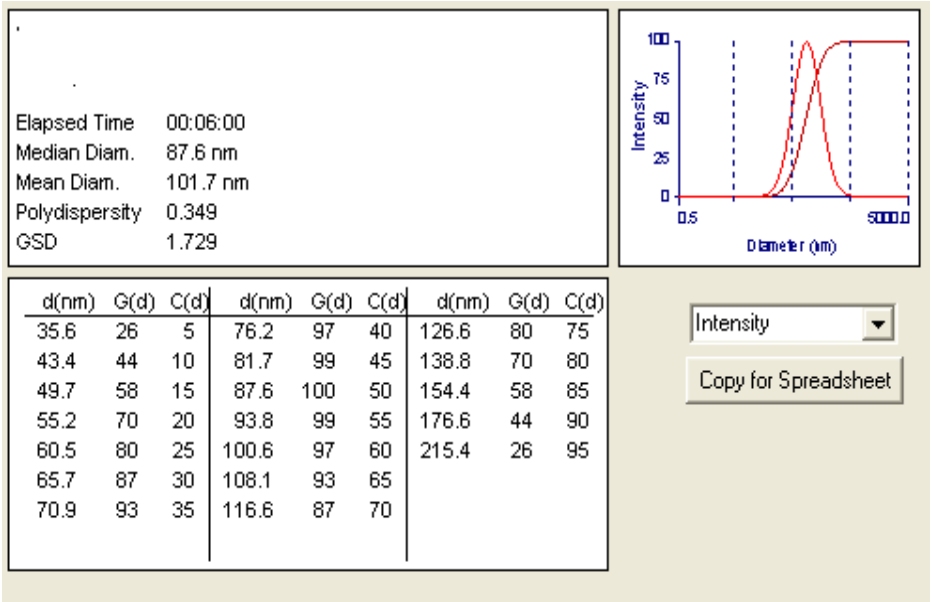

Figure A27: 2% concentration, unsonicated, day 12

APPENDIX B

The following are the snapshots of the DLS results of the four Zinc Oxide samples (section 3.4).

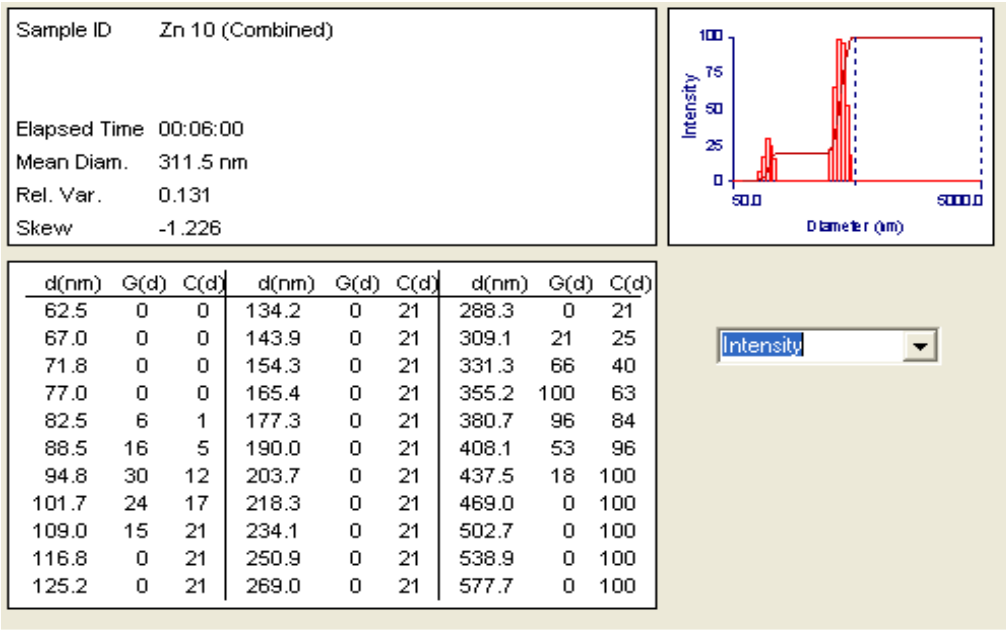

d(nm)	G(d)	C(d)	d(nm)	G(d)	C(d)	d(nm)	G(d)	C(d)
62.5	0	0	134.2	0	21	288.3	0	21
67.0	0	0	143.9	0	21	309.1	21	25
71.8	0	0	154.3	0	21	331.3	66	40
77.0	0	0	165.4	0	21	355.2	100	63
82.5	6	1	177.3	0	21	380.7	96	84
88.5	16	5	190.0	0	21	408.1	53	96
94.8	30	12	203.7	0	21	437.5	18	100
101.7	24	17	218.3	0	21	469.0	0	100
109.0	15	21	234.1	0	21	502.7	0	100
116.8	0	21	250.9	0	21	538.9	0	100
125.2	0	21	269.0	0	21	577.7	0	100

Figure B1: ZnO sample, DLS results

Sample Details:

The sample ZnO contains ZnO: 0.02%, SDS: 0.4%. The sample was sonicated for 2.5 hours after adding ZnO and SDS to the base fluid (DI water). Mean nanoparticle diameter is 311.5nm.

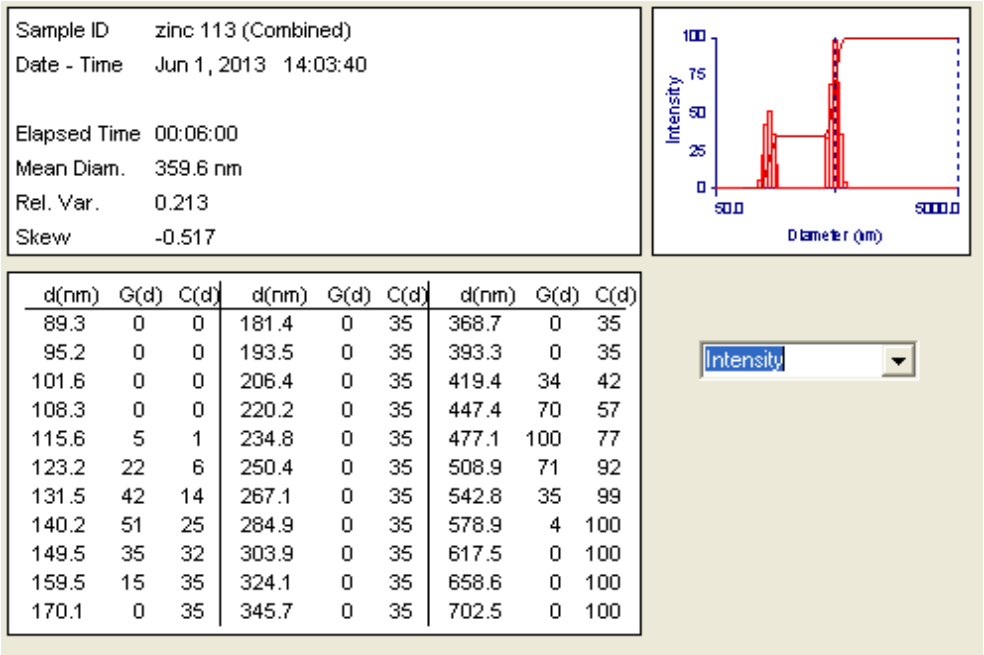

d(nm)	G(d)	C(d)	d(nm)	G(d)	C(d)	d(nm)	G(d)	C(d)
89.3	0	0	181.4	0	35	368.7	0	35
95.2	0	0	193.5	0	35	393.3	0	35
101.6	0	0	206.4	0	35	419.4	34	42
108.3	0	0	220.2	0	35	447.4	70	57
115.6	5	1	234.8	0	35	477.1	100	77
123.2	22	6	250.4	0	35	508.9	71	92
131.5	42	14	267.1	0	35	542.8	35	99
140.2	51	25	284.9	0	35	578.9	4	100
149.5	35	32	303.9	0	35	617.5	0	100
159.5	15	35	324.1	0	35	658.6	0	100
170.1	0	35	345.7	0	35	702.5	0	100

Figure B2: ZnO sample, DLS results

Sample Details:

The sample ZnO contains ZnO: 0.02%, SDS: 0.4%. The sample was sonicated for 6 hours after adding ZnO and SDS to the base fluid (DI water). Mean nanoparticle diameter is 359.6nm.

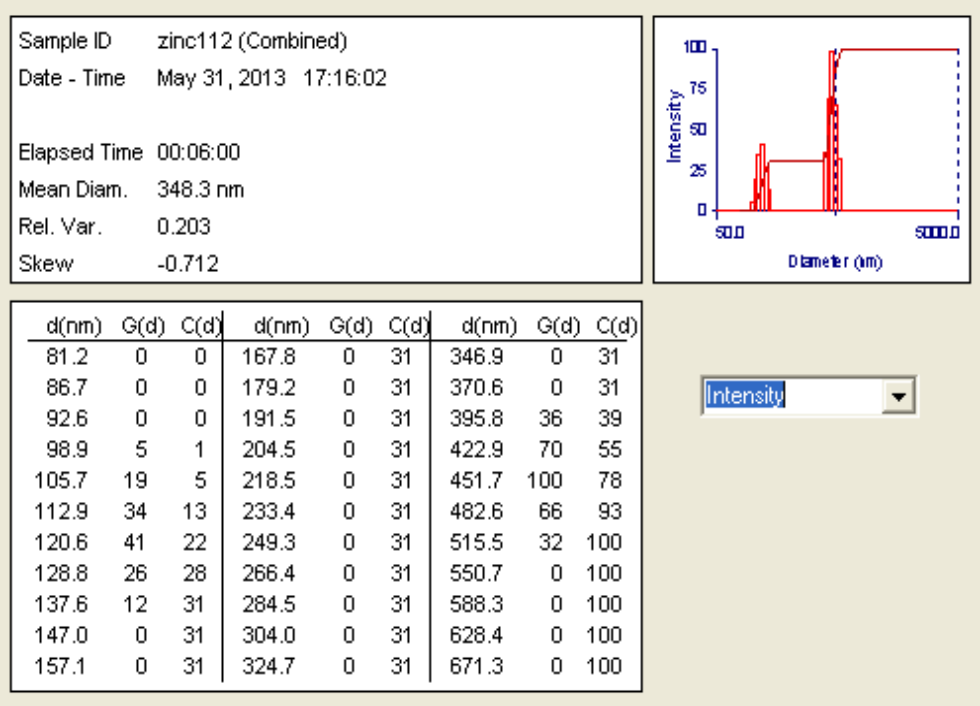

d(nm)	G(d)	C(d)	d(nm)	G(d)	C(d)	d(nm)	G(d)	C(d)
81.2	0	0	167.8	0	31	346.9	0	31
86.7	0	0	179.2	0	31	370.6	0	31
92.6	0	0	191.5	0	31	395.8	36	39
98.9	5	1	204.5	0	31	422.9	70	55
105.7	19	5	218.5	0	31	451.7	100	78
112.9	34	13	233.4	0	31	482.6	66	93
120.6	41	22	249.3	0	31	515.5	32	100
128.8	26	28	266.4	0	31	550.7	0	100
137.6	12	31	284.5	0	31	588.3	0	100
147.0	0	31	304.0	0	31	628.4	0	100
157.1	0	31	324.7	0	31	671.3	0	100

Figure B3: ZnO sample, DLS results

Sample Details:

The sample ZnO contains ZnO: 0.03%, SDS: 0.4%. The sample was sonicated for 2.5 hours after adding ZnO and SDS to the base fluid (DI water). Mean nanoparticle diameter is 348.3nm.

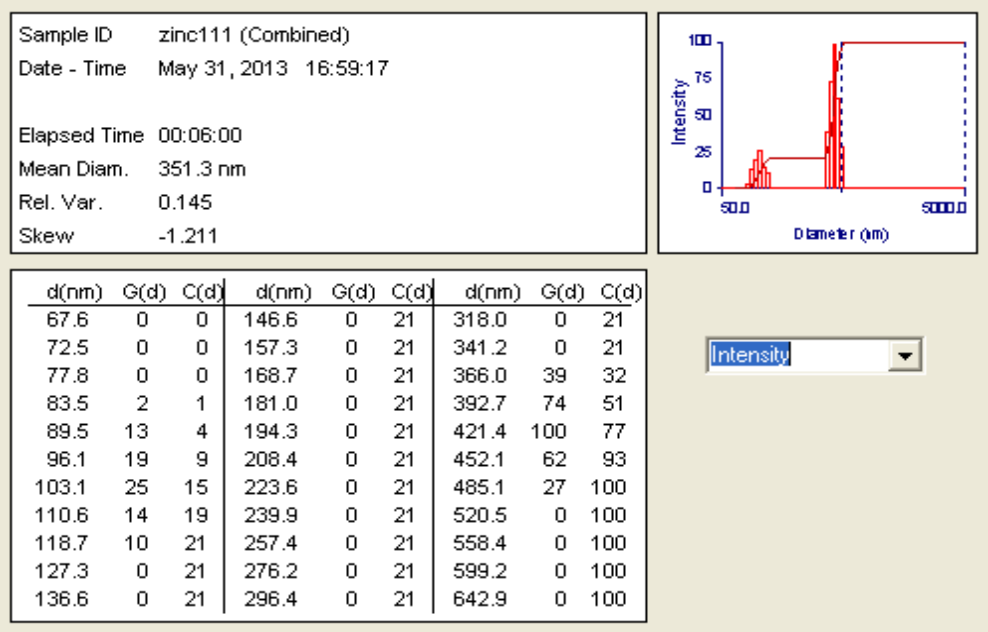

d(nm)	G(d)	C(d)	d(nm)	G(d)	C(d)	d(nm)	G(d)	C(d)
67.6	0	0	146.6	0	21	318.0	0	21
72.5	0	0	157.3	0	21	341.2	0	21
77.8	0	0	168.7	0	21	366.0	39	32
83.5	2	1	181.0	0	21	392.7	74	51
89.5	13	4	194.3	0	21	421.4	100	77
96.1	19	9	208.4	0	21	452.1	62	93
103.1	25	15	223.6	0	21	485.1	27	100
110.6	14	19	239.9	0	21	520.5	0	100
118.7	10	21	257.4	0	21	558.4	0	100
127.3	0	21	276.2	0	21	599.2	0	100
136.6	0	21	296.4	0	21	642.9	0	100

Figure B4: ZnO sample, DLS results

Sample Details:

The sample ZnO contains ZnO: 0.03%, SDS: 0.4%. The sample was sonicated for 6 hours after adding ZnO and SDS to the base fluid (DI water). Mean nanoparticle diameter is 351.3nm